

EIDESSTATTLICHE ERKLÄRUNG

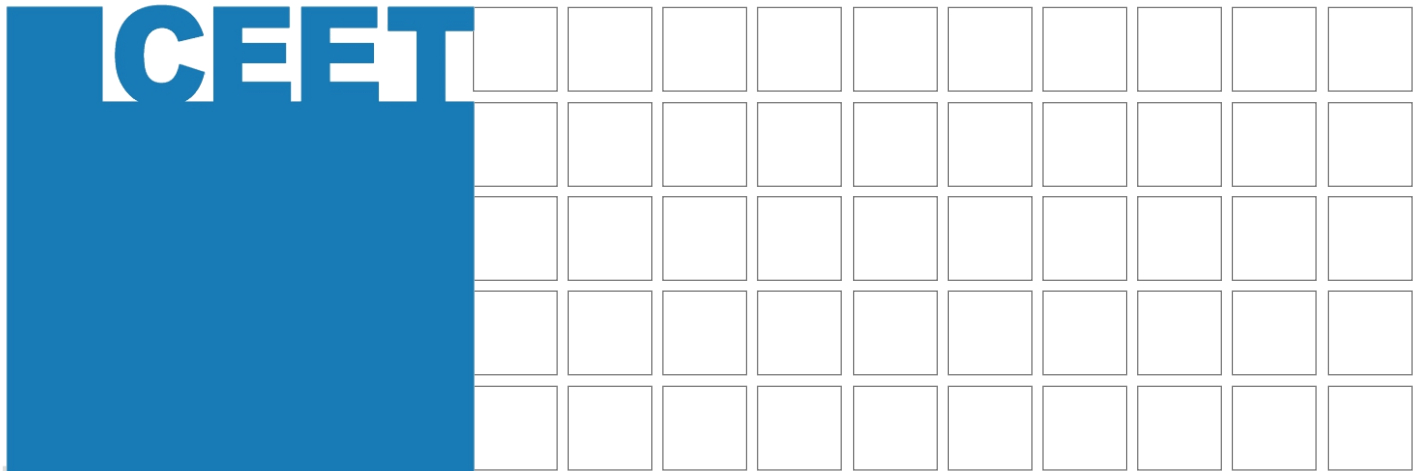
Ich erkläre an Eides statt, dass ich die vorliegende Arbeit selbstständig verfasst, andere als die angegebenen Quellen/Hilfsmittel nicht benutzt, und die den benutzten Quellen wörtlich und inhaltlich entnommenen Stellen als solche kenntlich gemacht habe. Das in TUGRAZonline hochgeladene Textdokument ist mit der vorliegenden Masterarbeit identisch.

5.12.2017

Datum

Manuel J. Faull

Unterschrift



Evaluation of the Thermo-Catalytic Depolymerisation of Lignin

Manuel J. Tandl

Graz, October 2017





Manuel J. Tandl, BSc

Evaluation of the Thermo-Catalytic Depolymerisation of Lignin

Master Thesis

Handed in at the

Graz University of Technology

Supervisor:

Priv.-Doz. Dipl.-Ing. Dr.techn. Nikolaus Schwaiger

Institute of Chemical Engineering and Environmental Technology

Graz, October 2017

Declaration

Decision of the Curricula-Commission for Bachelor, Master and Diploma studies from 10.11.2008
Permission of the Senate on 1.12.2008

STATUTORY DECLARATION

I declare that I have authored this thesis independently, that I have not used other than the declared sources/resources, and that I have explicitly marked all material which has been quoted either literally or by content from the used sources.

Graz, _____
Date

Signature

EIDESSTATTLICHE ERKLÄRUNG

Ich erkläre an Eides statt, dass ich die vorliegende Arbeit selbstständig verfasst, andere als die angegebenen Quellen/Hilfsmittel nicht benutzt und die den benutzten Quellen wörtlich und inhaltlich entnommenen Stellen als solche kenntlich gemacht habe.

Graz, _____
Datum

Unterschrift

Abstract

This work is focused on the evaluation of a process for the thermo-catalytic depolymerisation of lignin. Lignin is a component of wood and can be separated from a black liquor stream of a kraft process pulp and paper mill. Various ways to isolate lignin out of the black liquor are investigated and compared. Precipitation is identified as the most promising method. Subsequently, precipitation is used as basis of the further calculation. After this separation step, lignin is dispersed in tetralin, which is used as carrier and H₂ donor. Lignin is depolymerised at high temperatures and pressures. Thereby, tetralin is dehydrogenated to obtain naphthalene, which has to be separated and rehydrogenated in a further process step. Afterwards, a concept of the overall process is designed. Furthermore, mass and energy balances, depending on the purities of the process components, is simulated. It is observed that 35.8% of the organic content of the black liquor can be liquefied. The result of a carbon-based balance shows that 45.2% of dry matter carbon can be transferred into the liquid product. More specific component data is collected and shown in a database. Thereof, a simulation model which is used for the evaluation is prepared. Finally, an economic evaluation of the whole process is performed. It shows a comparable product price as for other similar biogenic fuels.

Kurzfassung

Diese Arbeit beschäftigt sich mit der Evaluierung eines Prozesses zur thermisch-katalytischen Depolymerisation von Lignin. Lignin ist ein Holzbestandteil und soll aus dem Ablaugestrom einer Papier- und Zellstofffabrik isoliert werden. Verschiedene Methoden zur Abscheidung von Lignin aus Ablauge wurden untersucht. Fällung stellt die vielversprechendste Methode dar. Daher wurde diese Methode als Basis für die weitere Berechnung herangezogen. Im Anschluss an diesen Trennprozess kann Lignin bei harschen Prozessbedingungen depolymerisiert werden. Tetralin dient dabei als Trägermedium und als H₂-Donor. Das Tetralin wird dabei zu Naphthalin dehydriert, welches in einem weiteren Prozessschritt wieder zu Tetralin hydriert wird. Es wurde festgestellt, dass 35.8% des organischen Anteils aus der Ablauge beziehungsweise 45.2% des Kohlenstoffs aus der Trockensubstanz verflüssigt werden kann. Hierzu wurde ein gesamtes Prozesskonzept entworfen. Des Weiteren ist das Augenmerk auf erforderliche Reinheiten der Stoffe gerichtet. Stoff- und Energiebilanzen sowie Stoffdatenbanken wurden erstellt, um daraus anschließend ein Simulationsmodell zu designen, mit dem die Evaluierung durchgeführt wurde. Zum Schluss wurde mit den berechneten Daten eine wirtschaftliche Beurteilung des Prozesses durchgeführt und gezeigt, dass die Herstellungskosten des erhaltenen Produkts mit anderen biogenen Treibstoffen vergleichbar sind.

Content

1	Introduction	1
1.1	Biomass to Liquid.....	1
1.2	Biorefinery concept	2
1.3	Objective of the thesis	3
1.4	Flipp ^o (Future Lignin and Pulp Processing Research)	4
2	From biomass to fuel.....	7
2.1	Wood.....	7
2.1.1	Structure and chemical composition of wood	7
2.1.2	Lignin	8
2.2	Pulping process.....	9
2.2.1	Kraft process.....	10
2.2.2	Black liquor.....	11
2.3	Decomposition process.....	11
3	Lignin separation.....	13
3.1	The LignoBoost process.....	13
3.2	Ultrafiltration.....	14
3.3	Characterisation of different precipitation products.....	14
4	Depolymerisation.....	17
4.1	Equilibrium data of tetralin-naphthalene-hydrogen system.....	19
5	Analytics	21
5.1	Dry matter and ash content	21
5.2	Elemental analysis.....	22
6	Experimental.....	23
6.1	Lignin precipitation with H ₂ SO ₄ as precipitant	23
6.1.1	Process parameter overview	24

6.1.2	Analytical results	25
6.1.3	Mass balance.....	29
6.1.4	Carbon transfer.....	31
6.2	Lignin precipitation with CO ₂ as precipitant	33
6.3	Depolymerisation balances	35
6.3.1	Process parameter overview	35
6.3.2	Analytical results	36
6.3.3	Mass balance.....	37
6.3.4	Carbon transfer.....	40
6.4	Rehydrogenation balances.....	45
6.4.1	Rehydrogenation with low dwell time and maximum tetralin concentration.....	49
6.4.2	Rehydrogenation with low dwell time and decalin prevention.....	49
6.4.3	Rehydrogenation with high dwell time and decalin prevention	51
6.4.4	Rehydrogenation hydrogen consumption.....	53
6.5	Key figures.....	54
6.5.1	Liquid product theoretical composition.....	54
6.5.2	Van Krevelen plot	55
6.5.3	Heating value of the liquid product	55
7	Modelling.....	57
7.1	Basic process flowsheet	57
7.2	Precipitation simulation model.....	62
7.3	Distillation of carrier	65
8	Entire process evaluation	67
8.1	Overall mass balance.....	67
8.2	Cost estimation	68
8.2.1	Operating cost estimation – Case #1	70

8.2.2	Operating cost estimation – Case #2	71
8.2.3	Operating cost estimation – Case #3	72
8.2.4	Capital costs	73
8.3	Availability	73
9	Conclusion and forecast.....	77
10	Appendix	79
10.1	Credits	79
10.2	Glossary	80
10.2.1	General acronyms.....	80
10.2.2	Formula symbols	80
10.2.3	Formula indices	80
10.3	Bibliography	82
10.4	Figures.....	86
10.5	Tables	89
10.6	Equations.....	92
10.7	Substance data.....	95
10.8	Experimental – amendment.....	97
10.9	Modelling.....	98
10.9.1	Matlab code	98

1 Introduction

Lignin is a valuable source for the production of chemicals. At the same time, the high amount of lignin in black liquor can be a bottleneck in paper mills, especially in the recovery boiler [1]–[4]. This is the reason, why new opportunities beyond the traditional production of cellulose are being explored for pulp and paper mills [5]. One possibility of lignin upgrading is depolymerisation [6]. Simultaneously, the demand of new second and third generation biogenic diesel substitute fuels has increased enormously. In particular, research concerning fuels from wooden sources has expedited. Therefore, not only the comparability with the diesel or the crude oil price is of major importance, but also the comparability with other fuels of biogenic origin is relevant. One way to reach new CO₂ emission legislation targets is to increase the required biogenic share in automotive fuels. Even in the on-road transport sector, the capacity of a full electrification in the next decades is not given.

1.1 Biomass to Liquid

Since 2006, scientists are working at the Institute of Chemical Engineering and Environmental Technology (CEET) at Graz University of Technology on research in the field of biomass liquefaction. The main topics are the upgrading of liquid phase pyrolysis oils [7]–[10] and biochar liquefaction [11]. Figure 1-1 shows a process overview in which the HDO process and the pyrolysis char hydrogenation are included.

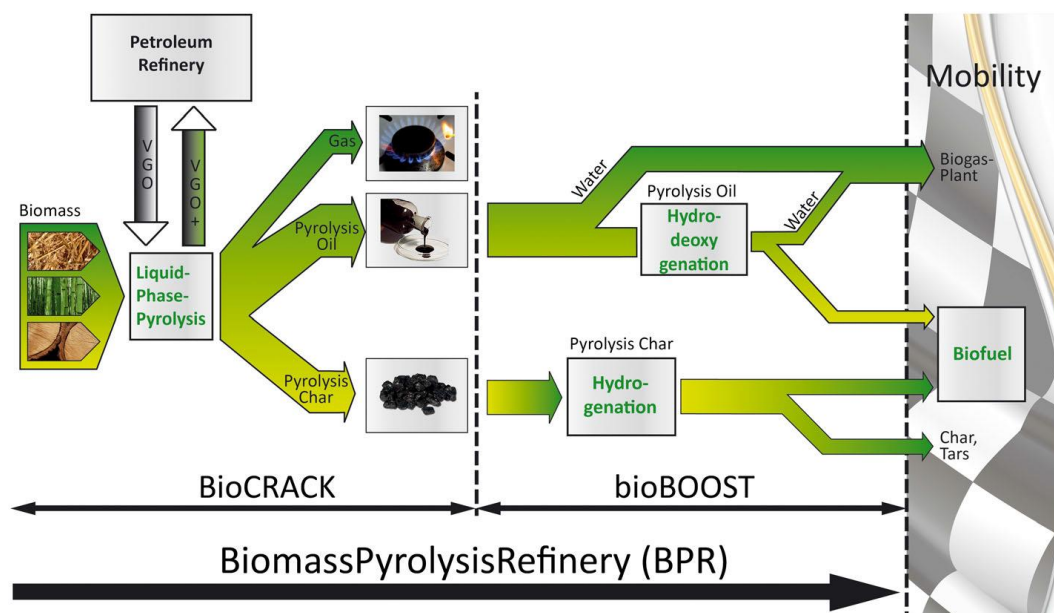


Figure 1-1: Biomass Pyrolysis Refinery process

1.2 Biorefinery concept

The definition of biorefining is the sustainable processing of biomass into marketable products and fuels [12]. Another definition is that a biorefinery is a facility which integrates biomass transfer processes and equipment to produce fuels, power and chemicals from biomass [13]. The biorefinery concept is based on the following twelve principles of green chemistry [14]:

1. Prevent waste
2. Design safer chemicals and products
3. Design less hazardous chemical syntheses
4. Use renewable feedstock chemicals
5. Use catalysts, not stoichiometric reagents
6. Avoid chemical derivatives
7. Maximize atom economy
8. Use safer solvents and reaction conditions
9. Increase energy efficiency
10. Design chemicals and products to degrade after use
11. Analyse in real time to prevent pollution
12. Minimize the potential of accidents

In Figure 1-2 the biorefinery value chain is depicted [15].

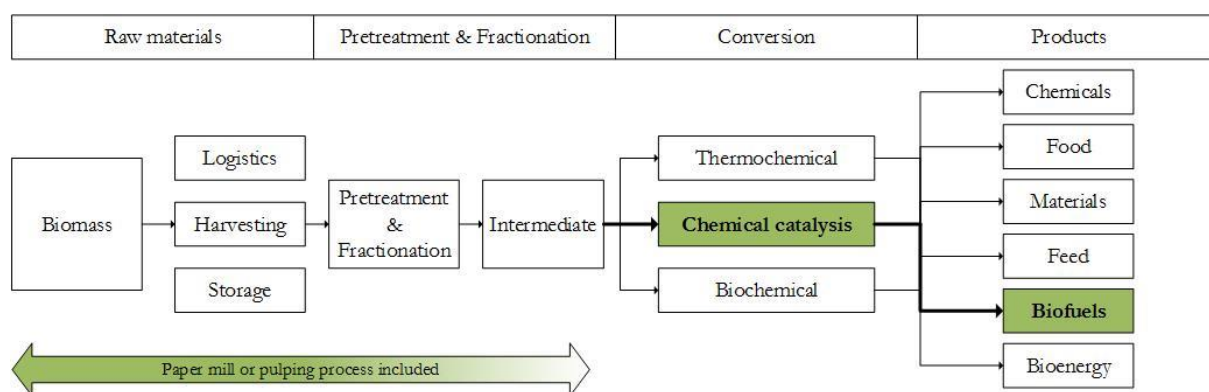


Figure 1-2: Biorefinery - value chain [15]

The advantages of integrating a biorefinery site in a paper mill are numerous [15].

- Saves 1/3rd of infrastructure capital (versus Greenfield)
 - Steam and power, water and effluent stations, warehouse, wood yards, storage tanks etc.

- Already has operation permits
- Expertise in cellulosic procurement and logistics
- Modern kraft mill produces 30% excess energy
- Produces chemicals on-site (NaOH, CaO etc.)

1.3 Objective of the thesis

The goal of this project is the design of a concept of lignin separation and upgrading out of black liquor to generate high-value products, especially fuels and chemicals. A carbon enrichment from the paper mill to the petrol refinery site in the products is the main aim. Therefore, various methods of lignin extraction and recovery from pulp mill waste streams will be evaluated. The most promising separation method will then be used for further calculations. For the following calculations, the gathering of material and process data, in order to carry out material and energy balances, is of utmost importance. Material and process data can be obtained from referenced literature and experiments conducted for this work.

Afterwards, the lignin depolymerisation and the solvent recovery are investigated. To do so, experimental data, materials and kinetics analysed by TU Graz may be used. The broad process of depolymerisation is defined beforehand, based on an existing patent from TU Graz, in which tetralin is used as carrier and as hydrogen donor. Here, tetralin is dehydrogenated to obtain naphthalene which has to be recycled in a solvent recovery step through hydrogen.

Moreover, a rough process scheme of the overall process flow has to be designed. This scheme is the basis of the modelling. The connection between paper mill and refinery, which is crucial, should be clearly observable in this step.

Finally, a coupled basic simulation model has to be set up for a new process, which contains lignin recovery, lignin depolymerisation and solvent recycling. The expected outcome of these simulations and calculations are liquid fuel yield data, as well as preliminary energy demand and cost estimations. Also, it should be applicable for later reverse specification and control use. A graphical user interface (GUI) has to be implemented in order to enhance the understanding of the model and corresponding documentation must be provided.

1.4 Flippr^o (Future Lignin and Pulp Processing Research)

Flippr^o is a cooperative research project with companies of the Austrian pulp and paper industry and Austrian universities as scientific partners [16]. The task is to develop future business areas based on lignin and modern fibre utilization for the involved companies. The Flippr^o project is divided into two sectors – the lignin sector and the pulp sector. This thesis belongs to the former, i.e. the lignin sector. Figure 1-3 shows the industrial partners on the left side and scientific project partners on the right side.



Figure 1-3: Industrial (left) and scientific (right) project partners

Following acronyms for project partners were used:

- Graz University of Technology Institute of Chemical Engineering and Environmental Technology (subsequently CEET)
- University of Natural Resources and Life Sciences, Vienna (subsequently BOKU)
- BioEnergy 2020+ GmbH (subsequently BioEnergy)
- BDI – BioEnergy International AG (subsequently BDI)

Flippr^o is funded as part of COMET (Competence Centers for Excellent Technologies) promoted by BMVIT, BMWFJ, Styria and Carinthia. The COMET program is managed by FFG. Figure 1-4 shows the funders of the Flippr^o project.

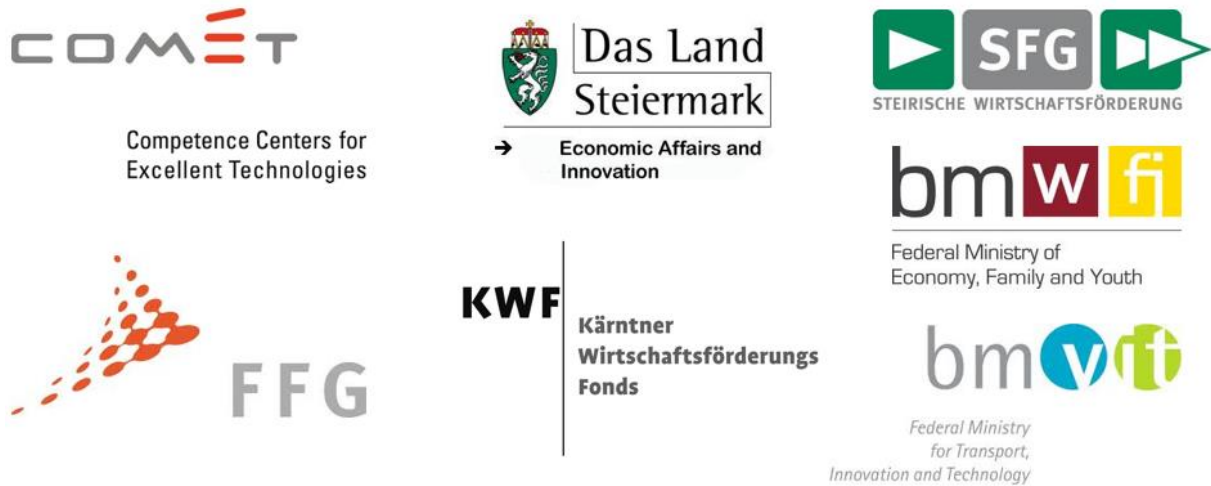


Figure 1-4: Funders

2 From biomass to fuel

In this chapter, the process starting from the tree and finishing with the liquid product is discussed.

2.1 Wood

Wood is a porous and fibrous material which can be found in trees, for example. Trees are seed-bearing plants. They can further be subdivided into gymnosperms, to which softwoods belong, and angiosperms, which include hardwoods [17].

2.1.1 Structure and chemical composition of wood

The macro- and microstructure of wood is depicted in Figure 2-1. The three major constituents of wood are celluloses, hemicelluloses and lignin.

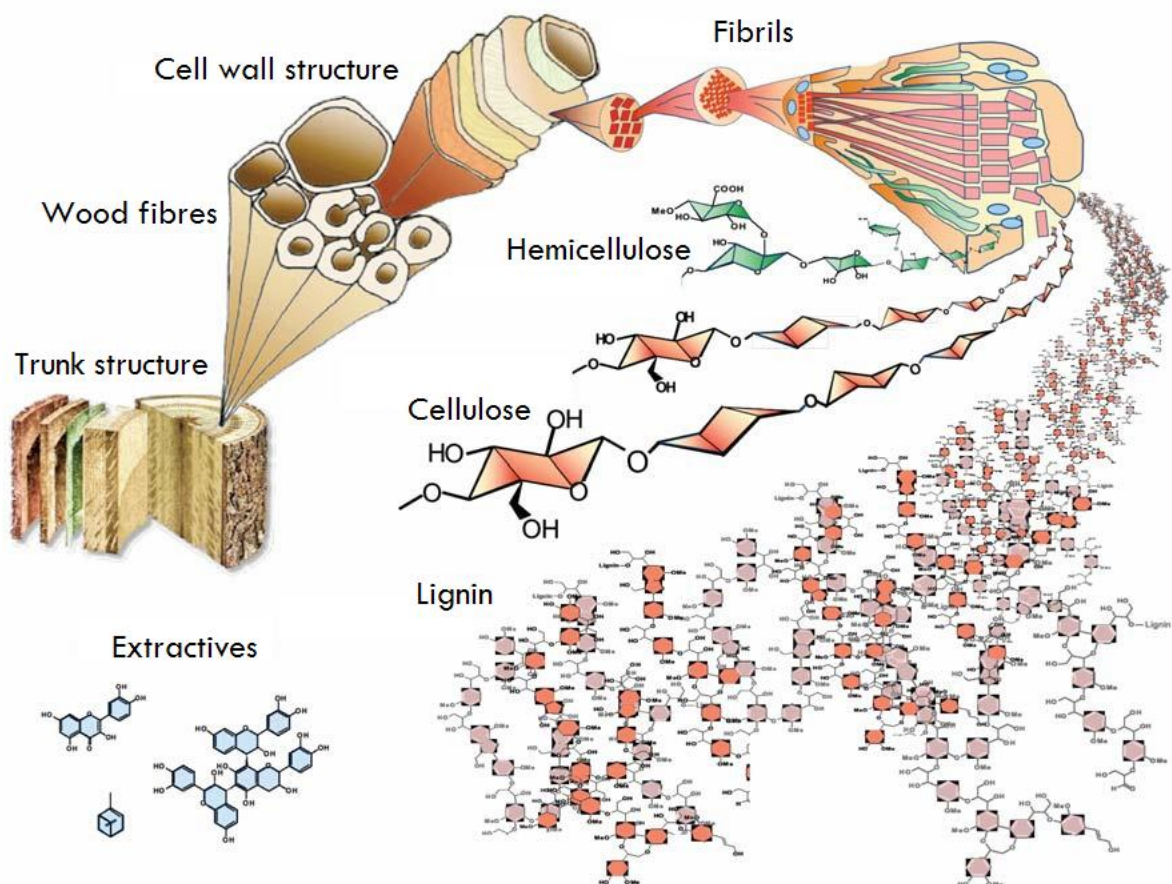


Figure 2-1: Macro- and microstructure of wood [18]

The macro molecules are distributed as shown in Table 2-1. There is a major difference in hardwood and softwood lignin content. In the investigated pulping processes softwood is mainly used.

Table 2-1: Organic constituents of wood [19]

Type	Cellulose (% dry weight)	Hemicellulose (% dry weight)	Lignin (% dry weight)
Hardwood	40-44	15-35	18-25
Softwood	40-44	20-32	25-35

The elemental composition of wood is shown in Table 2-2.

Table 2-2: Elemental composition of wood [19]

Element	% dry weight
Carbon	49.0
Hydrogen	6
Oxygen	44
Nitrogen	0.1
Ash	0.2-0.5

2.1.2 Lignin

Lignin is one of the three major constituents of wood and the most important component for this study. The organic polymer is formed by polymerisation of the three monolignols viz., *p*-coumaryl, coniferyl and sinapyl alcohol (Figure 2-2). These three molecules are formed from D-glucose [20].

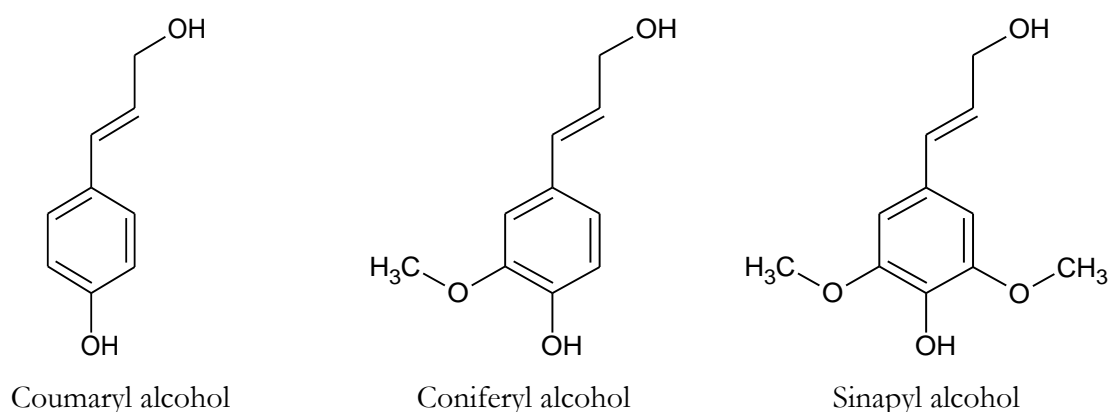


Figure 2-2: Main lignin components [21]

Lignin in wood is responsible for binding the cells together, rigidity of the cells themselves, reducing geometrical change with moisture content fluctuation and increasing wood's toxicity and, thus,

the resistance against decay and insect attack [19]. As an example, a possible construction of spruce lignin polymer is shown in Figure 2-3. This also shows the complexity to describe the molecule holistically.

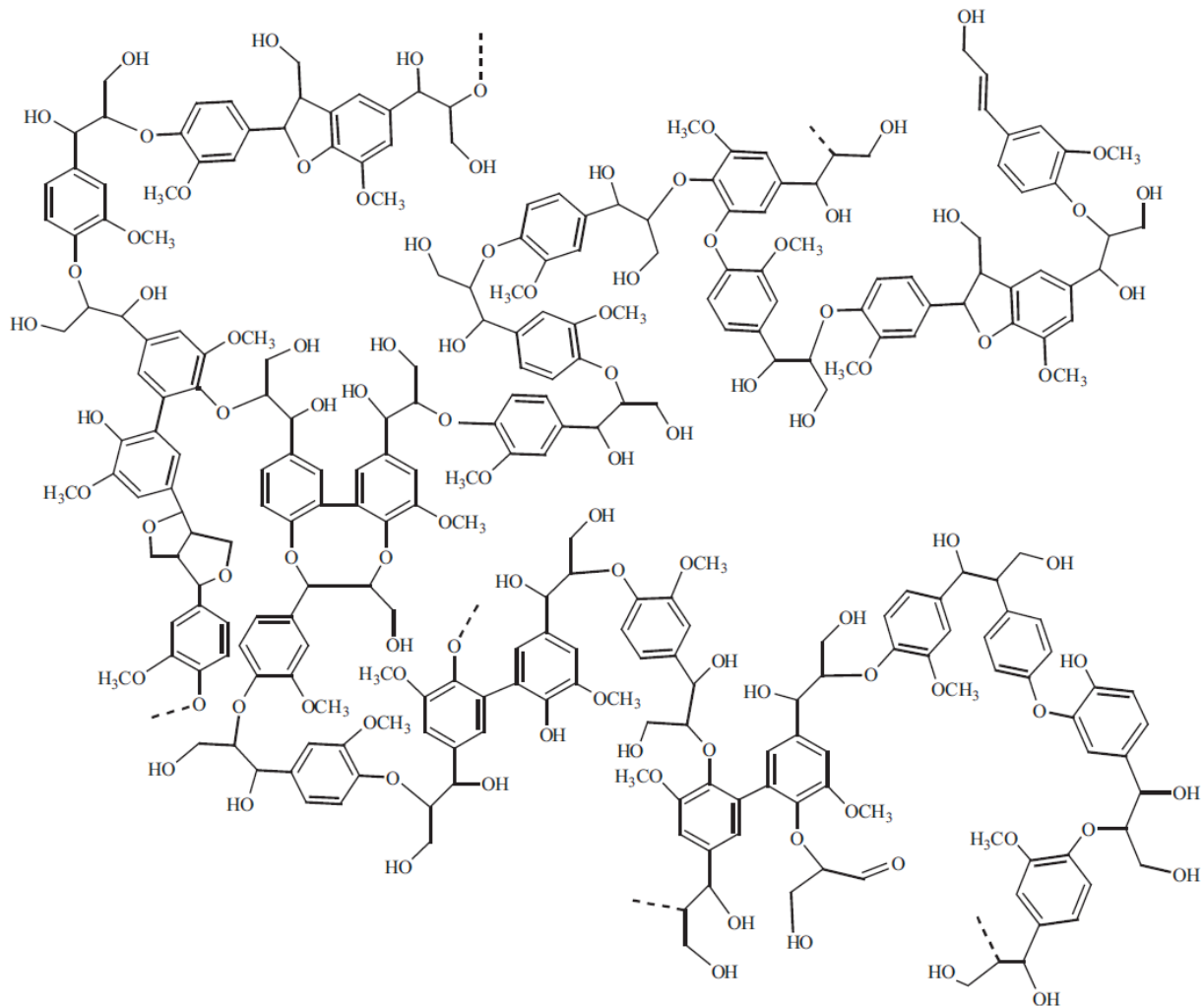


Figure 2-3: Chemical structure of Spruce Lignin [22], [23]

2.2 Pulping process

Different pulping methods exist [24]. One possible way of classification is to distinguish between chemical pulping and mechanical pulping. An additional way to produce fibres is to recover them, by means of recycling, of waste paper. In this study the focus is set on chemical pulping. Chemical pulping is further subdivided into sulphate or kraft pulping, sulphite pulping and semi-chemical pulping.

2.2.1 Kraft process

The aim of the pulping process is the separation of cellulose and lignin into its individual parts. Therefore, in a so-called pulping step, the wood reacts with an aqueous solution of NaOH and Na₂S. This reaction agent is named white liquor. The fibres (cellulose and partly hemicellulose) remain solid whereas lignin is dissolved into the liquor as Figure 2-4 shows [25].

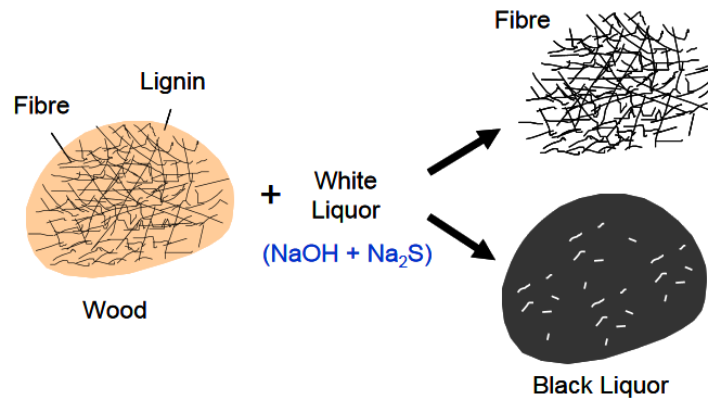


Figure 2-4: Principle behind the kraft pulping process [25]

In Figure 2-5 the kraft pulping process is characterized [26]. Depending on the desired product, the process can be divided into sub-cycles. A possible classification is to divide the process into chipping, pulping, washing, bleaching, stock preparation, blending, papermaking, recovery of chemicals, plant processing [27] and aftertreatment. In this study the main focus is set on the recovery of the chemicals, specifically, the liquor recovery path (Figure 2-5, green and orange cycle).

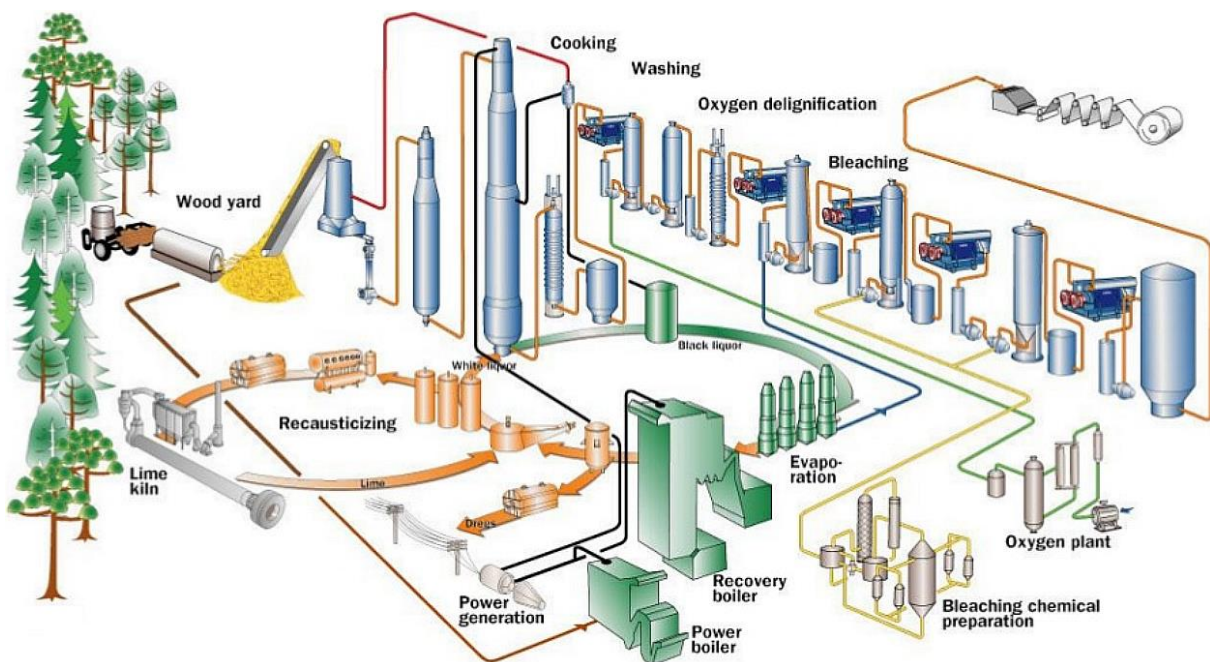


Figure 2-5: Kraft process - principle flow sheet [26]

2.2.2 Black liquor

After the pulping process, the black liquor is collected. To raise the heating value of the black liquor, water is partially evaporated. The product is called heavy or thick black liquor, which is then burnt in the recovery boiler. The ash of this combustion process is mixed with water to form the so called green liquor. In the causticizing plant the green liquor is recycled into the white liquor which is the main reactant of the pulping process. The lignin produced in a kraft pulping process is called kraft lignin or more rarely named as alkali lignin [6].

2.3 Decomposition process

The following lignin decomposition pathways are possible (Figure 2-6). In modern paper mills lignin is almost burnt for energy production and chemicals recovery.

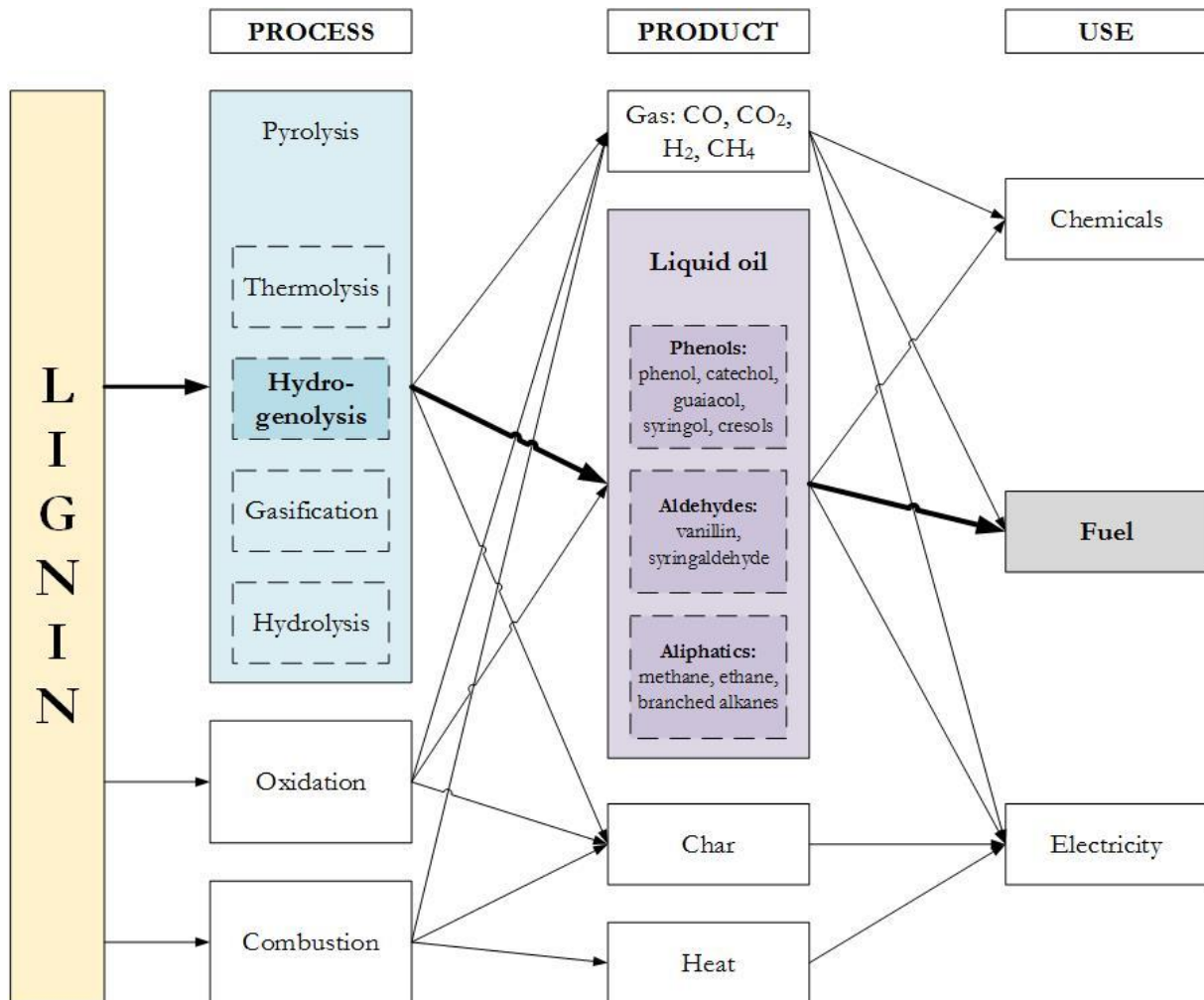


Figure 2-6: Lignin decomposition pathways [6]

Thermo-catalytic lignin depolymerisation is assigned to hydrogenolysis. Lignin pyrolysis is not taken into account due to its high amount of solid residue.

3 Lignin separation

Different ways to extract lignin out of kraft black liquor were investigated [28]. The most common methods are precipitation [29]–[32], ultrafiltration or a combination of both of them. Further classifications based on process control are possible. In this chapter, the most common processes are described and compared. Additionally, a precipitation experiment was performed to obtain samples as the basis for dry matter, ash and elemental analysis. Furthermore, a mass balance of the separation process evaluation and of the ensuing lignin depolymerisation investigations was set up.

3.1 The LignoBoost process

The LignoBoost process is a common way of lignin separation from black liquor (BL). The process was developed within the FRAM2 (Future Resource Adapted Pulp Mill, part 2) R&D program [29], [30]. The process is described on the basis of the scheme illustrated in Figure 3-1.

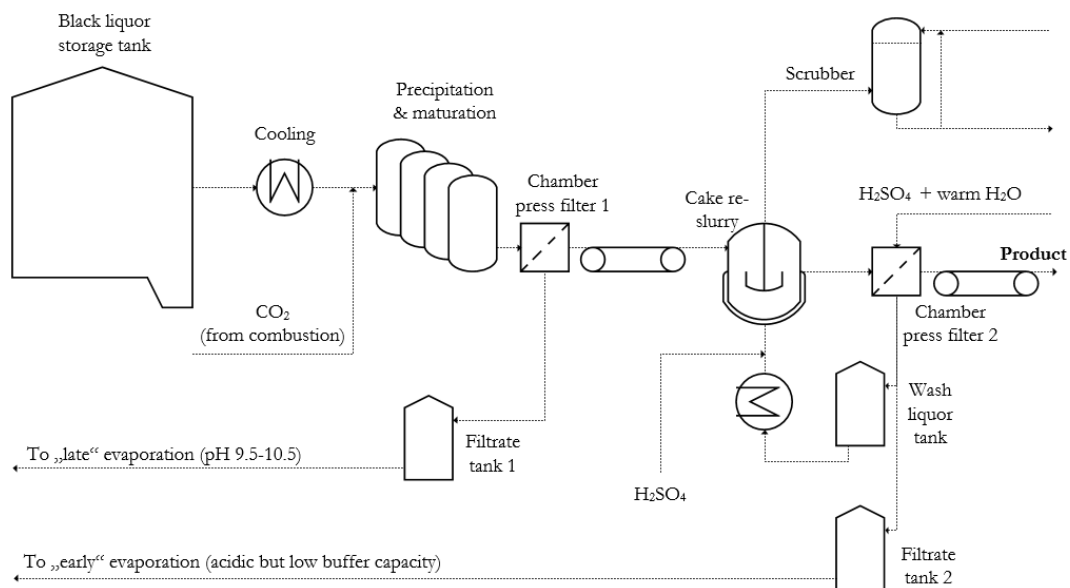


Figure 3-1: The LignoBoost process

BL with a dry matter content of 35-45% is the starting material of this process. First BL is cooled. CO₂ is used as precipitant in the first precipitation step. After this step, the precipitable solids are separated with a chamber filter press. The filtrate which has a pH of about 9.5-10.5 is pumped back to a late evaporation step. The filter cake is moved into a slurry reactor where it is dispersed and acidified. Afterwards, a combined filtration and washing step is used. The filtrate of this second filtration step is recycled to the weak black liquor.

The main advantages of the LignoBoost process are:

- reduced filter area and wash water consumption
- lower sulfuric acid consumption
- higher lignin yield
- lower ash and carbohydrate content and higher dry solid content in the lignin

3.2 Ultrafiltration

Furthermore, ultrafiltration is a process that can be used to extract lignin from black liquor[33], [34]. Figure 3-2 shows schematically a multi-stage ultrafiltration as it is expected to be managed for lignin separation.

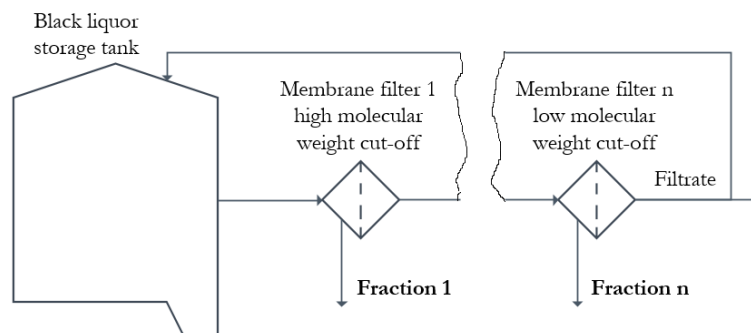


Figure 3-2: Ultrafiltration

3.3 Characterisation of different precipitation products

The composition of black liquor varies depending upon different factors such as used wood mixture, vaporising degree or process management. Trends can be determined. But even similar black liquors seem to behave completely differently during the precipitation process. Project partner BOKU analysed different black liquor samples.

Pöls black liquor precipitation behaviour is shown in Figure 3-3. It is the black liquor with the highest lignin yields at high pH values. At pH 6, 52% of the whole lignin in black liquor can be precipitated.

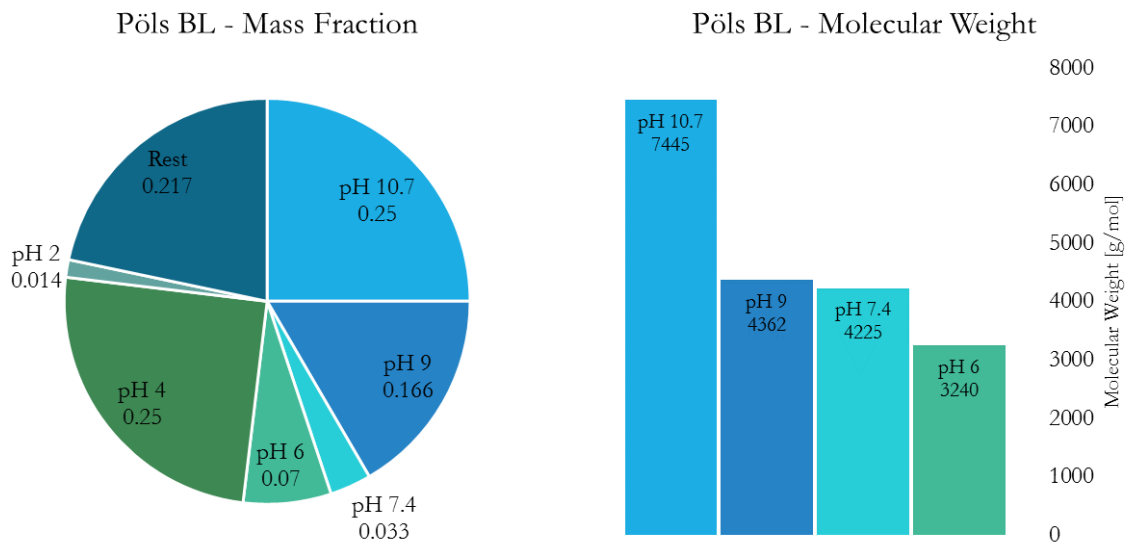


Figure 3-3: Pöls black liquor behaviour of precipitation at different pH values

Yield of precipitated lignin from Mondi black liquor is depicted in Figure 3-4. Although the precipitation yield above pH 9, which is the important pH range for the further use as lignin depolymerisation feed, is not as high as for Pöls lignin the yield below pH 6 is 28% higher. Mondi black liquor shows no clear decreasing trend of molecular weight with decreasing pH as observed by Pöls black liquor precipitation.

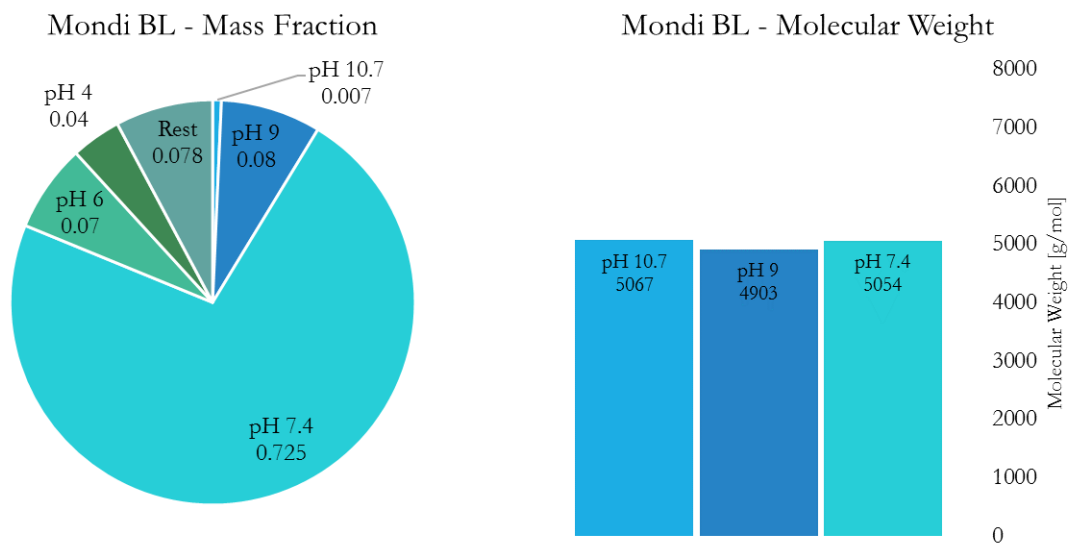


Figure 3-4: Mondi black liquor behaviour of precipitation at different pH values

In literature comparable results can be found. Alekhina et al. describe a similar black liquor precipitation behaviour as observed with Pöls black liquor [32]. An extract is shown in Figure 3-5.

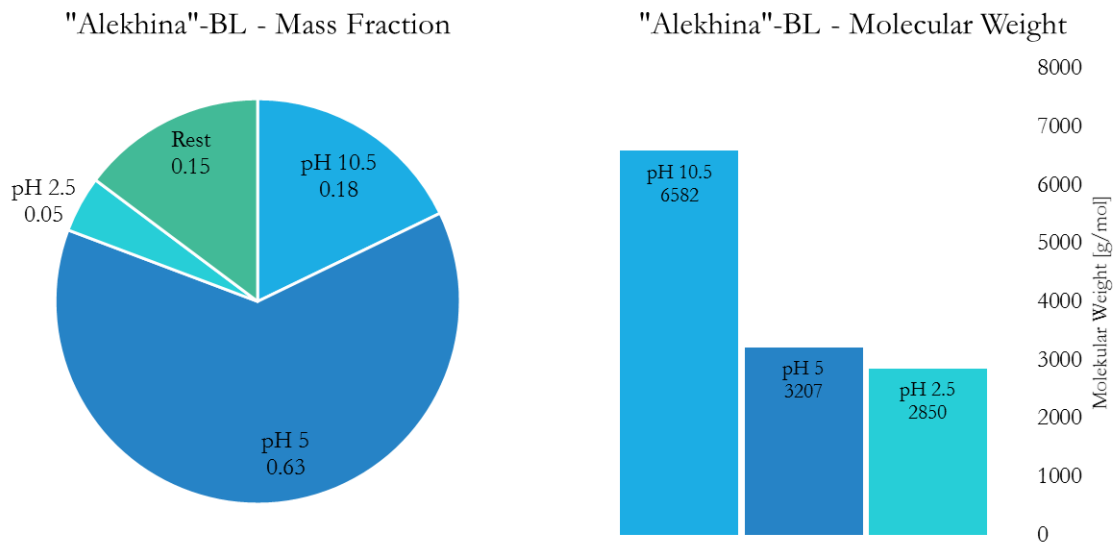


Figure 3-5: "Alekhina" black liquor behaviour of precipitation at different pH values

In Figure 3-6, a comparison of lignin precipitation behaviour of different black liquors is shown. Further products of lignin separation from literature were taken into account [31].

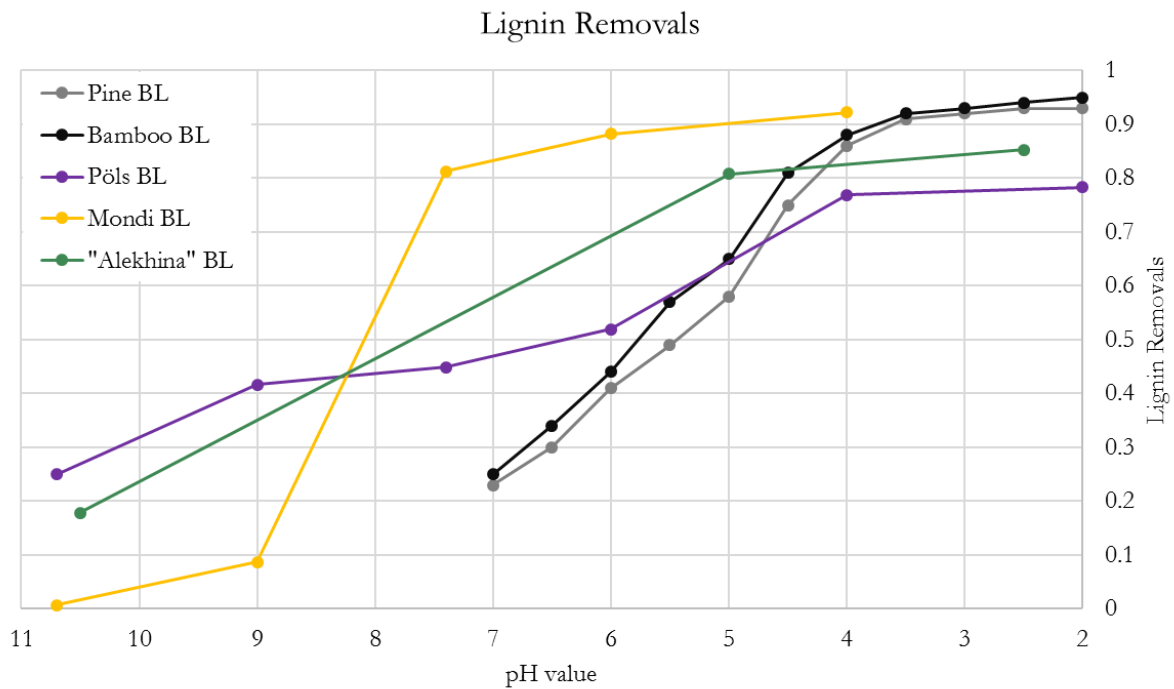


Figure 3-6: Lignin removals behaviour of different black liquors

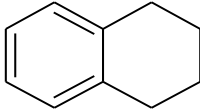
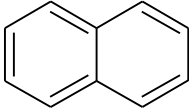
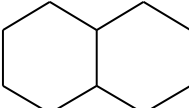
When comparing the lignin removability of different black liquor, a trend can be observed: the lower the pH value, the higher the lignin yield. In case of precipitation, product usage as educt for thermo-catalytic lignin depolymerisation the Pöls black liquor is most suitable due to the highest yields already achieved at high pH values.

4 Depolymerisation

The depolymerisation of lignin is induced in the presence of H₂ or a hydrogen donor at high temperatures and high pressures with a catalyst [35]–[37]. The large lignin molecules break down to smaller, more stable fragments.

In this study, tetralin is used as solvent. It is also responsible for the hydrogen donation. During depolymerisation, tetralin is converted to naphthalene and degradation products. A side product is the desired highly reactive hydrogen. In a further process step, the tetralin has to be rehydrogenated at less harsh process conditions with hydrogen and a catalyst. During the rehydrogenation, stable and unreactive decalin is built [11]. *Cis*- and *trans*-decalin exists. The carrier and products are shown in Table 4-1.

Table 4-1: Carrier and products after depolymerisation and rehydrogenation

Trivial name	Name	Structure	Formula
tetralin	1,2,3,4-tetrahydro-naphthalene		C ₁₀ H ₁₂
naphthalene	-		C ₁₀ H ₈
decalin	decahydro-naphthalene		C ₁₀ H ₁₈

Important data of the three molecules is shown in Table 4-2.

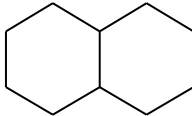
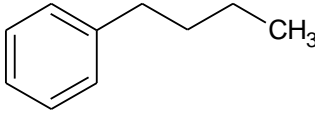
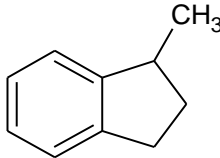
Table 4-2: Characterisation of tetralin, naphthalene and decalin

Item	Acronym	tetralin	naphthalene	decalin	Unit
molar mass	M	132.2	128.17	138.25	[kg/kmol]
density	ρ	970	1140	880	[kg/m ³]
carbon content	μ_C	0.9085	0.9370	0.8687	[-]
hydrogen content	μ_H	0.0917	0.0630	0.1315	[-]
melting point	T _m	-35.8	80.3	-43	[°C]
boiling point	T _b	208	218	190	[°C]
critical temperature [38]–[40]	T _c	446	475	n.a.	[°C]
critical pressure [38]–[40]	p _c	34	41	n.a.	[bar]
critical volume [38]–[40]	v _c	0.428	n.a.	n.a.	[m ³ /kg]

Other potential hydrogen donors are isopropylalcohol, formic acid or formaldehyde, but they have a high vapour pressure for usage in this process.

Significant degradation products are decalin, butylbenzene and 1-methylindan [36]. Properties are shown in Table 4-3.

Table 4-3: Description of significant degradation products

Trivial name	Name	Structure	Formula
decalin	decahydro-naphthalene		C ₁₀ H ₁₈
butylbenzene	n-butyl-benzene		C ₁₀ H ₁₄
1-methyl-indan	2,3-dihydro-1-methyl-1H-indene		C ₁₀ H ₁₂

Various factors such as evaporability and molecular size are important for liquefaction. These parameters can be specified in part by the specific molecules in the educt and their functional groups.

4.1 Equilibrium data of tetralin-naphthalene-hydrogen system

To evaluate the properties of hydrocarbons and the interactions between those, the PENG-ROBINSON equations are used [41]. However, PENG-ROBINSON equations seem to have numerical problems at the high pressures in the depolymerisation process. The evaluation of the equilibrium at 50 bar is not feasible. Consequently, PSRK and NRTL were tested and compared with PENG-ROBINSON equations. Finally, the NRTL method was used to evaluate the interactions between the different hydrocarbons and their properties. The difference between the three methods is shown in Figure 4-1. At a temperature of 200°C the difference is neglectable. Similarly, the difference at 425°C and 50 bar is expected to be neglectable as well.

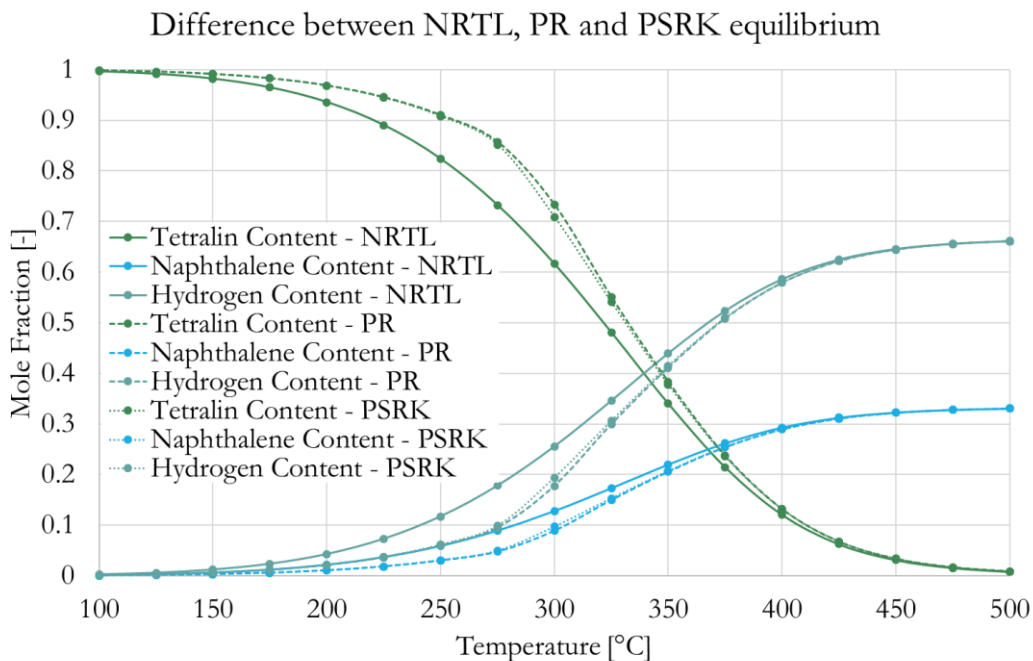


Figure 4-1: Equilibrium of tetralin-naphthalene-hydrogen system – difference between NRTL, Peng-Robinson and PSRK

The equilibrium data of the tetralin-naphthalene-hydrogen system was evaluated with the NRTL method concerning following two operating points:

- 200°C and 20 bar
- 425°C and 50 bar

The results are shown in Figure 4-2.

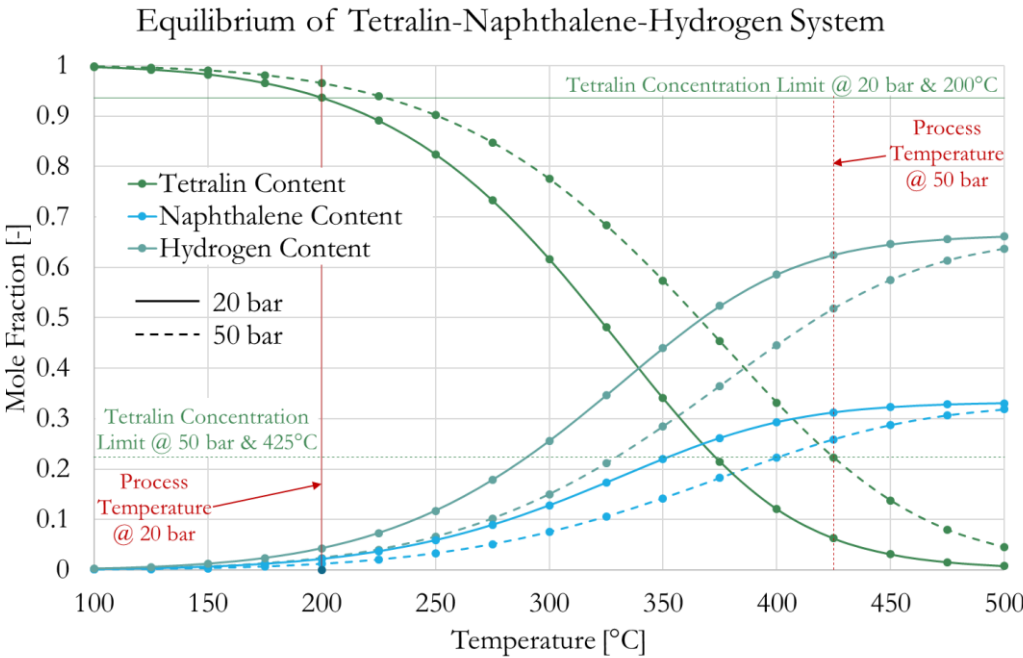


Figure 4-2: Equilibrium of tetralin-naphthalene-hydrogen system

5 Analytics

Dry matter content, ash content, elemental composition and fixed carbon were evaluated. Analytics were performed by CEET. Further extended analysis work was conducted by BOKU, BioEnergy and BDI.

5.1 Dry matter and ash content

Dry matter and ash content analyses were performed by CEET. Counter-measurements were done by BDI. The mass balance is based on these results. Used equipment is listed in Table 5-1.

Table 5-1: Dry matter and ash content analysis devices

Device	Name	Supplier	Analyser
Drying cabinet	UN 500	Memmert	CEET
Muffle furnace	M110	Heraeus	CEET
Drying cabinet			BDI
Muffle furnace			BDI

Dry matter content was determined according to ISO EN 18134-3:2015. The samples were dried for 24 h at 105°C. Each of the samples C1, C2, BL1 and F1 were divided into 4 subsamples. Results of the dry matter content analysis are presented in Table 6-5

Ash content of the dry samples was established according to SIS-CEN/TS 14775:2004 [42]. The samples were placed in the muffle furnace for more than 6 h at a constant temperature of 550°C with a preheating phase of 2 h where the furnace was ramped-up stepwise. The results of the ash content analysis are listed in Table 6-6.

5.2 Elemental analysis

Elemental analysis was performed by CEET, BOKU and BioEnergy. Used equipment is listed in Table 2-1.

Table 5-2: Elemental analysis device

Device	Name	Supplier	Analyser
Elemental analyser	Vario Macro CHN (V5.19.7)	Elementar	BDI
Elemental analyser			BOKU
Elemental analyser	Vario EL III	Elementar	BioEnergy
Multiwave	Multiwave 3000	Anton Paar	BioEnergy
Calorimetric bomb			BioEnergy

Results of the elemental analysis conducted by BDI are listed in Table 6-7. The samples were measured three times.

6 Experimental

To perform the mass balance and the carbon transfer calculations the experimental, the analytical data and literature data were the basis. The outcomes of the calculation are the precipitation yield, the liquefaction degree of the depolymerisation step, the precipitation and depolymerisation carbon transfer and the overall carbon transfer. These calculations, the experimental measurements and the analytical characterisation of the used and produced substances are necessary. In this chapter these parameters, values and the results of the calculation are presented. The calculation is divided in two steps, i.e. the precipitation and the depolymerisation. Two different precipitation pathways were investigated. The basic approach was to calculate with the data from the experiment performed at Zellstoff Pöls AG with H_2SO_4 as precipitation agent. The second calculation path is based on the analysis data of the experiments performed by BOKU Wien with CO_2 as precipitation agent. The acronyms and indices are explained in appendix 10.2.

6.1 Lignin precipitation with H_2SO_4 as precipitant

To perform a lignin precipitation, the Zellstoff Pöls AG precipitation pilot plant (Figure 6-1) was used. Semi-dehydrated Black Liquor was used as feedstock. H_2SO_4 was used as precipitant.

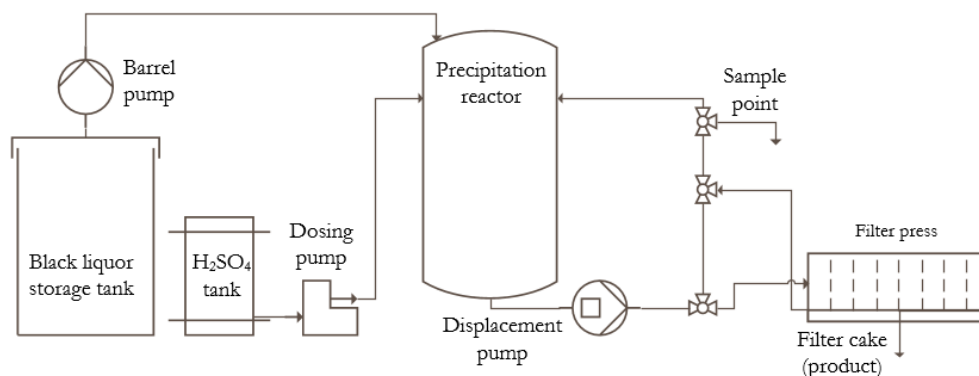


Figure 6-1: Zellstoff Pöls AG precipitation pilot plant - process scheme

The precipitation reactor was filled via a barrel pump with 78 litres of BL. To ensure the correct volume, the redundant BL was removed through an outlet valve which was positioned at the necessary height of the storage tank. The temperature of the BL at the beginning of the experiment was 50°C . After filling the reactor, the H_2SO_4 dosing was started. For a better dispersion, the mixture was circulated by means of a displacement pump. When a pH 9.1 was achieved, H_2SO_4 dosing was stopped. Afterwards the valves were switched so that the suspension could pass the filter press. The precipitated solid particles were separated in the filter chambers. The filtrate was pumped back

into the reactor. The first two filtration steps, i.e. during the first experiment phase, only one filtration chamber was used. The filter cake of these two steps was the first sample for analysis purposes (subsequently referred to as C1). The process temperature decreased to 45°C during the first experiment phase. A second sample (subsequently referred to as C2) was precipitated and sent to TU Graz for analysis purposes by Zellstoff Pöls AG after two further precipitation steps on the following days. In this second part of the experiment, the black liquor temperature decreased further and reached ambient temperature. It is expected that the precipitation yield increases with decreasing temperature [43]–[46].

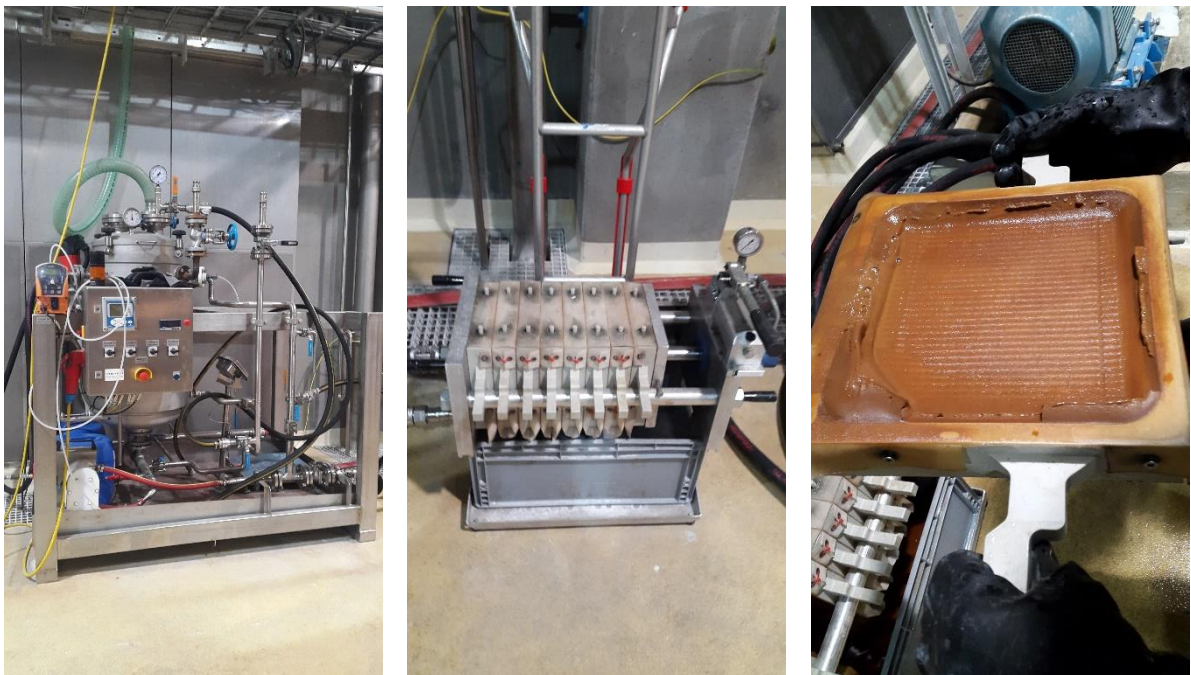


Figure 6-2: Precipitation pilot plant: reactor construction (left), chamber filter press (middle) and emptied filter chamber with cake residue (right)

6.1.1 Process parameter overview

The input components of the experiment were semi-dehydrated BL and a 50% H_2SO_4 as characterized in Table 6-1 and Table 6-2.

Table 6-1: Black liquor input data

Item	Acronym	Value	Unit
initial black liquor volume	V _{BL}	78	[l]
black liquor density	ρ _{BL}	1100	[kg/m ³]
initial black liquor mass	m _{BL}	85.8	[kg]
initial black liquor pH	pH _{BL}	13.5	[-]
black liquor dry matter content	w _{DS,BL}	0.2254	[-]
black liquor ash content	w _{Ash,BL}	0.5116	[-]

Table 6-2: H₂SO₄ input data

Item	Acronym	Value	Unit
initial H ₂ SO ₄ solution mass	m _{H₂SO₄,Lsg}	6.85	[kg]
H ₂ SO ₄ content in the solution	w _{H₂SO₄}	0.5	[-]
initial H ₂ SO ₄ mass	m _{H₂SO₄}	3.425	[kg]

The outcome streams are measured at the end of the experiment. They are shown in Table 6-3.

Table 6-3: Outcome streams

item	acronym	value	unit
filtrate mass after experiment	m _{F,meas}	45.19	[kg]
filter cake mass after part 1 (C1)	m _{C1}	2.050	[kg]
filter cake mass after part 2 (C2)	m _{C2}	2.960	[kg]

6.1.2 Analytical results

Results of the analysis are presented in this chapter. An overview of the samples, their description and acronyms are shown in Table 6-4.

Table 6-4: Sample overview

S-#	Sample	Acronym	Description
#1	Filter cake	C1	Filter cake of first precipitation, CEET analysed, 33%ds
#2	Filter cake	C2	Filter cake after further precipitation time, CEET analysed, ~41%ds
#3	Filtrate	F1	Filtrate, CEET analysed, pH 9
#4	Black Liquor	BL1	Black Liquor sample, precipitation feed, CEET analysed, pH13.5, ~22%ds
#5	Dry filter cake	DC1	Dry matter of the C1 sample
#6	Filter cake ash	AC1	Residue of C1 after incineration
#7	Filtrate ash	AF1	Residue of F1 after incineration
#8	Black Liquor ash	ABL1	Residue of BL1 after incineration
#9	Filter cake	C3	Filter cake from CO ₂ -driven precipitation, BOKU analysed

In Figure 6-3, the samples are depicted.

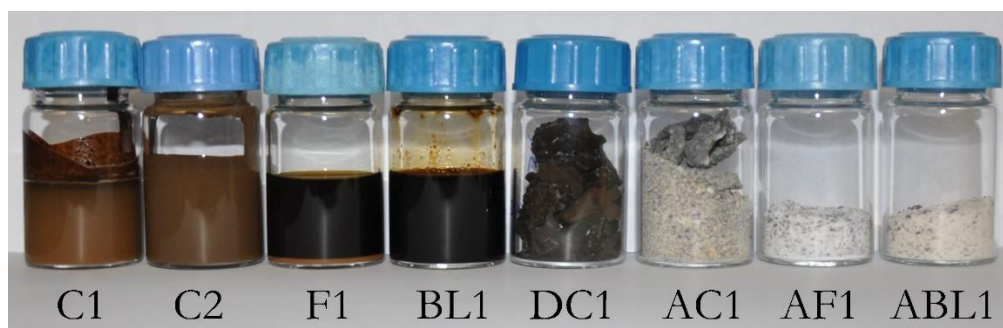


Figure 6-3: Samples

6.1.2.1 Dry matter and ash content

Results of the dry matter content analysis are presented in Table 6-5 where n is the number of samples and w_{DS} is the average dry matter value. The used devices are shown in chapter 5.1.

Table 6-5: Dry matter content

Sample	n	w _{DS}
	[-]	[%]
C1	4	32.70
C2	4	39.86
F1	4	18.22
BL1	4	22.54

Results of the ash content analysis are listed in Table 6-6 where n is the number of samples and w_{Ash} is the average ash content value.

Table 6-6: Ash content

Sample	n	w _{Ash}
	[-]	[%]
C1	2	46.12
F1	2	64.05
BL1	2	51.16

The residues after the incineration of the samples are shown in Figure 6-4, Figure 6-5 and Figure 6-6. Black lumps in the residues are apparent. Especially in the filter cake residue (Figure 6-4), they are distinctive. Even after five days in the furnace the size and the number of lumps were not decreased.

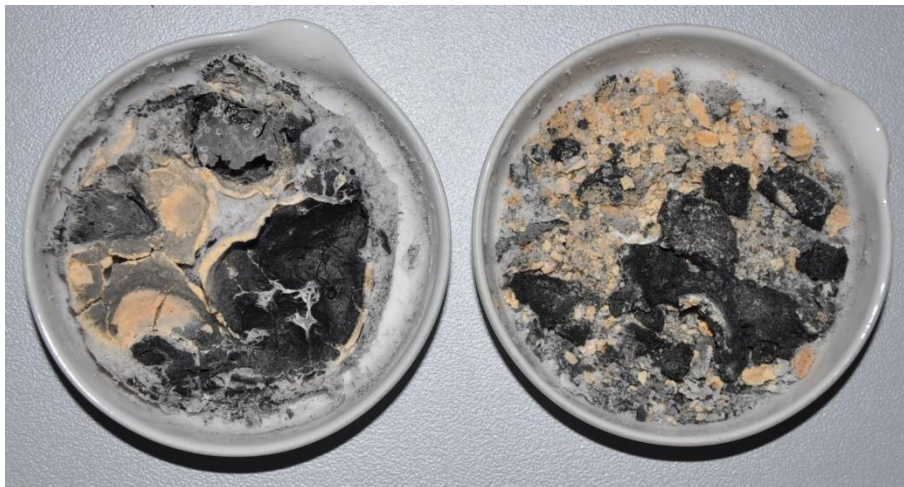


Figure 6-4: Filter cake ash after the incineration



Figure 6-5: Filtrate ash after the incineration



Figure 6-6: Black Liquor ash after the incineration

6.1.2.2 Elemental analysis

The results of the elemental analysis done by BDI are listed in Table 6-7 where n is the number of samples and μ_i are the values of the average content of the analysed elements. The used devices are shown in chapter 5.2.

Table 6-7: Elemental analysis

Sample	n	Carbon	Hydrogen	Nitrogen	Rest
		μ_C [%]	μ_H [%]	μ_N [%]	μ_R [%]
C1	3	52.79	4.76	0.06	42.39
F1	3	17.76	2.65	0.03	79.56
BL1	1	38.40	3.88	0.10	57.62

6.1.3 Mass balance

The balance boundaries are shown in Figure 6-7. Input streams are the black liquor stream and the sulfuric acid stream. Data is listed in Table 6-1 and Table 6-2. There are two product streams - the filtrate and the filter cake. The analysis of the stream data is shown in Table 6-1 and Table 6-2. The most important characteristics of the mass balance are the dry matter content and the ash content. The results are summarized in Table 6-8.

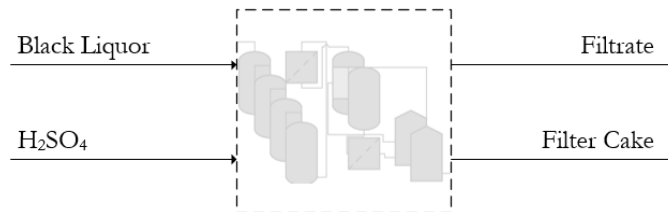


Figure 6-7: Balance boundaries - precipitation with H₂SO₄

Following assumptions are the basis of the calculation:

- process is treated as quasi-continuous
 - no mass accumulation in the system (input = output)
- filtration efficiencies of almost 100% are feasible
 - filtration efficiency is based on the maximum filterable mass by Nutsche Filtration
- The ash content of the sample filtered with Nutsche Filter is the same as the ash content of the analysed samples
- H₂SO₄ is totally dissociated
- The difference between the dry matter and the residue after ash content analysis is the organic amount.

The overall balance (6-1) is defined as

$$\frac{dm}{dt} = \sum m_{in} - \sum m_{out} \quad (6-1)$$

Because of the assumption that the process is quasi-continuous, the transient term drops out and the equation (6-2) is simplified to

$$\sum m_{in} = \sum m_{out} \quad (6-2)$$

With the black liquor volume V_{BL} , the density ρ_{BL} and the measured mass of consumed H_2SO_4 , the sum of the input mass (6-3) is calculated.

$$\sum m_{in} = m_{BL} + m_{H_2SO_4} = \rho_{BL} \cdot V_{BL} + m_{H_2SO_4} \quad (6-3)$$

The organic amount of black liquor (6-4) can be calculated with the dry matter $w_{DS,BL}$ and the ash content $w_{Ash,BL}$.

$$m_{org,BL} = m_{BL} \cdot w_{DS,BL} \cdot (1 - w_{Ash,BL}) \quad (6-4)$$

Due to filtrate loss during the experiment the measured input and output masses are not equal. The filtrate loss (6-5) and consequently the expected filtrate mass of a feasible, lossless, managed process (6-6) is calculable via the measured filter cake mass m_C .

$$m_{F,loss} = \sum m_{in} - (m_C + m_{F,meas}) \quad (6-5)$$

$$m_{F,pred} = \sum m_{in} - m_C \quad (6-6)$$

To calculate the precipitation yield, the organic mass in the filter cake is necessary. As an initial approach, the received dry filter cake mass after the whole experiment duration $m_{DS,C}$ was taken into account. With the analysed dry matter content $w_{DS,C}$ and the ash content $w_{Ash,C}$, a first yield of organic substance in the product (6-7) is evaluated.

$$W_{org,C,meas} = \frac{m_{DS,C} \cdot (1 - w_{Ash,C})}{m_{org,BL}} \quad (6-7)$$

With the residual filtrate mass $m_{F,meas}$ and the filtrate dry matter concentration $c_{DS,F}$ as well as with the filterable mass $m_{DS,C}$, the measurement-based filtration efficiency (6-8) is defined.

$$\mathcal{E}_{filtration,meas} = \frac{m_{DS,C}}{m_{DS,C} + m_{F,meas} \cdot c_{DS,F}} = \frac{m_{DS,C}}{m_{DS,prec,meas}} \quad (6-8)$$

If the filtrate loss can be prevented, the filter cake mass can be increased. Under the premise that the filtration duration is sufficiently long and the number of filter chambers in use is defined cor-

rectly, filtration efficiencies up to 100% (based on Nutsche Filter filterable dry matter) are predicted. The filtrate loss after the first two filtration steps was about one litre. This causes a margin deviation. Under the assumption that all the dry matter which is filterable with the Nutsche Filter is also filterable with the chamber filter press and the filtrate dry matter concentration is constant, a new predicted dry filter cake mass $m_{DS,C,pred}$ (6-9) can be evaluated. With this filter cake mass, the predicted yield of organic substance in the product (6-10) increases significantly.

$$m_{DS,C,pred} = m_{DS,C} + m_{F,pred} \cdot c_{DS,F} \quad (6-9)$$

$$W_{org,C,pred} = \frac{m_{DS,C,pred} \cdot (1 - w_{Ash,C})}{m_{org,BL}} \quad (6-10)$$

The results of the calculation concerning the precipitation yield are shown in Table 6-8.

Table 6-8: Mass balance result summary of precipitation with H₂SO₄ as precipitant

item	acronym	value	unit
organic amount of black liquor	$m_{org,BL}$	9.44	[kg]
sum of the input mass	Σm_{in}	92.65	[kg]
predicted filtrate mass	$m_{F,pred}$	66.32	[kg]
filtrate loss	$m_{F,loss}$	21.13	[kg]
yield of organic substance in the product	$W_{org,C,meas}$	0.107	[-]
predicted dry filter cake mass	$m_{DS,C,pred}$	9.61	[kg]
predicted yield of organic substance in the product	$W_{org,C,pred}$	0.548	[-]
measurement-based filtration efficiency	$\epsilon_{filtration,meas}$	0.264	[-]

6.1.4 Carbon transfer

The data from the elemental analysis (Table 6-7) and the results of the mass balance in chapter 5 are of major importance for the carbon transfer investigations. The measurements viz., the analysis data of the inputs and outputs are shown in Table 5-1. The balance boundaries are the same as for the mass balance. They are shown in Figure 6-7. The black liquor input data is listed in Table 6-1. The results of the calculation are summarized in Table 6-9.

The following consideration was made:

- All carbon mass in the black liquor originates from the lignin in the black liquor. This means all carbon in the process is from a biogenic source.

The first step is to calculate the initial carbon mass (6-11). Therefore, the initial black liquor mass m_{BL} is multiplied with the dry matter content $w_{DS,BL}$ and the black liquor carbon content $\mu_{C,BL}$.

$$m_{C,in} = m_{BL} \cdot w_{DS,BL} \cdot \mu_{C,BL} \quad (6-11)$$

This is the base value of the precipitation carbon transfer. With the evaluated dry filter cake mass from the mass balance $m_{DS,C,pred}$ and the filter cake carbon content $\mu_{C,C}$, the carbon mass in the product (6-12) is determined. For the calculation of the carbon balance deviation the carbon mass in the filtrate (6-13) is established. To do so, the predicted filtrate mass $m_{F,pred}$ of the mass balance and the filtrate carbon content $\mu_{C,F}$ are necessary.

$$m_{C,C} = m_{DS,C,pred} \cdot \mu_{C,C} \quad (6-12)$$

$$m_{C,F} = m_{F,pred} \cdot w_{DS,F} \cdot \mu_{C,F} \quad (6-13)$$

Thus, an absolute (6-14) and a relative (6-15) balance deviation are calculated.

$$\Delta m_C = \Sigma m_{C,in} - \Sigma m_{C,out} = m_{C,BL} - (m_{C,C} + m_{C,F}) \quad (6-14)$$

$$e_{C,prec} = \left| \frac{\Sigma m_{C,in} - \Sigma m_{C,out}}{\Sigma m_{C,in}} \right| = \left| \frac{\Delta m_C}{m_{C,BL}} \right| \quad (6-15)$$

Three different reference values are used to calculate the carbon transfer degree: the whole black liquor mass (6-16), the black liquor dry matter mass (6-17) and the black liquor carbon mass (6-18). The black liquor carbon mass specific carbon transfer degree is of major importance for further calculations.

$$C_{C,BL} = \frac{m_{C,C}}{m_{BL}} \quad (6-16)$$

$$C_{C,DS,BL} = \frac{m_{C,C}}{m_{DS,BL}} \quad (6-17)$$

$$C_{C,prec} = \frac{m_{C,C}}{m_{C,BL}} \quad (6-18)$$

The results of the calculation concerning the carbon transfer are shown in Table 6-9.

Table 6-9: Carbon transfer result summary of precipitation with H₂SO₄ as precipitant

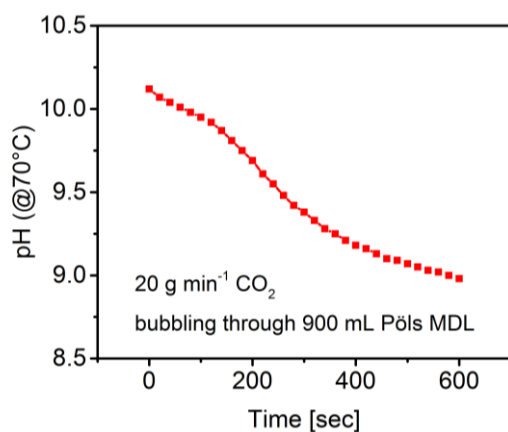
item	acronym	value	unit
initial carbon mass	$m_{C,in}$	7.43	[kg]
carbon mass in filter cake	$m_{C,C}$	5.07	[kg]
carbon mass in filtrate	$m_{C,F}$	2.15	[kg]
absolute carbon balance deviation	Δm_C	0.21	[kg]
relative carbon balance deviation	e_C	2.78	[%]
carbon transfer degree black liquor based	$C_{C,BL}$	0.059	[-]
carbon transfer degree dry black liquor based	$C_{C,BL,DS}$	0.262	[-]
carbon transfer degree	C_C	0.683	[-]

6.2 Lignin precipitation with CO₂ as precipitant

The BOKU team is developing a special CO₂-based precipitation process [47]. The process using CO₂ as precipitant is expected to reduce the inorganic amount in the intermediate viz., the educt of the depolymerisation step. It is also expected that this can be the preferred process due to further advantages of the CO₂-based precipitation such as lower precipitant costs and easier handling and, thus, a simpler overall process. As a reactor, it may be possible to use a simple bubble column. Since the development of this process is still ongoing, data for the calculation are not available.

Nevertheless, trends can be determined. Pöls black liquor, similar to what was used in TU Graz experiments, was the educt of these analyses.

The pH drop over the experiment time, induced by bubbling of CO₂ through 900 ml of this Pöls black liquor sample at 70°C with a flow rate of 20 g/min for 10 minutes, is shown in Figure 6-8.

Figure 6-8: pH drop induced by CO₂

This would mean that 200 g CO₂ is necessary to decrease the pH to 9. It is assumed that with better mixing and bubble size distribution and, thus, a better mass transport, the amount of necessary CO₂ can be massively decreased. Therefore, many further experiments have to be performed. Figure 6-9 shows the lab scale setup of the CO₂-based precipitation.

Figure 6-9: Lab scale precipitation experiment with CO₂ as precipitant

6.3 Depolymerisation balances

The depolymerisation balance is based on an experiment performed by CEET [35]–[37]. Kraft lignin from a black liquor evaporation was the initial product. The used chemicals were tetralin, γ -FeOOH and sulphur. Tetralin served as carrier and H_2 donor. γ -FeOOH was used as catalyst. Sulphur was applied to activate the catalyst. The experiments were performed in a batch reactor [37].

6.3.1 Process parameter overview

Physical and chemical properties are to be found in appendix 10.7. The process parameters are shown in Table 6-10.

Table 6-10: Depolymerisation process parameter

item	acronym	value	unit
temperature	T	425	[°C]
H_2 pressure	p_{H_2}	50	[bar]
process pressure	p	180	[bar]
catalyst content	w_{cat}	0.1	[-]

The initial quantities of the used materials are listed in Table 6-11.

Table 6-11: Initial quantities of depolymerisation experiment

item	acronym	value	unit
initial tetralin mass	$m_{tetralin}$	97.67	[g]
initial lignin mass	m_{lignin}	30.5	[g]
lignin dry matter content	$w_{DS,L}$	1	[-]
initial hydrogen mass	m_{H_2}	1.33	[g]
initial γ -FeOOH mass	$m_{\gamma\text{-FeOOH}}$	1.42	[g]
initial sulphur mass	$m_{sulphur}$	1.77	[g]

The state of aggregation of the starting material is important concerning the calculation of the liquefaction yield. Dry lignin, catalyst and sulphur represent the solids. Tetralin is the only liquid and H_2 is the only gaseous starting material. Solid, liquid and gaseous mass of the starting material are shown in Table 6-12.

Table 6-12: Physical state distribution

item	acronym	value	unit
solid input mass	$m_{\text{solid,in}}$	33.69	[g]
liquid input mass	$m_{\text{liquid,in}}$	97.67	[g]
gaseous input mass	$m_{\text{gas,in}}$	1.33	[g]

The product streams are declared as solid, liquid and gaseous product or residue. The analysis of the stream data is shown in Table 6-13.

Table 6-13: Output fractions

item	acronym	value	unit
solid output fraction	$m_{\text{solid,out}}$	22	[g]
liquid output fraction	$m_{\text{liquid,out}}$	107.4	[g]
gaseous output fraction	$m_{\text{gas,out}}$	3.4	[g]

6.3.2 Analytical results

In this chapter, the results of the analysis are presented.

6.3.2.1 Chemical composition of the liquid carrier outcome

It is assumed that the liquid carrier decomposition during the reaction with lignin as start product has a similar behaviour as with pyrolysis char as start product. The chemical composition after a heating phase to 425°C was used for further calculations [36]. The analytical results are shown in Table 6-14.

Table 6-14: Chemical composition of liquid carrier after reaction with lignin

item	acronym	value	unit
tetralin content after reaction	$W_{\text{tetralin,out}}$	0.846	[-]
naphthalene content after reaction	$W_{\text{naphthalene,out}}$	0.142	[-]
degradation products after reaction	$W_{\text{DM,out}}$	0.012	[-]

6.3.2.2 Elemental analysis

The results of the elemental analysis done by BDI are listed in Table 6-15 where μ_i are the average content of the analysed elements' value. For the elemental composition of the degradation products a mean hydrogen content of the components listed in Table 4-3 was evaluated. The used devices are shown in chapter 5.2.

Table 6-15: Elemental composition of depolymerisation educts and products

Substance	Carbon	Hydrogen	Nitrogen	Rest
	μ_C [%]	μ_H [%]	μ_N [%]	μ_R [%]
tetralin	0.908	0.092	0.000	0.000
naphthalene	0.937	0.063	0.000	0.000
decalin	0.869	0.132	0.000	0.000
degrad. products	0.890	0.105	0.000	0.000
hydrogen	0.000	1.000	0.000	0.000
lignin	0.354	0.039	0.000	0.607
solid residue	0.127	0.011	0.000	0.882
gaseous residue	0.371	0.435	0.000	0.194

6.3.3 Mass balance

The balance boundaries are shown in Figure 6-10. Input streams are the lignin stream, the tetralin stream, the hydrogen stream, the catalyst stream and the sulphur stream.

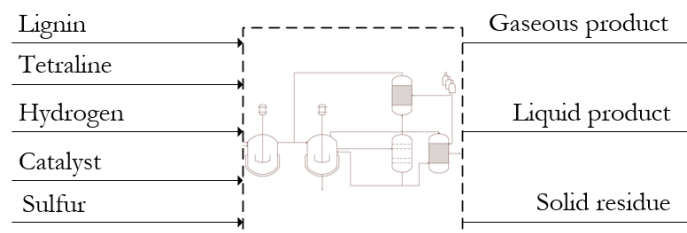


Figure 6-10: Balance boundaries - depolymerisation

The overall balance is shown in equations (6-1) and (6-2). The sum of the input mass (6-19) is calculable with the initial tetralin mass m_{tetralin} , the initial lignin mass m_{lignin} , the initial hydrogen mass m_{H_2} , the initial catalyst mass $m_{\gamma\text{-FeOOH}}$ and the initial sulphur mass m_{sulphur} .

$$\sum m_{\text{in}} = m_{\text{tetraline}} + m_{\text{lignin}} + m_{\text{H}_2} + m_{\gamma\text{-FeOOH}} + m_{\text{sulphur}} \quad (6-19)$$

The sum of the output mass (6-20) is calculated with the solid output fraction $m_{\text{solid,out}}$, the liquid output fraction m_{liquid} and the gaseous output fraction $m_{\text{gas,out}}$.

$$\sum m_{\text{out}} = m_{\text{solid,out}} + m_{\text{liquid,out}} + m_{\text{gas,out}} \quad (6-20)$$

An absolute (6-21) and a relative (6-22) mass balance deviation were evaluated.

$$\Delta m_{\text{dpm}} = \sum m_{\text{in}} - \sum m_{\text{out}} \quad (6-21)$$

$$e_{\text{dpm}} = \left| \frac{\sum m_{\text{in}} - \sum m_{\text{out}}}{\sum m_{\text{in}}} \right| = \left| \frac{\Delta m}{\sum m_{\text{in}}} \right| \quad (6-22)$$

The liquefaction degree and the depolymerisation degree can be determined with the knowledge of all solid, liquid and gaseous input and output masses under the following assumptions:

- Catalyst and sulphur are unaffected by the depolymerisation (6-23). This implies that the dry lignin is the only solid affected starting product.
- Lignin is absolutely dry \rightarrow no liquid or gas content.
- Hydrogen originates partially from the tetralin which is thereby reduced to naphthalene. The mass loss because of the hydrogen transfer into the product is almost negligible.
- Solid (6-24), liquid (6-25) and gaseous (6-26) mass change is the basis of the calculation.

$$m_{\gamma\text{-FeOOH},\text{in}} + m_{\text{sulphur},\text{in}} = m_{\gamma\text{-FeOOH},\text{out}} + m_{\text{sulphur},\text{out}} \quad (6-23)$$

$$\Delta m_{\text{solid}} = m_{\text{solid,out}} - m_{\text{solid,in}} \quad (6-24)$$

$$\Delta m_{\text{liquid}} = m_{\text{liquid,out}} - m_{\text{liquid,in}} \quad (6-25)$$

$$\Delta m_{\text{gas}} = m_{\text{gas,out}} - m_{\text{gas,in}} \quad (6-26)$$

The liquefaction degree follows in (6-27).

$$W_l = \frac{\Delta m_{\text{liquid}}}{m_{\text{lignin}}} \quad (6-27)$$

The depolymerisation degree follows in (6-28).

$$W_{dpm} = \frac{|\Delta m_{solid}|}{m_{lignin}} \quad (6-28)$$

The results are presented in Table 6-16 and depicted in Figure 6-11 and Figure 6-12.

Table 6-16: Results of the depolymerisation mass balance

item	acronym	value	unit
all incoming mass	Σm_{in}	132.69	[g]
all outgoing mass	Σm_{out}	132.80	[g]
absolute mass balance deviation	Δm_{dpm}	-0.11	[g]
relative mass balance deviation	ϵ_{dpm}	0.08	[%]
solid mass change	Δm_{solid}	-11.69	[g]
liquid mass change	Δm_{liquid}	9.73	[g]
gaseous mass change	Δm_{gas}	2.07	[g]
depolymerisation degree	W_{dpm}	0.387	[-]
liquefaction degree	W_l	0.319	[-]

In Figure 6-11 the input and output quantities are shown. The liquid fraction dominates due to the three times higher concentration of initial tetralin with respect to the initial lignin. The solid input fraction is reduced during the depolymerisation. Liquid and gaseous fractions are increased.

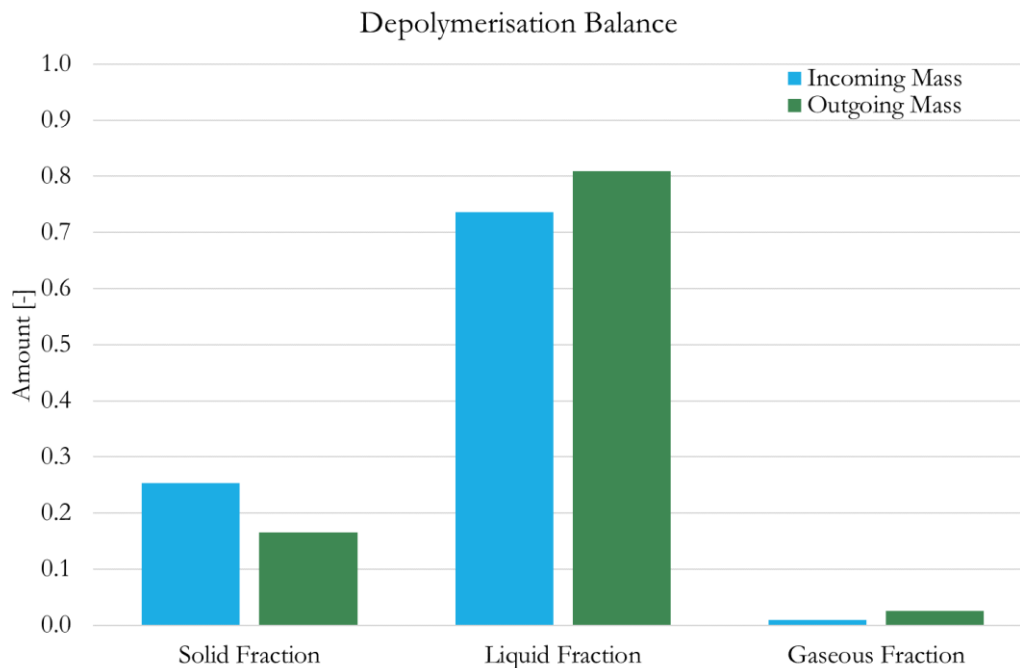


Figure 6-11: Depolymerisation balance

In Figure 6-12 the effect of the depolymerisation is shown in more detail. The different fractions are dependent upon the initial lignin mass in this graph.

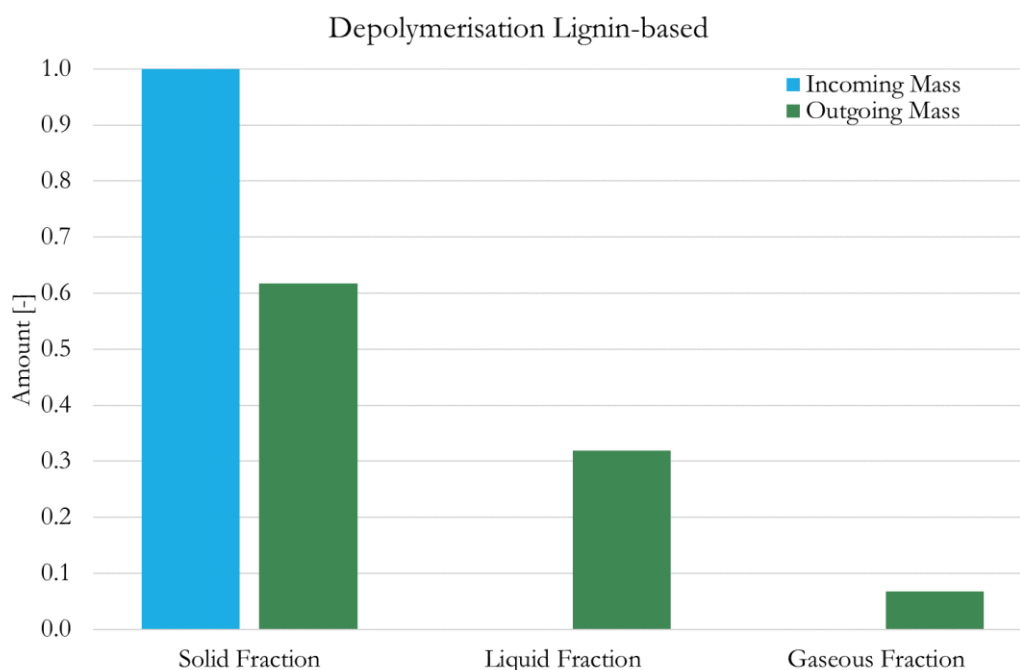


Figure 6-12: Depolymerisation lignin-based

6.3.4 Carbon transfer

The data from the elemental analysis (Table 6-15) and the results of the depolymerisation mass balance in chapter 6.3.3 are the basis of the establishment of the carbon transfer into the liquid phase. The characterisation of the input and output streams is shown in Table 6-11, Table 6-12 and Table 6-13. The balance boundaries are the same as for the depolymerisation mass balance (Figure 6-10). The black liquor input data is listed in Table 6-1. The results of the calculation are summarized in Table 6-17.

Following considerations were made:

- Carbon from tetralin stays in tetralin and its degradation products. All additional carbon in the liquid product originates from the lignin.
- Significant degradation products are decalin, butylbenzene and 1-methylindan, which are expected to be the components with the highest amount. A theoretical degradation molecule with a mean hydrogen and carbon content was used in the calculations.

- The product oil was not separated from the liquid carrier. The composition of the oil is calculable via the carbon balance. In the following, the product is called liquid product.
- Nitrogen and sulphur content in the liquid product is assumed to be negligibly low. The liquid product only contains carbon, hydrogen and oxygen. The oxygen content results from the evaluated sum of the other elements.
- Hydrogen content in the catalyst was not taken into account.

For the evaluation of the initial carbon mass (6-29), which is the basis of the depolymerisation carbon transfer, the lignin mass m_{lignin} is multiplied by the lignin carbon content $\mu_{\text{C,lignin}}$. Furthermore, the evaluation of the composition of the liquid product, the lignin-based initial hydrogen mass (6-30) was investigated in the same way.

$$m_{\text{C,lignin}} = m_{\text{lignin}} \cdot \mu_{\text{C,lignin}} \quad (6-29)$$

$$m_{\text{H,lignin}} = m_{\text{lignin}} \cdot \mu_{\text{H,lignin}} \quad (6-30)$$

The carbon, hydrogen and nitrogen content of the solid and gaseous residue were analysed. Multiplied by the evaluated quantities, establishing the carbon and hydrogen mass in solid and gaseous residue is possible.

$$m_{\text{C,solid}} = m_{\text{solid}} \cdot \mu_{\text{C,solid}} \quad (6-31)$$

$$m_{\text{C,gas}} = m_{\text{gas}} \cdot \mu_{\text{C,gas}} \quad (6-32)$$

$$m_{\text{H,solid}} = m_{\text{solid}} \cdot \mu_{\text{H,solid}} \quad (6-33)$$

$$m_{\text{H,gas}} = m_{\text{gas}} \cdot \mu_{\text{H,gas}} \quad (6-34)$$

The carbon mass (6-35) and therewith the carbon content in the liquid product (6-36) can be determined with the initial carbon mass and the carbon mass in solid and gaseous residue resulting from (6-31) and (6-32).

$$m_{\text{C,liquid}} = m_{\text{C,lignin}} - (m_{\text{C,solid}} + m_{\text{C,gas}}) \quad (6-35)$$

$$\mu_{C,liquid} = \frac{m_{C,liquid}}{m_{liquid}} \quad (6-36)$$

The carbon transfer degree (6-37) is now evaluable with the carbon mass in the liquid product and the initial carbon mass.

$$W_{C,dpm} = \frac{m_{C,liquid}}{m_{C,lignin}} \quad (6-37)$$

Furthermore, for the liquid product chemical composition, a tetralin-specific carbon balance to obtain the hydrogen content in the liquid product is necessary because tetralin donates hydrogen during the process. The chemical composition of the liquid carrier after the reaction with lignin is presented in Table 6-14. Tetralin, naphthalene and degradation product carbon and hydrogen contents are listed in Table 6-15. Their molecule structure is shown in Table 4-1 and Table 4-3. The component balance (6-47) is defined as follows, where $m_{carrier,out}$ is the mass of the degraded carrier and $m_{H_2,dpm}$ is the transferred hydrogen from the carrier into the liquid product.

$$m_{tetralin} = m_{carrier,out} + m_{H_2,dpm} \quad (6-38)$$

The carrier outcome mass is calculated via a carbon balance (6-39) focusing on the tetralin input and the tetralin output with the assumption that the carbon content of the carrier is constant during the reaction. This means that no carbon from the tetralin carrier is transferred into the liquid product. The carbon content of the transferred hydrogen is zero.

$$m_{C,tetralin} = m_{C,carrier,out} = m_{tetralin} \cdot \mu_{C,tetralin} \quad (6-39)$$

The linkage of the carrier output mass and the individual components can be described by using the known chemical and elemental composition ((6-40) - (6-46)). The residual tetralin $m_{C,tetralin,out}$, the naphthalene $m_{C,naphthalene,out}$ and the degraded product carbon mass $m_{C,DM,out}$ can be calculated by multiplication with the individual carbon contents.

$$m_{carrier,out} = m_{tetralin,out} + m_{naphthalene,out} + m_{DM,out} \quad (6-40)$$

$$m_{C,carrier,out} = m_{C,tetralin,out} + m_{C,naphthalene,out} + m_{C,DM,out} \quad (6-41)$$

$$m_{C,tetralin,out} = m_{carrier,out} \cdot w_{tetralin,out} \cdot \mu_{C,tetralin} \quad (6-42)$$

$$m_{C,naphthalene,out} = m_{carrier,out} \cdot w_{naphthalene,out} \cdot \mu_{C,naphthalene} \quad (6-43)$$

$$m_{C,DM,out} = m_{carrier,out} \cdot w_{DM,out} \cdot \mu_{C,DM} \quad (6-44)$$

$$m_{C,carrier,out} = m_{carrier,out} \cdot \left(w_{tetralin} \cdot \mu_{C,tetralin} + w_{naphthalene} \cdot \mu_{C,naphthalene} + w_{DM} \cdot \mu_{C,DM} \right)_{out} \quad (6-45)$$

$$m_{carrier,out} = m_{tetralin} - m_{H_2,dpm} \quad (6-46)$$

The combination of (6-45) with (6-46) leads to the result of the transferred hydrogen from the carrier into the product during the depolymerisation (6-47). By backwards calculation, the carrier output mass (6-46) is evaluated.

$$m_{H_2,dpm} = m_{tetralin} \cdot \left(1 - \frac{\mu_{C,tetralin}}{w_{tetralin,out} \cdot \mu_{C,tetralin} + w_{naphthalene,out} \cdot \mu_{C,naphthalene} + w_{DM,out} \cdot \mu_{C,DM}} \right) \quad (6-47)$$

The hydrogen input mass consists of the hydrogen of the tetralin, the lignin and the hydrogen gas stream. The calculation of the individual fractions and the whole hydrogen input is shown in (6-30) and (6-48) - (6-50).

$$m_{H,tetralin} = m_{tetralin} \cdot \mu_{H,tetralin} \quad (6-48)$$

$$m_{H,H_2} = m_{H_2} \quad (6-49)$$

$$\sum m_{H,in} = m_{H,tetralin} + m_{H,lignin} + m_{H_2} \quad (6-50)$$

The hydrogen output mass consists of the hydrogen of the carrier (6-47), the solid (6-33) and the gaseous (6-34) residue as well as the hydrogen in the liquid product. All other variables, besides the hydrogen content in the liquid product, are known. The product hydrogen mass and content are evaluated ((6-51) - (6-54)).

$$\sum m_{H,out} = m_{H,carrier,out} + m_{H,solid} + m_{H,gas} + m_{H,liquid} \quad (6-51)$$

$$m_{H,carrier,out} = \sum m_{H,in} - m_{H_2,dpm} \quad (6-52)$$

$$m_{H,liquid} = \sum m_{H,in} - (m_{H,carrier,out} + m_{H,solid} + m_{H,gas}) \quad (6-53)$$

$$\mu_{H,liquid} = \frac{m_{H,liquid}}{m_{liquid}} \quad (6-54)$$

The nitrogen and sulphur contents in the product are expected to be marginal. It is assumed that the rest of the liquid product is oxygen (6-55).

$$\mu_{O,liquid} = 1 - (\mu_{C,liquid} + \mu_{H,liquid}) \quad (6-55)$$

The results of the calculation concerning the carbon transfer and chemical composition of the liquid product are shown in Table 6-9.

Table 6-17: Carbon conversion during the depolymerisation and liquid product elemental composition

item	acronym	value	unit
initial carbon mass	$m_{C,lignin}$	10.80	[g]
initial hydrogen mass	$m_{H,lignin}$	1.19	[g]
carbon mass in solid residue	$m_{C,solid}$	2.39	[g]
carbon mass in gaseous product	$m_{C,gas}$	1.26	[g]
hydrogen mass in solid residue	$m_{H,solid}$	0.21	[g]
hydrogen mass in gaseous product	$m_{H,gas}$	1.48	[g]
carbon mass in liquid product	$m_{C,liquid}$	7.15	[g]
carbon content in liquid product	$\mu_{C,liquid}$	0.7345	[-]
carbon transfer	$W_{C,dpm}$	0.662	[-]
initial tetralin mass	$m_{tetralin}$	97.67	[g]
initial tetralin carbon mass	$m_{C,tetralin}$	88.73	[g]
carrier output mass	$m_{carrier\ out}$	-88.00	[g]
hydrogen transfer	$m_{H2,dpm}$	0.4110	[g]
initial tetralin hydrogen mass	$m_{H,tetralin}$	8.95	[g]
hydrogen residue in carrier	$m_{H,carrier\ out}$	8.5433	[g]
hydrogen mass in liquid product	$m_{H,liquid}$	1.24	[g]
hydrogen content in liquid product	$\mu_{H,liquid}$	0.1279	[-]
oxygen content in liquid product	$\mu_{O,liquid}$	0.1376	[-]

6.4 Rehydrogenation balances

The BtL research group at CEET developed a process during their research concerning biomass liquefaction in which naphthalene can be rehydrogenated to tetralin [35]–[37]. The focus was on three different process possibilities:

- in-situ process
 - separation of carrier from the liquid product
 - mixing with catalyst for the rehydrogenation
 - re-slurry with the starting product
- ex-situ process
 - separation of carrier from the liquid product
 - rehydrogenation in a separate reactor
 - re-slurry after the rehydrogenation with the starting product
- laissez-faire process
 - a fraction of the whole product is recycled without separation of the carrier

For the ex-situ rehydrogenation process a reaction kinetic was developed. Therefore, pure naphthalene was hydrated in a separate reactor at different temperatures and pressures and with varying catalyst amounts [11], [48]. A Ni-based catalyst was used. For the experiment the naphthalene was diluted with methyl-cyclohexane. Subsequently, the reaction system consisted of tetralin, naphthalene, decalin and hydrogen. Based on the experiment the process conditions were chosen. Table 6-18 shows the process conditions.

Table 6-18: Rehydrogenation process conditions

item	acronym	value	unit
temperature	T_{RH}	200	[°C]
pressure	p_{RH}	20	[bar]
catalyst amount	$w_{cat,RH}$	0.05	[-]

The reaction of naphthalene into its products is shown in Figure 6-13.

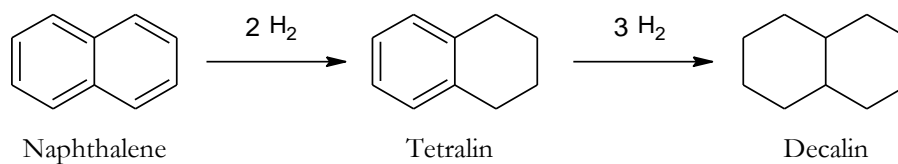


Figure 6-13: Reaction pathway of naphthalene with hydrogen

Under these conditions, the rehydrogenation reaction behaviour was observed (Figure 6-14).

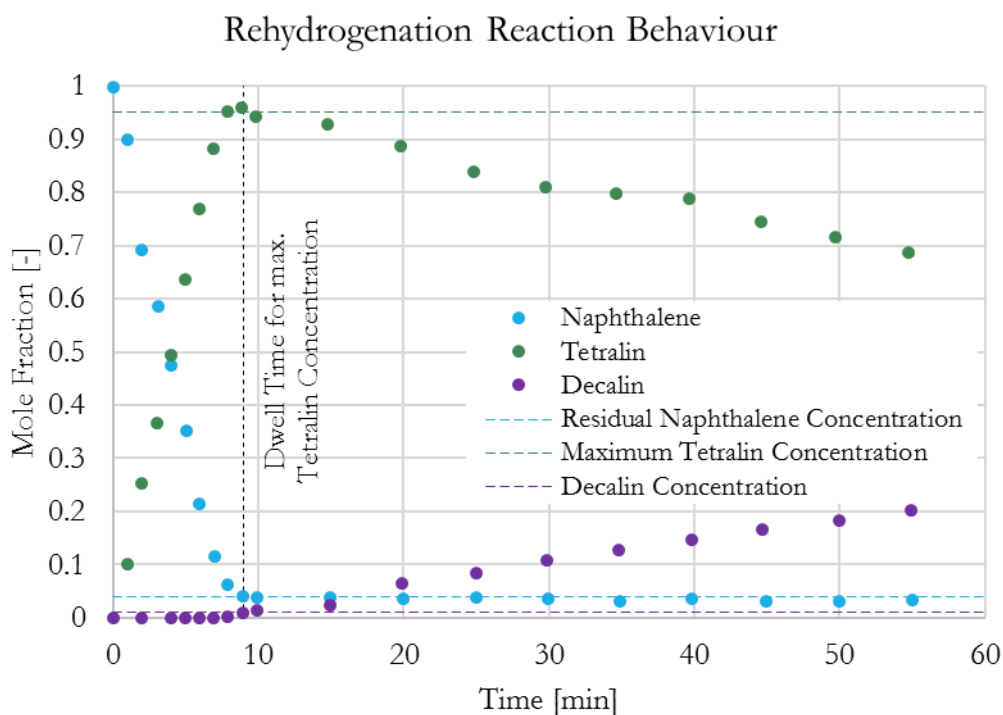


Figure 6-14: Rehydrogenation reaction behaviour – mole fraction versus time

The maximum tetralin concentration is achieved after a dwell time of nine minutes. The higher the dwell time in the depolymerisation reactor, the higher the dwell time in the rehydrogenation reactor that is necessary. Table 6-19 shows the concentrations after nine minutes of dwell time. *Cis*- and *trans*-decalin were not distinguished in these investigations.

Table 6-19: Mole fractions of components at dwell time for maximum tetralin concentration downstream rehydrogenation

item	acronym	value	unit
retention time	τ	9	[min]
tetralin concentration	$y_{\text{tetralin,us}}$	0.95	[-]
naphthalene concentration	$y_{\text{naphthalene,us}}$	0.04	[-]

decalin concentration	$y_{\text{decalin,us}}$	0.01	[-]
-----------------------	-------------------------	------	-----

The mass fraction equivalent graph can be calculated via the molecular weight of the components. The mass fractions are the basis of the rehydrogenation balance. Mass fraction over time is shown in Figure 6-15.

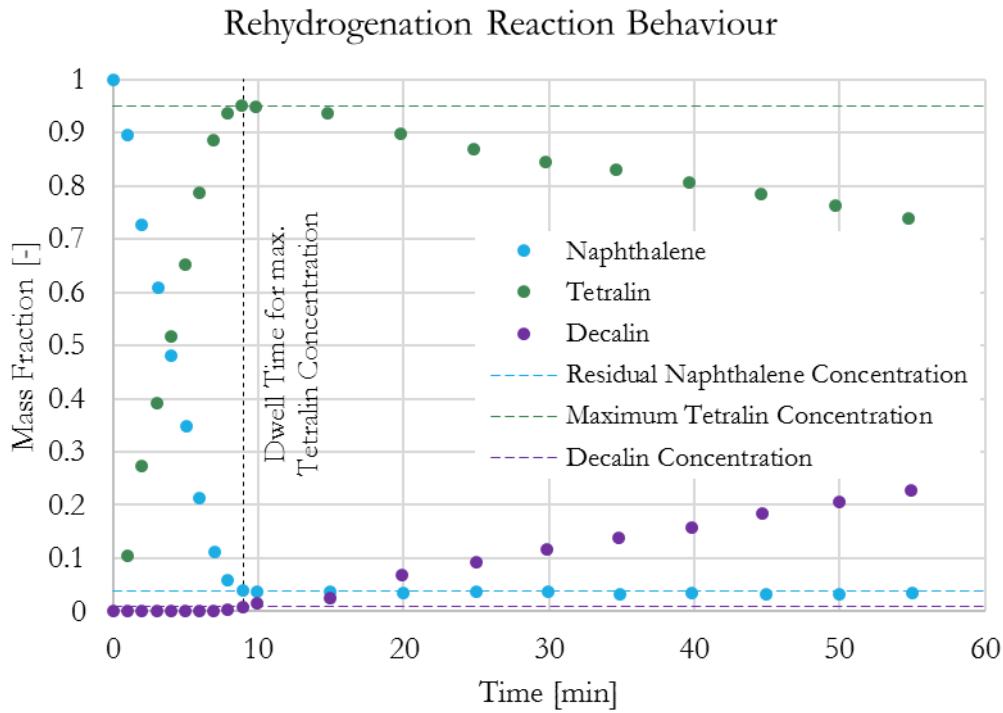


Figure 6-15: Rehydrogenation reaction behaviour - mass fraction versus time

The converted mass fractions at the dwell time of maximum tetralin concentration are shown in Table 6-20.

Table 6-20: Mass fractions of components at dwell time for maximum tetralin concentration downstream rehydrogenation

item	acronym	value	unit
retention time	τ	9	[min]
tetralin concentration	$w_{\text{tetralin,us}}$	0.951	[-]
naphthalene concentration	$w_{\text{naphthalene,us}}$	0.039	[-]
decalin concentration	$w_{\text{decalin,us}}$	0.01	[-]

The rehydrogenation balance is divided into three loops to present representative scenarios. In a first iteration, the maximum tetralin concentration should be reached after the rehydrogenation.

Therefore, the same carrier composition as in chapter 6.3.4 is assumed. In a second loop, the decalin should be decreased to zero with a constant dwell time. This also leads to a decrease of the tetralin yield. In a third scenario, the tetralin start concentration (concentration after depolymerisation reactor) can be reduced down to 40%. Therefore, the dwell time in the depolymerisation reactor should be increased. This leads to a higher tetralin conversion, but may lead to a higher product yield too.

The balance boundaries exclude the distillation column(s) which are treated separately. It is assumed that low boiling products are fully separated from the carrier. Higher boiling components are treated as inert components. The balance boundaries and the stream description are shown in Figure 6-16.

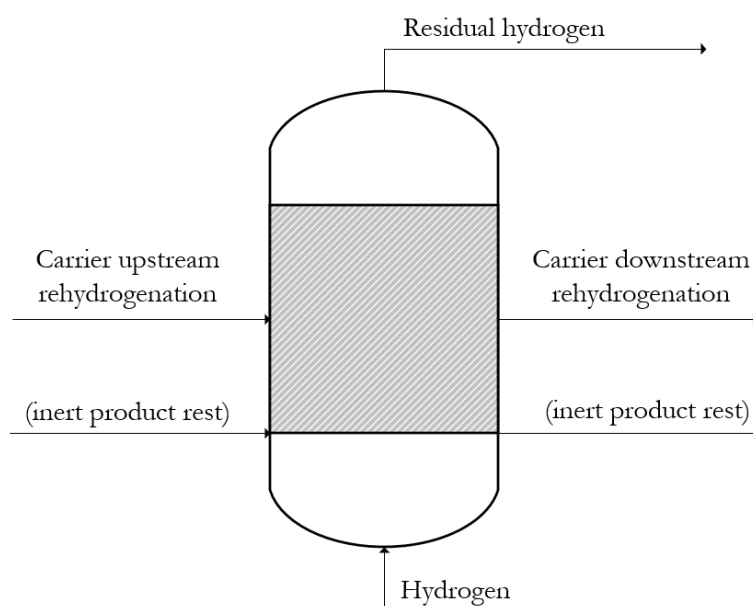


Figure 6-16: Rehydrogenation balance boundaries

The composition of the carrier upstream and downstream the reactor is presented in Figure 6-14, Figure 6-15, Figure 6-17, Figure 6-18 and Figure 6-19.

The basis of the calculation are the following assumptions:

- The whole product is separable from the carrier stream.
- The product which stays in the carrier is treated as inert in the rehydrogenation process and is depolymerised when it is transferred to the depolymerisation reactor.
- No fresh carrier is included in the calculations.

6.4.1 Rehydrogenation with low dwell time and maximum tetralin concentration

Low dwell time leads to reduced reactor volumes with constant throughputs and resulting lower investment costs. The product yield and quality can probably be lower. The reaction behaviour of the rehydrogenation with a certain start concentration from chapter 6.3.4 Table 6-17 is depicted in Figure 6-17.

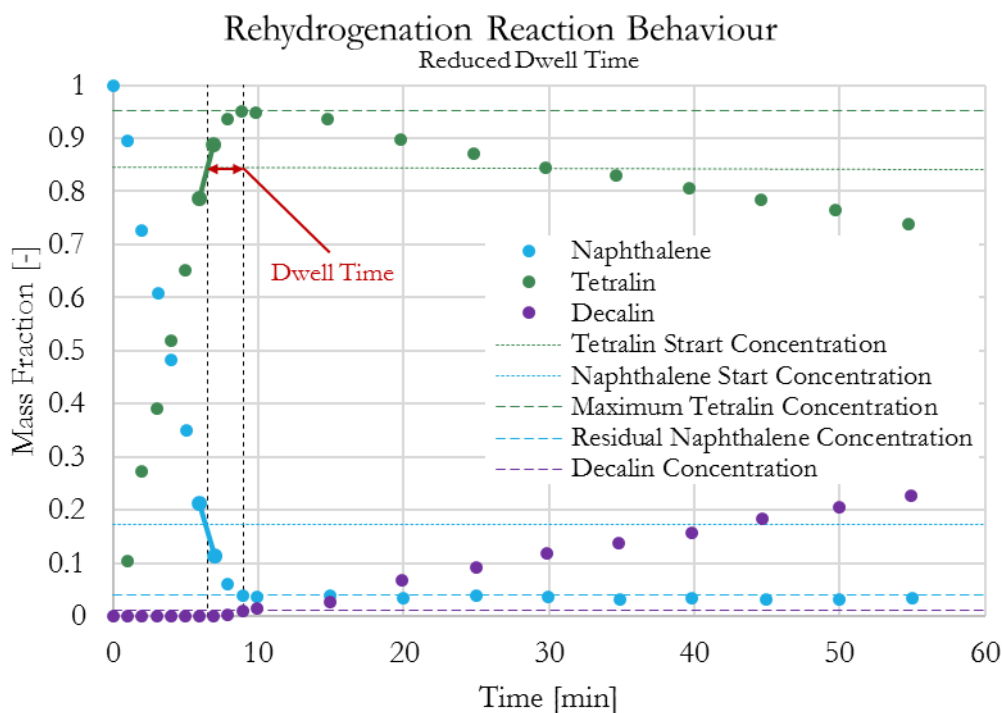


Figure 6-17: Rehydrogenation reaction behaviour - reduced dwell time

To rehydrogenate naphthalene to tetralin, the dwell time in the reactor can be reduced to 2.5 min. The main problem with operating with high upstream tetralin amounts and maximum tetralin downstream amount is the accruing decalin. Decalin is a stable molecule and cannot be used as hydrogen donor in the depolymerisation process. If decalin is not easily separable in the distillation step, the risk of accumulation of decalin in the process is given. A possibility to prevent decalin formation is described in chapter 6.4.2.

6.4.2 Rehydrogenation with low dwell time and decalin prevention

Tetralin is an intermediate product in reactions of naphthalene with hydrogen (Table 6-18). The thermodynamic equilibrium is on the decalin side in this case. A stoichiometric hydrogen amount

still leads to a high amount of decalin. The tetralin formation is predominant until a low naphthalene concentration is reached. Decalin formation begins when naphthalene amount decreases below 11% at the observed process conditions. If the reaction is terminated early enough, the decalin formation can be prevented.

The boundary assumptions for the decrease of decalin are listed below.

- Minimum naphthalene concentration to have no decalin formation.
- Same dwell time as in chapter 6.4.1.

The reaction behaviour is depicted in Figure 6-18.

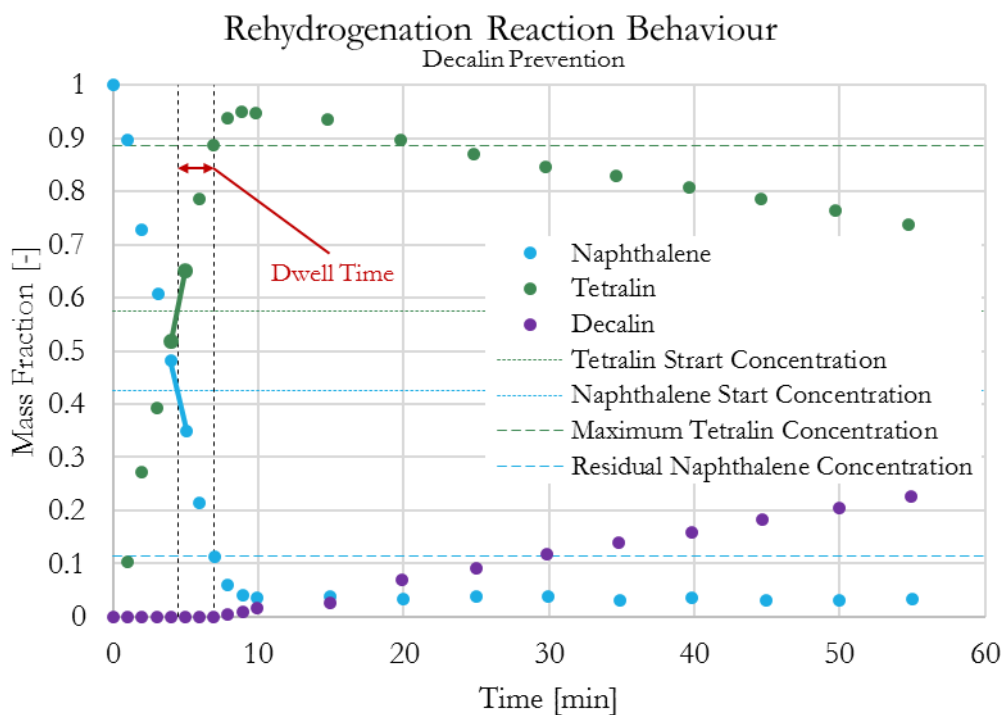


Figure 6-18: Rehydrogenation reaction behaviour - decalin prevention and low dwell time

This leads to the reduction of decalin without any change of the dwell time. Moreover, higher tetralin concentration downstream rehydrogenation reactor is possible with same flow rate. The needed hydrogen portion of the rehydrogenation is expected to be approximately constant too. The naphthalene and tetralin concentrations upstream and downstream the rehydrogenation reaction can be taken from Figure 6-18 at the calculated dwell time range. The upstream composition is evaluated by interpolation between the measured concentrations. Table 6-21 shows the results of this investigation.

Table 6-21: Mass fractions at low dwell time of maximum tetralin concentration without any decalin formation upstream and downstream rehydrogenation

item	acronym	value	unit
retention time range	$\Delta\tau$	2.5	[min]
upstream tetralin concentration	$w_{\text{tetralin,us}}$	0.575	[-]
upstream naphthalene concentration	$w_{\text{naphthalene,us}}$	0.425	[-]
upstream decalin concentration	$w_{\text{decalin,us}}$	0	[-]
downstream tetralin concentration	$w_{\text{tetralin,ds}}$	0.885	[-]
downstream naphthalene concentration	$w_{\text{naphthalene,ds}}$	0.115	[-]
downstream decalin concentration	$w_{\text{decalin,ds}}$	0	[-]

6.4.3 Rehydrogenation with high dwell time and decalin prevention

The depolymerisation product yield begins to decrease with tetralin contents in the carrier below 40%. This was determined in the experiments using the laissez-faire process method by Feiner [36]. Dwell time can be increased so that the relative tetralin yield reaches a maximum without increasing the decalin amount. This leads to a higher tetralin conversion and possibly to a higher product yield because of a higher possible dwell time in the depolymerisation reactor too. Drawbacks of a higher dwell time with a constant flow are higher equipment costs. Also, the process variability without having quality or yield losses is limited. If higher tetralin amounts occur, decalin will be generated. Lower tetralin amounts lead to lower product yields. However, it is assumed that this is the most advisable process strategy.

For the process evaluation, the boundary assumptions for the decrease of decalin are listed below.

- Minimum downstream naphthalene concentration to have no decalin formation.
- Minimum upstream tetralin concentration of 40%.

The reaction behaviour is depicted in Figure 6-19.

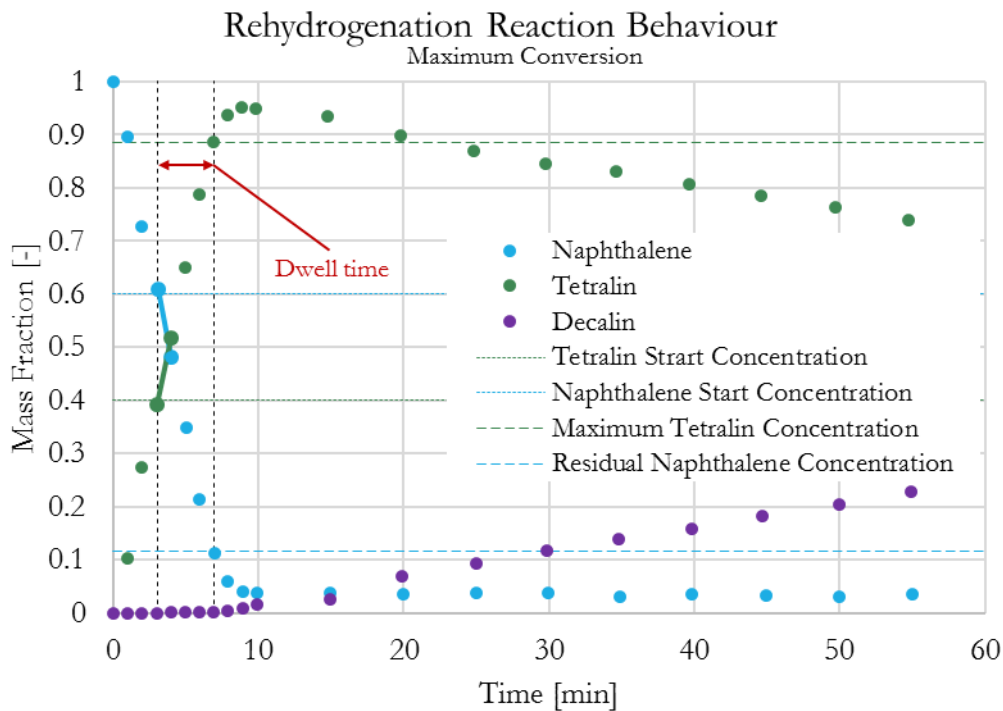


Figure 6-19: Rehydrogenation reaction behaviour - maximum tetralin conversion

Taking the limitations and assumptions into account, a dwell time of 3.9 min is needed for a maximum tetralin conversion without forming decalin as a by-product. The accuracy of the measurement is checked by interpolation between the measured concentrations. The naphthalene mass fraction is 60% in the analytic data too.

Results are shown in Table 6-22.

Table 6-22: Mass fractions at high dwell time range for maximum tetralin creation without decalin

item	acronym	value	unit
retention time range	$\Delta\tau$	3.9	[min]
upstream tetralin concentration	$w_{\text{tetralin,us}}$	0.4	[-]
upstream naphthalene concentration	$w_{\text{naphthalene,us}}$	0.6	[-]
upstream decalin concentration	$w_{\text{decalin,us}}$	0	[-]
downstream tetralin concentration	$w_{\text{tetralin,ds}}$	0.885	[-]
downstream naphthalene concentration	$w_{\text{naphthalene,ds}}$	0.115	[-]
downstream decalin concentration	$w_{\text{decalin,ds}}$	0	[-]

6.4.4 Rehydrogenation hydrogen consumption

By combining the results of the investigations in chapter 6.4.3 with the reaction itself (Figure 6-13), the hydrogen need is possible to estimate. The process strategy defined in chapter 6.4.3 was the basis of the hydrogen calculation. Concurrently, it is the case with the highest hydrogen consumption. The evaluation is based on the following assumptions:

- No degradation products during the rehydrogenation reaction. Hydrogen is only consumed for production of tetralin.
- Stoichiometric hydrogen requirements or total recycling of the stoichiometric excess hydrogen.

The reaction pathway is simplified as shown in Figure 6-20.

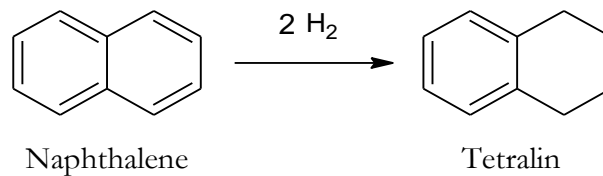


Figure 6-20: Simplified reaction equation

Two moles hydrogen are needed for a stoichiometric conversion of naphthalene to tetralin. By using the molecular weight of naphthalene and hydrogen (Table 4-2), the evaluation of the hydrogen consumption is feasible ((6-56), (6-57)).

$$m_{\text{H}_2} = \frac{n_{\text{H}_2}}{n_{\text{naphthalene}}} \cdot \frac{M_{\text{H}_2}}{M_{\text{naphthalene}}} \cdot m_{\text{naphthalene}} \quad (6-56)$$

$$W_{\text{H}_2, \text{RH}, E} = \frac{m_{\text{H}_2}}{m_{\text{naphthalene}}} = \frac{n_{\text{H}_2}}{n_{\text{naphthalene}}} \cdot \frac{M_{\text{H}_2}}{M_{\text{naphthalene}}} = 2 \cdot \frac{M_{\text{H}_2}}{M_{\text{naphthalene}}} \quad (6-57)$$

The same way of product-specific determination is possible ((6-58), (6-59)).

$$m_{\text{H}_2} = \frac{n_{\text{H}_2}}{n_{\text{tetralin}}} \cdot \frac{M_{\text{H}_2}}{M_{\text{tetralin}}} \cdot m_{\text{tetralin}} \quad (6-58)$$

$$W_{\text{H}_2, \text{RH}, P} = \frac{m_{\text{H}_2}}{m_{\text{tetralin}}} = \frac{n_{\text{H}_2}}{n_{\text{tetralin}}} \cdot \frac{M_{\text{H}_2}}{M_{\text{tetralin}}} = 2 \cdot \frac{M_{\text{H}_2}}{M_{\text{tetralin}}} \quad (6-59)$$

The results of the hydrogen requirement are shown in Table 6-23.

Table 6-23: Mass fractions at high dwell time range for maximum tetralin creation without decalin

item	acronym	value	unit
hydrogen need (educt-specific)	$W_{H_2,RH,E}$	0.0315	[-]
hydrogen need (product-specific)	$W_{H_2,RH,P}$	0.0306	[-]

6.5 Key figures

The key figures are summarized in this chapter.

6.5.1 Liquid product theoretical composition

It is possible to summarise the elemental composition of the theoretical oil to a model molecule. Based on the mass balance in chapter 6.3.4, a theoretical elemental composition was calculated. The mole fractions are shown in Table 6-24.

Table 6-24: Elemental distribution in the liquid product - mole fraction

item	acronym	value	unit
carbon mole fraction	$y_{C,liquid}$	0.31	[-]
hydrogen mole fraction	$y_{H,liquid}$	0.64	[-]
oxygen mole fraction	$y_{O,liquid}$	0.04	[-]

This leads to a molecule in the form of $C_xH_{2.07x}O_{0.14x}$.

6.5.2 Van Krevelen plot

A representative way to compare other biofuels with the depolymerisation product is the Van Krevelen Plot. A comparison of various fuels is shown in Figure 6-21.

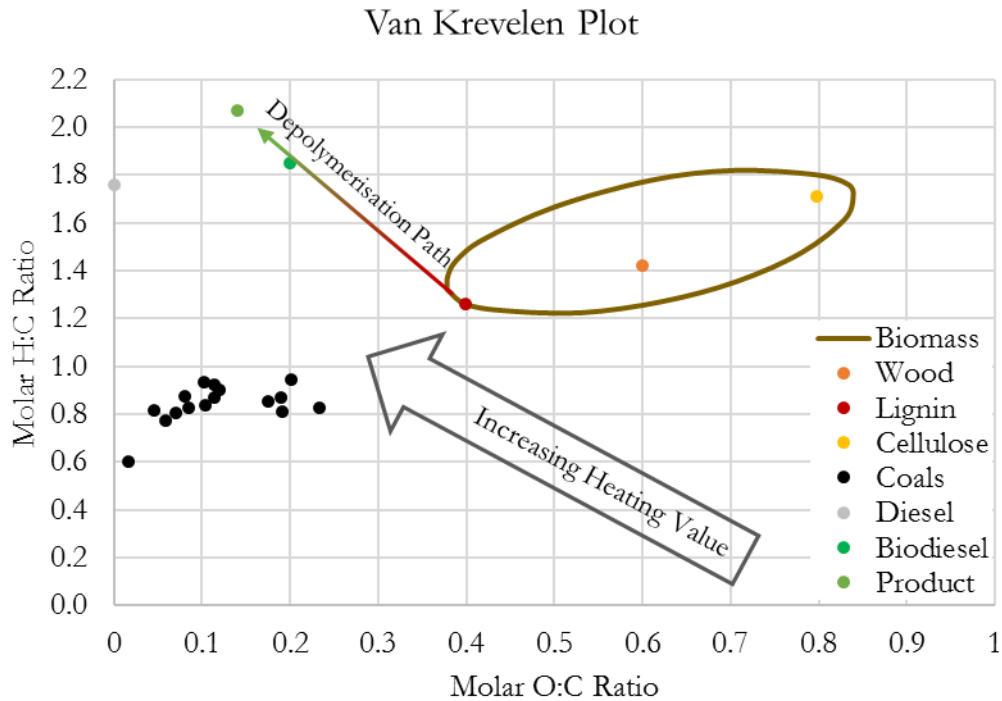


Figure 6-21: Van Krevelen plot

6.5.3 Heating value of the liquid product

The heat value can be estimated with empirical equations for substances with unknown molecular compositions on the basis of the elemental composition. One of these approaches was designed by Boie [49]. The equation to estimate the upper and the lower heating value contains the mass fractions of the individual elements and fixed factors as follows.

$$HV_{Boie} = w_C \cdot h_C + w_H \cdot h_H + w_N \cdot h_N + w_S \cdot h_S + w_O \cdot h_O \quad (6-60)$$

The specific factors h_i for each particular element, for the upper heating value (HHV) and for the lower heat value (LHV), are shown in Table 6-25.

Table 6-25: Specific factors for the heat value estimation

item	acronym	HHV	LHV	unit
carbon multiplication factor	h_C	35.16	35.16	[MJ]/kg
hydrogen multiplication factor	h_H	116.225	94.438	[MJ]/kg
nitrogen multiplication factor	h_N	6.28	6.28	[MJ]/kg
sulphur multiplication factor	h_S	10.465	10.465	[MJ]/kg
oxygen multiplication factor	h_O	-11.09	-11.09	[MJ]/kg

Including the element mass fractions evaluated in chapter 6.3.4 and shown in Table 6-17, the upper and the lower heating value can be estimated. Table 6-26 shows the heat values of the liquid product.

Table 6-26: Upper and lower heat value of liquid product

item	acronym	value	unit
upper heating value (Boie)	HHV	39.17	[MJ]/kg
lower heating value (Boie)	HLV	36.38	[MJ]/kg

The heat value of the liquid product is similar to that of biodiesel [50].

7 Modelling

With the mass balance and the carbon transfer calculation as well as with literature data as basis, a combined simulation model can be designed. The model should serve as a basic calculation tool for estimations. Furthermore, it should be expandable for more complex systems like controlled continuous simulation. For easier handling and better reproducibility, a GUI (graphical user interface) should be implemented.

Different tools to create simulation models were considered. Two of the used tools (subsequently SP1 and SP2) have the advantage of a large implemented component database. On the basis of this database pure component data and binary interaction parameters of the almost “simple” components were evaluated. The decisive disadvantage is that there is no possibility to handle the large molecules with a mostly unknown structure. Merely pseudo-components could be generated, but there is no possibility to validate the model without at least a second calculation way or experiments. The advantage of common software like MS Excel VBA and Matlab is the individuality and easy handling. The main drawback of MS Excel VBA is the low data capacity. In the basic modelling, no problems would arise but with further extensions the amount of data could greatly increase.

For the setup of the model, the answer was to combine various different methods. Binary data and component interaction data come from the database. Also, particular process steps - like the distillation after the depolymerisation - can be simulated. The main calculation is done using Matlab. The verification is carried out with MS Excel.

7.1 Basic process flowsheet

Figure 7-1 shows the principle process flowsheet. The streams and blocks are listed in Table 7-1, Table 7-2 and Table 7-3.

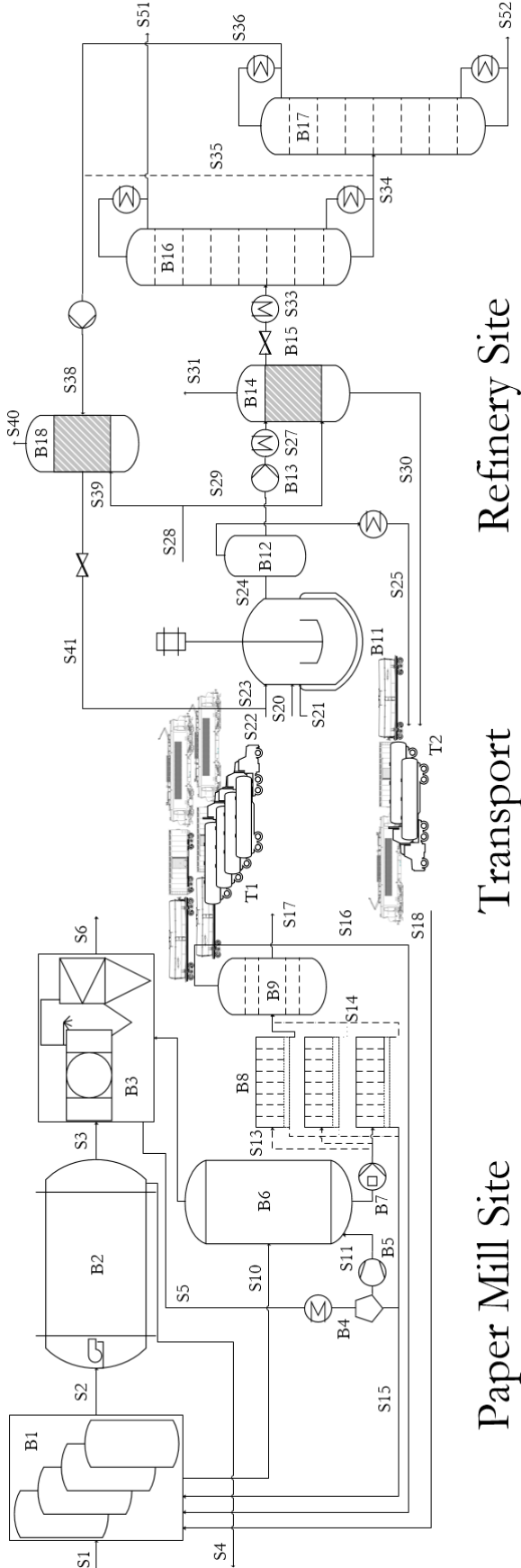


Figure 7-1: Principle process scheme

Table 7-1: Stream table

Acronym	Description	Calculation
S1	Weak Black Liquor	
S2	Thick Liquor	
S3	Raw Exhaust Gas	
S4	Inorganics for Liquor Recycling	
S5	Pretreated Exhaust Gas	
S6	Clean Exhaust Gas	
S10	Treated Black Liquor for Precipitation	BL
S11	Precipitant Stream	H ₂ SO ₄ , CO ₂
S12	Exhaust Gas after Precipitation	
S13	pH-reduced Black Liquor Dispersion	
S14	Filter Cake	C
S15	Filtrate	F
S16	Residual Moisture	
S17	Product Cake for Refinery	
S18	Residue from Depolymerisation Process	
S19	free	
S20	Product Cake from Paper Mill	lignin
S21	Catalyst	
S22	Fresh Carrier	tetralin
S23	Initial Carrier	ds+tetralin, ds
S24	Educt Suspension	
S25	Dewatering Product	
S26	free	
S27	Initial Suspension for Depolymerisation	
S28	Hydrogen Supply	
S29	Hydrogen Supply for Depolymerisation	H ₂
S30	Solid Depolymerisation Residue	solid,out
S31	Gaseous Depolymerisation Residue	gas,out
S32	free	
S33	Depolymerisation Product	dpm
S34	Carrier and Bottoms	
S35	Carrier and Bottoms (alt.: w/o separation)	
S36	Isolated Carrier	
S37	free	
S38	Carrier Upstream Rehydrogenation	us
S39	Hydrogen Supply for Rehydrogenation	H ₂
S40	Gaseous Rehydrogenation Residue	
S41	Recycled Carrier Downstream Rehydrogenation	ds
S42	Fresh Carrier	
S51	Overheads	
S52	Bottoms	

Table 7-2: Block table

Acronym	Description
B1	Black Liquor Pretreatment (Evaporators)
B2	Recovery Boiler
B3	Exhaust Aftertreatment
B4	Condenser and Water Separator
B5	Exhaust Compressor
B6	Bubble Column
B7	Displacement Pump
B8	Parallel Chamber Filter Presses
B9	Product Treatment
B10	free
B11	Dispersion Vessel
B12	Dewatering Column
B13	Pressure Stage and Preheater
B14	Depolymerisation Reactor
B15	Throttle and Heat Exchanger
B16	Distillation Column #1
B17	Distillation Column #2
B18	Rehydrogenation Reactor

Table 7-3: Transport table

Acronym	Description
T1	Transport from Paper Mill to Refinery
T2	Transport from Refinery to Paper Mill

B1 schematically shows the black liquor pretreatment. S1 is the weak black liquor from the cooking process. Depending on the required dry matter content for further processing, concentrated black liquor is taken after a defined evaporation step. S10 is the pretreated feed stream for the precipitation. It is comparable with the BL feed in chapter 6.1. S2 is the rest of the concentrated black liquor. It is burnt in B3 - the recovery boiler. S4 is the recycling stream which is led back into the causticizing cycle. S5 describes the exhaust gas flow which is led to the precipitation. Alternatively, S3 can be led into the precipitation reactor without exhaust aftertreatment (B3). This has to be investigated experimentally. S6 represents the cleaned exhaust gas emission. After cooling, condensation and dewatering (B4) the exhaust stream S11 is induced into the precipitation reactor B6 via compressor B5. The process conditions are described in Table 6-1. S11 is high in CO₂, which serves as precipitant in the reactor. The residual exhaust gas is led back into the exhaust aftertreatment B3. Sulphur compounds in the exhaust gas due to the precipitation reaction are conceivable. After

the reaction, the black liquor feed is present as suspension. Suspension S13 is led to the filtration plant B8 via displacement pump B7. Different filtration methods are possible. High throughputs, continuous operation and low vulnerability against blockage are required. Therefore, chamber filter press batteries (quasi-continuous), vacuum drum filters or other self-cleaning filter concepts can be used. The most efficient filtration concept has to be investigated. In Figure 7-1 a chamber filter press battery is suggested. S14 represents the product stream viz., the filter cake. S15 is the filtrate stream which is led back to the evaporation step. B9 shows a possibly need for aftertreatment of the product, for example a further dewatering. Depending on the product quality and the requisite moisture for transport, the product can be treated, for example with a kiln. S16 is the residual water stream which is also led back to the evaporators. S17 shows the product of the precipitation.

S20 is equal to the product S17 of the precipitation and the feed to the depolymerisation unit. The carrier S23 (sum of fresh carrier S22 and recycle stream S41), the precipitation product S20 and the catalyst are dispersed in the dispersion vessel B11. Stream S24 shows the suspension. In a flash B12 residual water might be eliminated if present. It can be transferred back to the paper mill for recycling purposes (S25). The suspension is led via a pump and over a preheater (together B13) into the depolymerisation reactor B14. The process conditions are listed in Table 6-10. S28 is the main hydrogen supply. S29 is the hydrogen supply for the depolymerisation reaction. S29 is also led into the depolymerisation reactor. The solid residue S30, which contains the inorganics, is removed and led back to the paper mill. The gaseous residue S31 which contains almost only hydrogen can possibly be recycled and reused in the depolymerisation and rehydrogenation process. The liquid stream containing the converted carrier and the liquid product must be expanded and cooled for further processing. S33 is the feed for the carrier distillation. In a first distillation column B16 the product overheads S51 are separated. S51 represents one of the main product streams. For further processing, two possible pathways are plausible. One option is to lead the carrier stream with heavy product components S34 into a further distillation B17. The bottoms S52 are separable as the second main product. The advantage of a second distillation is to prevent possible accumulation in the process. The costs would be the main drawback. In this case, an almost pure carrier S36 is led to the rehydrogenation B18. The other option is to lead the carrier with the heavy product components directly back into the rehydrogenation step (S35). It has to be investigated if the heavy product components break down further. Also, it is assumed that a mixture of S35 and S36 is possible to relieve the second distillation. This depends on the carrier quality requirement for the

rehydrogenation. S38 represents the feed of the rehydrogenation reaction in reactor B18. The process conditions are shown in Table 6-18. Due to operated calculations it is comparable with S36, which means the almost pure carrier. S39 is the hydrogen supply. S40 represents the residual gas, which contains almost exclusively only hydrogen. It is assumed that recycling is feasible. The rehydrogenation product S41 is expanded to ambient pressure and is mixed with S22.

T1 and T2 describe the transport between paper mill and refinery site. The accruing precipitation product is transported to the refinery (T1). The solid residue (mostly inorganics) and the residual water are transferred back to the paper mill (T2).

7.2 Precipitation simulation model

A simple simulation model to evaluate the effectivity of the precipitation was created. Matlab Simulink was used as the software package. It can be used for estimations and as basis of advanced simulations. Mathematic models from literature were implemented [43]–[46]. Basis model parameters and equations from literature were used for the setup of the model and for comparison reasons. Verification was performed via an auxiliary calculation in MS Excel.

A GUI was created for better use and documentation as shown in Figure 7-2. Box 1 shows the calculation method. Switching between stationary and transient simulation is possible. Transient calculation was not implemented because it is not of major importance for preliminary estimations. In Panel 2, the stream data for stationary processes can be defined. In the mathematic models used, a specification of black liquor mass flow, initial pH and temperature and an acidification set point is necessary. It is expandable with further black liquor data as for example alkali data or molecular weight distribution. Label 3 provides input data for transient processing. It is disabled for stationary processing. The model and stream parameter set can be adjusted in Box 4. The basis of verification and first simulation results was the “Zhu parameter set” according to literature [43]–[46]. Panel 5 is relevant for the process control. An initialisation with default parameter set stored in workspace is possible by clicking on the “Initialisation” button. Model and parameter database can be read in by using the push-button. Also, it is possible to reset or to clear the input with the push-button. Panel 6 shows a parameter override.

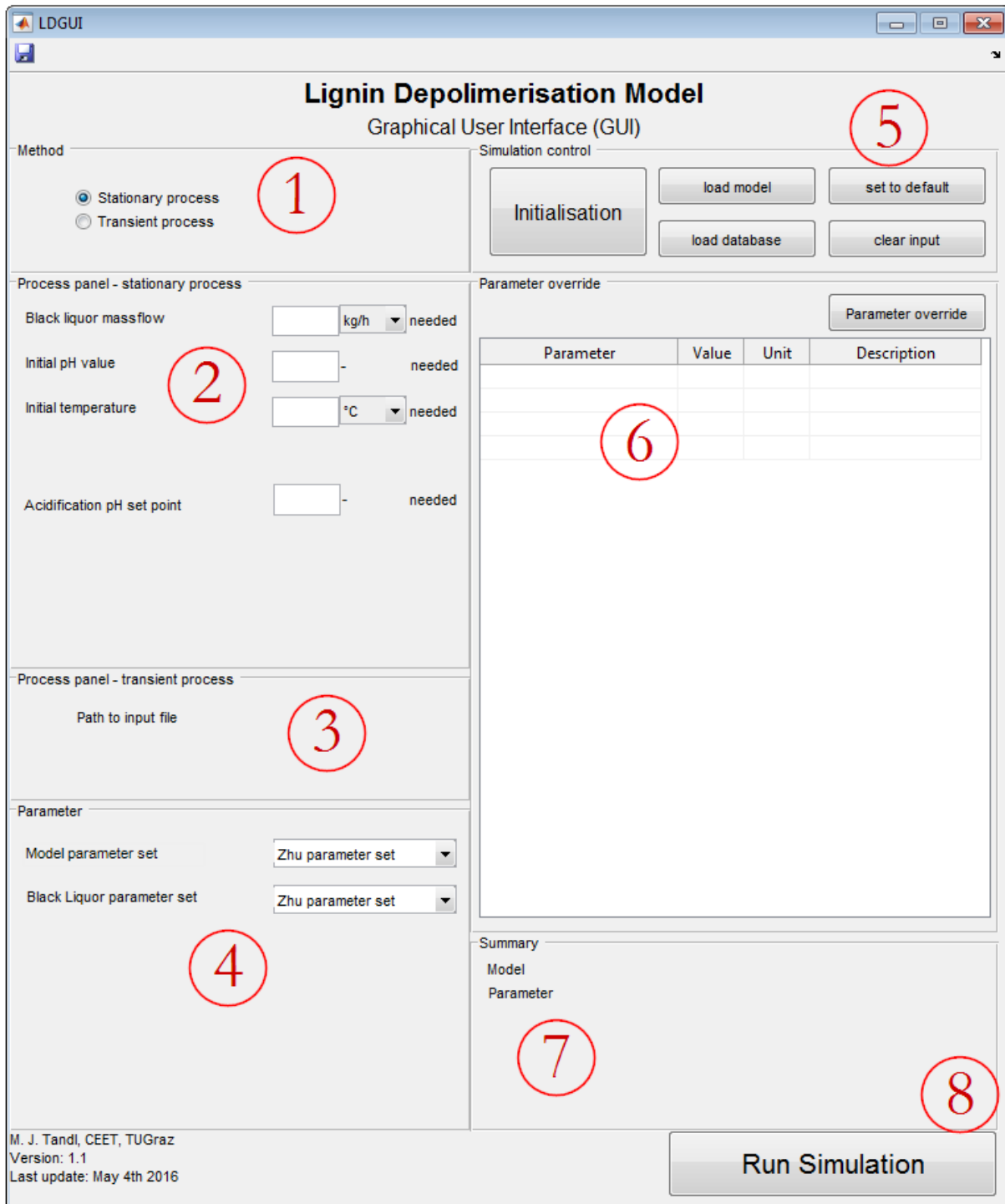


Figure 7-2: Precipitation simulation model – GUI

Table function does not work in older Matlab versions. Parameter number is low in these versions. Consequently, the parameter override is not implemented yet. Label 7 gives an overview of the defined settings, if model and parameter set is loaded. If the setup of the simulation is done and all necessary inputs are available, the simulation can be started by clicking Button 8, “Run Simulation”.

When starting the simulation, Matlab checks completeness of input. If no error messages pop up the program opens the model. The simulation model is shown in Figure 7-3.

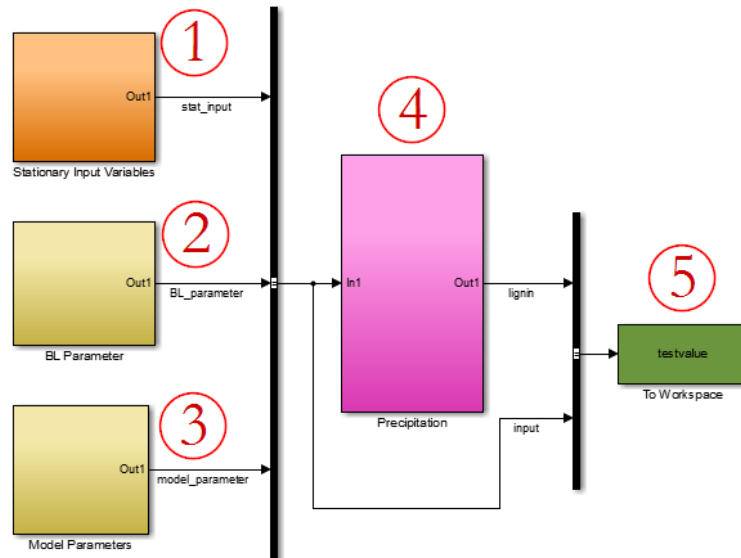


Figure 7-3: Precipitation simulation model

In Block 1 the stream data is read in and multiplied with unit factors which can be defined in the GUI. Block 2 contains the database and, later, the parameter override. In Block 3 the model parameter sets are implemented. Manual switching is possible. Core structure of the model reside in Block 4. Currently, a simple mathematic model is implemented. Control units and model improvements can be integrated. Block 5 represents the output to workspace. A file can also be generated directly.

The fairly simple structure of the model's inner workings is depicted in Figure 7-4, where 1 shows the stream data input and conversion, 2 - the manual switches of the model parameter sets and 3 - a part of the mathematic model.

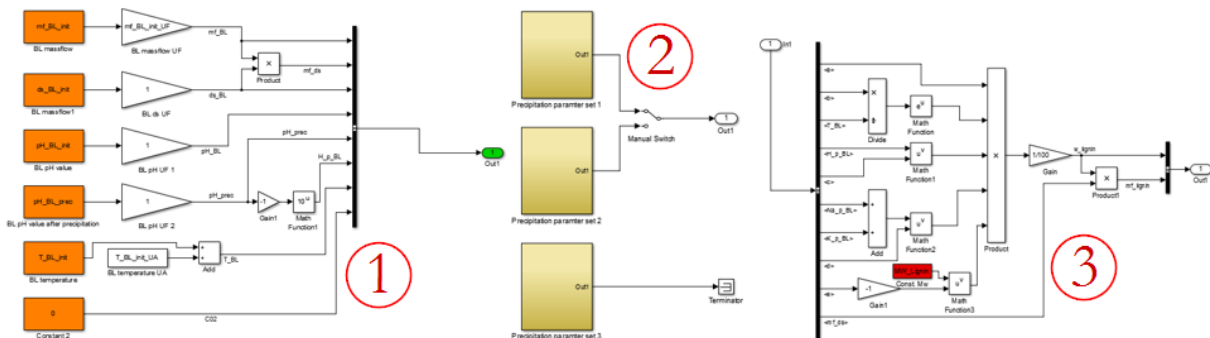


Figure 7-4: Precipitation simulation model - inner workings

7.3 Distillation of carrier

Before the carrier is rehydrogenated, the product has to be isolated from the depolymerisation product stream. Mandatorily, the overheads have to be separated. It is assumed that parts of the heavy components break down further when they are recycled with the carrier. The separation efficiency is evaluated by simulation. Therefore, a stream has to be specified. In Table 6-23, the carrier composition is shown. The carrier to product ratio after the depolymerisation (7-1), as well as the mass fractions ((7-2), (7-3)) are evaluable using the liquefaction degree, the hydrogen requirement, the initial lignin mass and the initial carrier mass.

$$R_{dist} = \frac{m_{tetralin} - m_{H_2,dpm}}{m_{lignin} \cdot W_l} \quad (7-1)$$

$$w_{carrier,dist} = \frac{m_{tetralin} - m_{H_2,dpm}}{(m_{tetralin} - m_{H_2,dpm} + m_{lignin} \cdot W_l)} \quad (7-2)$$

$$w_{product,dist} = \frac{m_{lignin} \cdot W_l}{(m_{tetralin} - m_{H_2,dpm} + m_{lignin} \cdot W_l)} \quad (7-3)$$

Additionally, a boiling point curve is important to define the stream. Therefore, an evaluated product boiling point curve of a pyrolysis coal liquefaction product was used because of the expected similar behaviour. A set of hypothetical components can be established with the knowledge of the input stream composition. Fine adjustment was done by setting hypothetical components manually. The summary of these hypothetical components is called hypothetical oil subsequently. The boiling point curve measurement and a comparison with the hypothetical oil are shown in Figure 7-5.

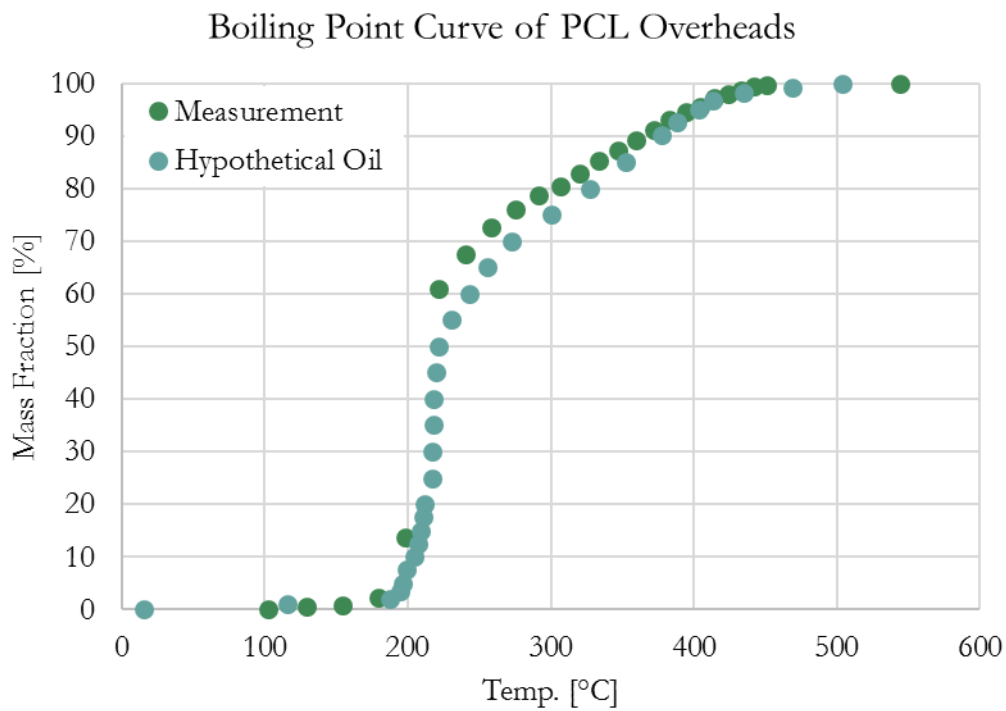


Figure 7-5: Boiling point curve of PCL overheads

Moreover, this set can be used for simulations with the evaluated composition downstream the depolymerisation reactor. In Table 7-4, the stream for the simulation of distillation is defined.

Table 7-4: Stream specification for distillation

item	acronym	value	unit
carrier to product ratio	R_{dist}	10	[-]
carrier mass fraction	$w_{\text{carrier,dist}}$	0.91	[-]
product mass fraction	$w_{\text{product,dist}}$	0.09	[-]
pressure	p_{dist}	20	[bar]
boiling point curve	defined		

8 Entire process evaluation

In this chapter, the calculation from chapter 6 and the simulations from chapter 7 are summarised. Sankey graphs are carried out for a better illustration of the processes involved.

8.1 Overall mass balance

The results of the partial mass balances can be combined to one overall mass balance. The result is the liquid product yield as a percentage of three different bases: the black liquor quantity, the black liquor dry matter and the organic content in the black liquor. Figure 8-1 shows a Sankey graph which represents the liquefaction degree of the three different references.

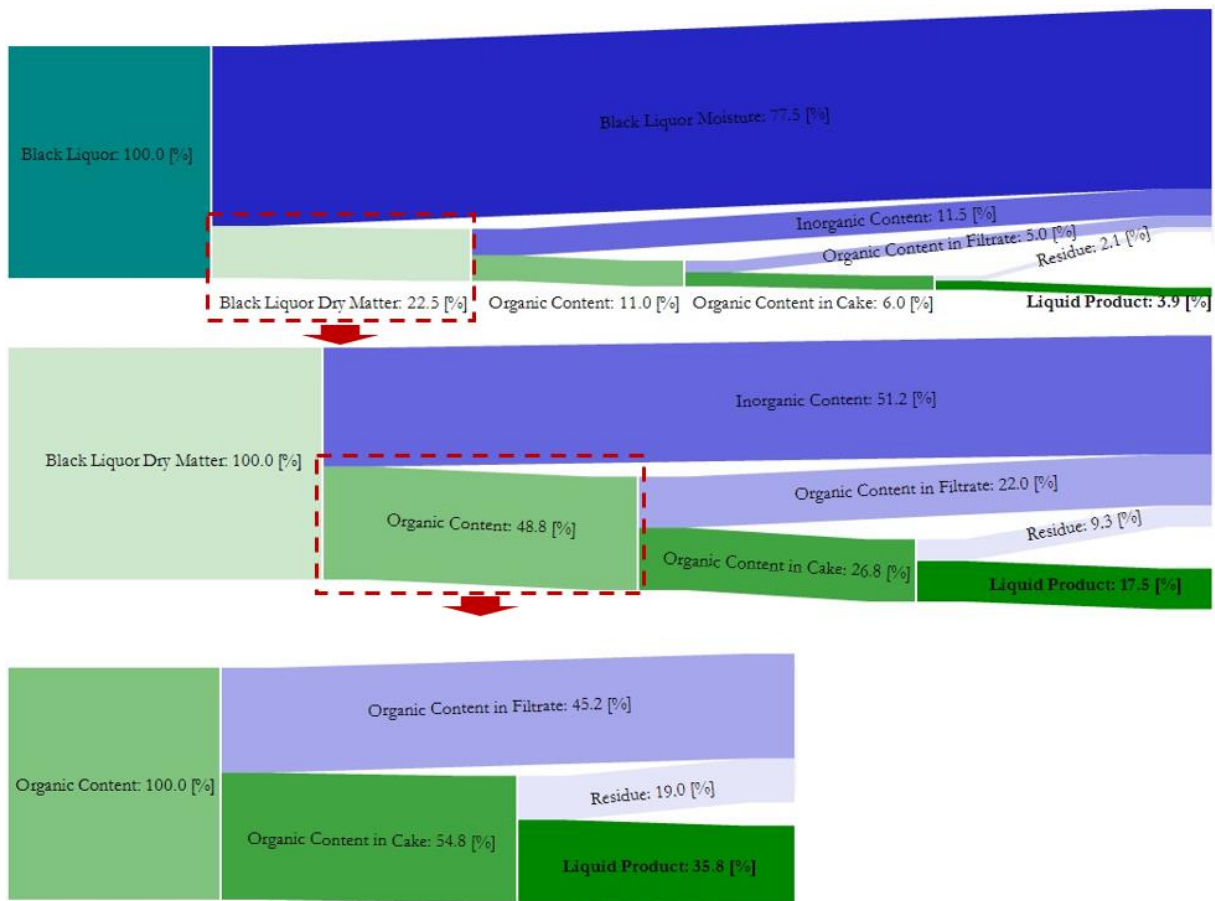


Figure 8-1: Liquefaction

3.9% of the whole black liquor can be liquefied. Black liquor moisture, inorganics, filtrate with organic residue and the liquefaction residue are led back to the paper mill recycling process. The liquid product yield is 17.5% when the black liquor dry matter is the basis. 35.8% of the whole black liquor organic content can be liquefied.

Concerning the carbon balance, the black liquor carbon content is the basis. The following Sankey graph (Figure 8-2) shows the carbon transfer degree of three different references.

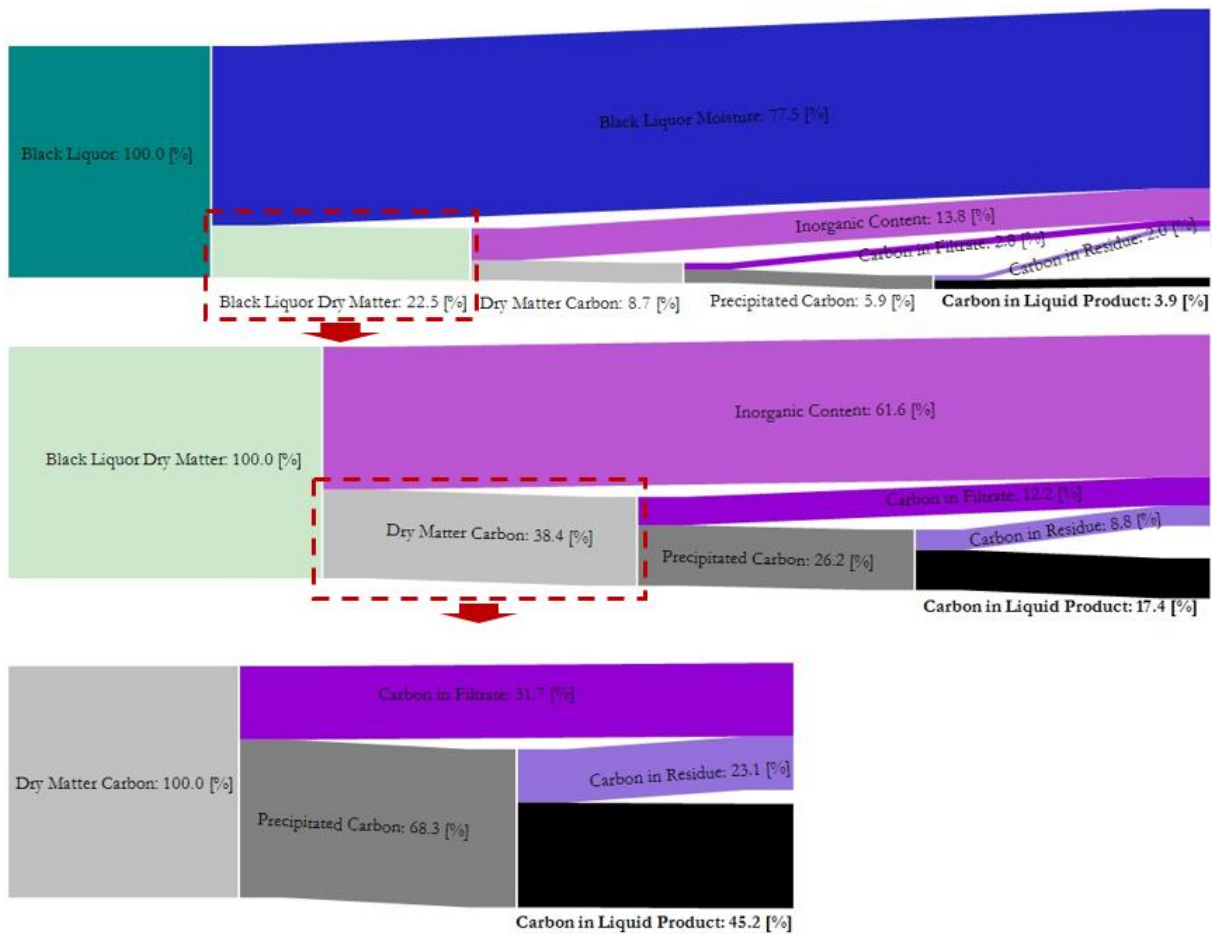


Figure 8-2: Carbon transfer

3.9% of the whole black liquor mass is carbon which can be transferred into the liquid product. Moreover, 17.4% of the black liquor dry matter can be found as carbon in the liquid product. This means, as a consequence, that 45.2% of the whole carbon fraction in the dry matter can be transferred into the liquid product.

8.2 Cost estimation

The cost estimation is based on former projects [50]–[52] and on information from project partners [53]. The calculation is subdivided in four parts: the precipitation in the paper mill, the transport, the depolymerisation and rehydrogenation as a whole and the carrier distillation. The cost estimation is based on a defined product yield which is set to 250 000 tons per year. Basis data is summarised in Table 8-1.

Table 8-1: Annual operation time and product mass

item	acronym	value	unit
operating hours	t_o	8000	[h/a]
product mass	m_p	250000	[t/a]
product mass	m_p	31.25	[t/h]

Process costs consist of raw materials, chemicals, energy, transport, personnel, maintenance, after-treatment and other unassigned operating costs. The process cost estimation is split into two parts for each process. Raw material and chemical costs have the highest influence. Subsequently, these costs are summarised to material costs which are the basis of the calculation. Personnel, maintenance, aftertreatment and other unassigned operating costs defined as a percentage of the material costs. In the same manner, the energy costs of all processes at ambient conditions, e.g. the precipitation, are also treated as a percentage of the material costs. Energy costs are treated separately for processes at high temperatures and pressures due to higher operation costs (chapter 7.3).

The basis of the transport cost estimation is a transport route between a paper mill location and a refinery location. Pöls, Styria was chosen as the paper mill location. The refinery site is located in Schwechat, Vienna. The transport by long-haulage truck, prices are estimated to be between 20 and 30 €/t for this route. Transport costs influence the operating costs. Table 8-2 shows a cost range of material, transport and utility costs supplied by the project partners, while Table 8-3 shows the cost impact factors collected in [50]–[52].

Table 8-2: Material, transport and utility costs per reference unit [53]

item	value		unit
	min	max	
Liquor	80	120	€/t
Lignin	200	300	€/t
Sulphuric acid	80	100	€/t
CO2	100	140	€/t
Transport	20	30	€/t
Electrical energy	35	50	€/MWh
Heat	35	50	€/MWh
Aftertreatment	2	3	€/m ³
Hydrogen	2000	3000	€/t
Tetralin	1500	4000	€/t
Naphthalene	1500	2000	€/t
FeOOH catalyst	800	1500	€/t
rehydrogenation catalyst	1000	2000	€/t

Table 8-3: Cost impact factors

item	value		unit
	min	max	
energy costs (if ambient)	0.0042	0.0041	[-]
maintenance costs	0.0018	0.0227	[-]
personnel costs	0.0059	0.0041	[-]
aftertreatment costs	0.0005	0.0021	[-]
Unassigned operation costs	0.0050	0	[-]

Known process streams (chapter 8.1) are priced with factorised material costs (Table 8-2) and impinged with additional processing costs (Table 8-3). Minimum and maximum prices are used to calculate a cost scatter band as a result. Different cases were considered and evaluated. As a reference, two known processes are shown additionally in the cost estimation plots:

- bioboost fast pyrolysis process by BTG [54]–[56]
- Fischer-Tropsch Carbo V process [57]–[59]

8.2.1 Operating cost estimation – Case #1

In the first case, a transport of black liquor from paper mill site to refinery site was assumed. This means that the whole treatment is conducted at the refinery site. Figure 8-3 shows the result of the estimation.

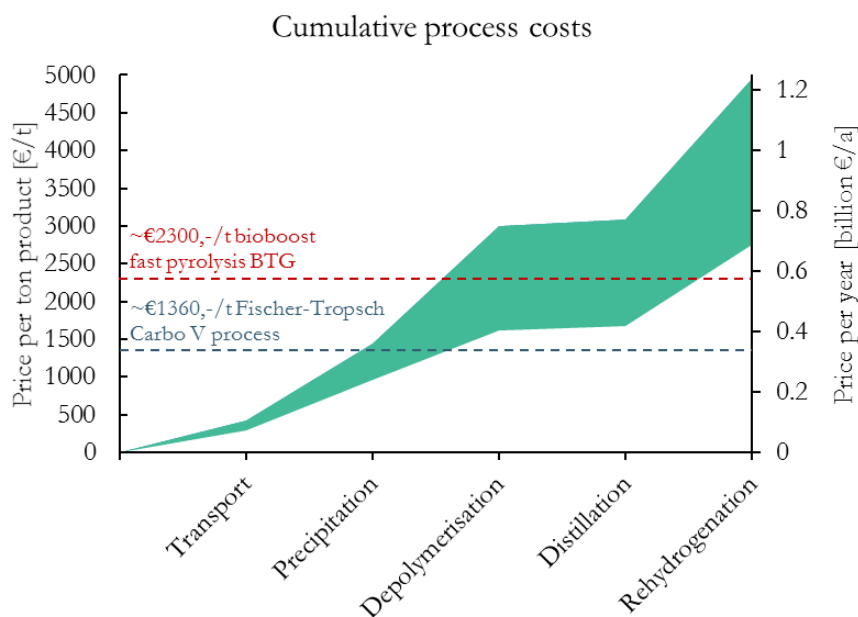


Figure 8-3: Cumulative process costs – case #1

The transport costs are high in this case. Black liquor with high moisture content is transferred to the refinery. The occurring wastewater has to be transferred back to the paper mill for recycling. This almost doubles the transport expense.

In the category precipitation, the raw material price is included. Due to the high quantity, the costs increase rapidly.

The costs of the depolymerisation step includes the necessary fresh carrier, the catalyst and the hydrogen costs which are based on the cake quantity. Also, the energy costs are included. These were estimated by approximately calculating the required heating power and pump capacity of the flow and requisite process temperature and pressure. To define the heat capacity of the flow, an average value of the overall temperature range was taken. Moreover, it is assumed that the differential pressure has the highest influence on the pump capacity. Discharge heat and losses were not considered. An average summarised pump and engine efficiency of 0.5 was chosen. Because of the relatively low influence of the pump capacity on the energy, an estimation in this way is sufficient.

The distillation costs are an outcome of the simulation work in chapter 7.3. The verification was done with auxiliary calculation and estimation of the energy requirement.

The rehydrogenation causes high costs due to a high hydrogen and catalyst requirement. Energy costs were estimated in the same way as in the depolymerisation part. These costs could possibly be avoided because of heat energy recuperation from the other processes.

The estimated process costs of this case are in a range between 0.68 and 1.24 billion €/a and 2 750 and 4 950 €/t of product respectively.

8.2.2 Operating cost estimation – Case #2

In the second cost estimation case, precipitation in the paper mill, transport of the cake to the refinery and depolymerisation at the refinery site were considered. Therefore, the precipitation cake is priced according to data provided by the project partners. The price of the cake strongly depends on the way of precipitation. If precipitation with exhaust gas from the recovery boiler is feasible, prices of the filter cake can be lower. Also, washing and treating the cake at the paper mill site would prevent costs due to lower transport quantities. The results of case #2 cost investigations are depicted in Figure 8-4.

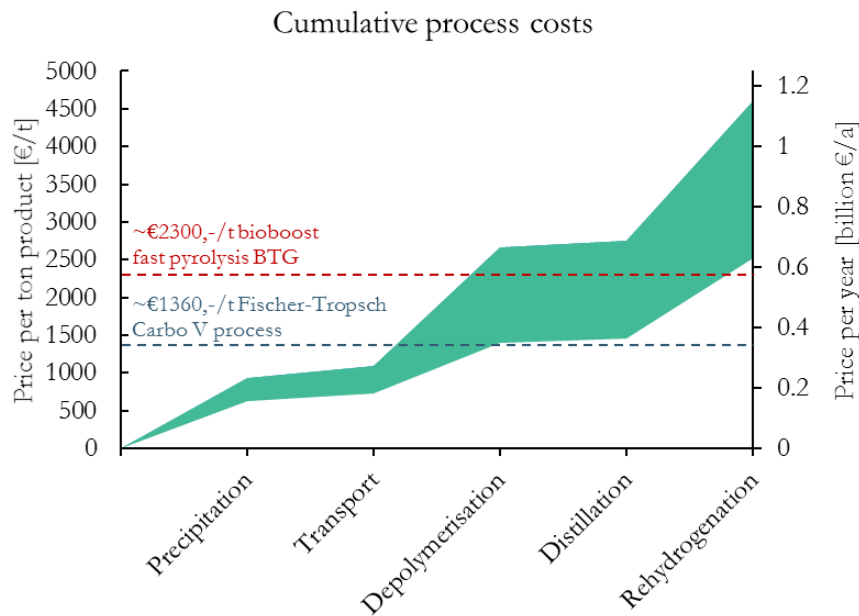


Figure 8-4: Cumulative process costs - case #2

The costs can be reduced with the concept of case #2. Transportation costs decrease by over 90%. The depolymerisation process includes the raw material costs. The energy costs of the depolymerisation, the rehydrogenation and the distillation process steps were evaluated in the same way as in chapter 8.2.1. This is possible due to the same input quantities.

The estimated process costs for this case are in a range between 0.63 and 1.15 billion €/a and 2 500 and 4 600 €/t of product respectively.

8.2.3 Operating cost estimation – Case #3

In a further step, case #3, it is assumed that the catalyst quantity can be greatly decreased and the product quality can be increased, which leads to a further essential cost reduction. Here, the catalyst quantity of the depolymerisation step as well as for the rehydrogenation is reduced.

Table 8-4: Catalyst quantity for depolymerisation and rehydrogenation

item	acronym	value	unit	description
catalyst mass fraction for depolymerisation	W _{γ-FeOOH}	0.005	[-]	of cake mass
catalyst mass fraction for rehydrogenation	W _{Ni-cat}	0.005	[-]	of carrier mass

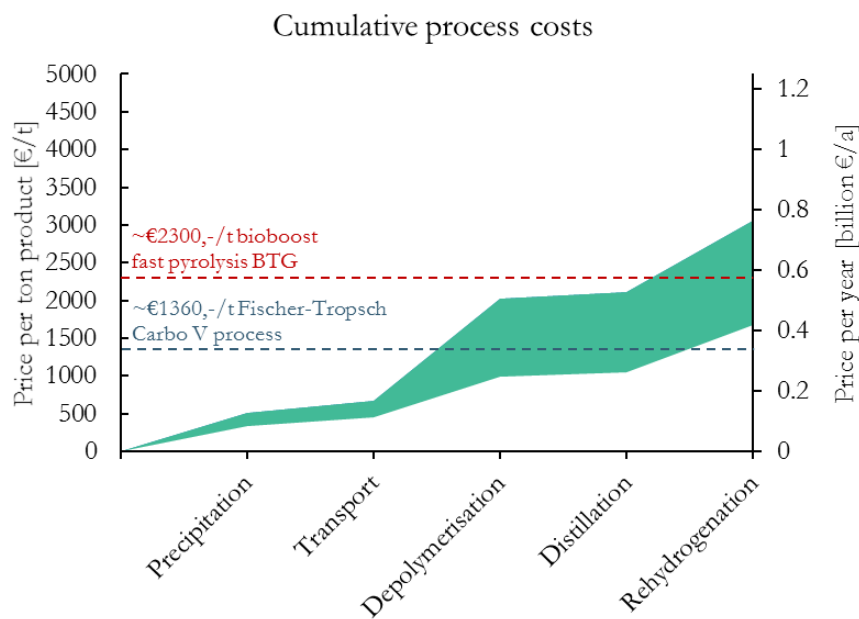


Figure 8-5: Cumulative process costs - case #3

The estimated process costs of this case are in a range between 0.42 and 0.76 billion €/a and 1 700 and 3 050 €/t of product respectively.

This is comparable with the bioboost fast pyrolysis process by BTG. However, the lowest estimated process costs of the thermo-catalytic lignin depolymerisation are above the processing costs of the Fischer-Tropsch Carbo V process. (Note: no information about included depreciation).

8.2.4 Capital costs

A capital cost estimation without knowledge of the precise process streams, the required capacity (equipment volume or surface) and processing site would be implausible. More information and more detailed calculation is necessary. Possible approaches for rough capital cost estimations are shown in literature [15], [60].

8.3 Availability

Open statistical data concerning accruing of lignin or black liquor in paper mills do not exist. A derivation of black liquor quantities is possible with the assumption that 1 kg black liquor (dry) accrues during the production of about 1 kg pulp (dry). In literature, amounts of 3 to 7 kg black liquor per kg pulp can be found [24], [61]. About 20% of the black liquor accruing in a paper mill can be used without having energy distress or process instabilities [62]. Concerning a liquefaction product yield of 3.9%, this would lead to possible product quantities of 43.6 kt/year in Austria,

1.1 Mt in Europe and 4.6 Mt worldwide (average values 2011-2014). In the following graphs (Figure 8-6, Figure 8-7, Figure 8-8), the trend of pulp production over the last years as well as the black liquor and, consequently, the predicted liquid product quantities are shown. Furthermore, the worldwide chemical pulp production distribution is shown in Figure 8-9.

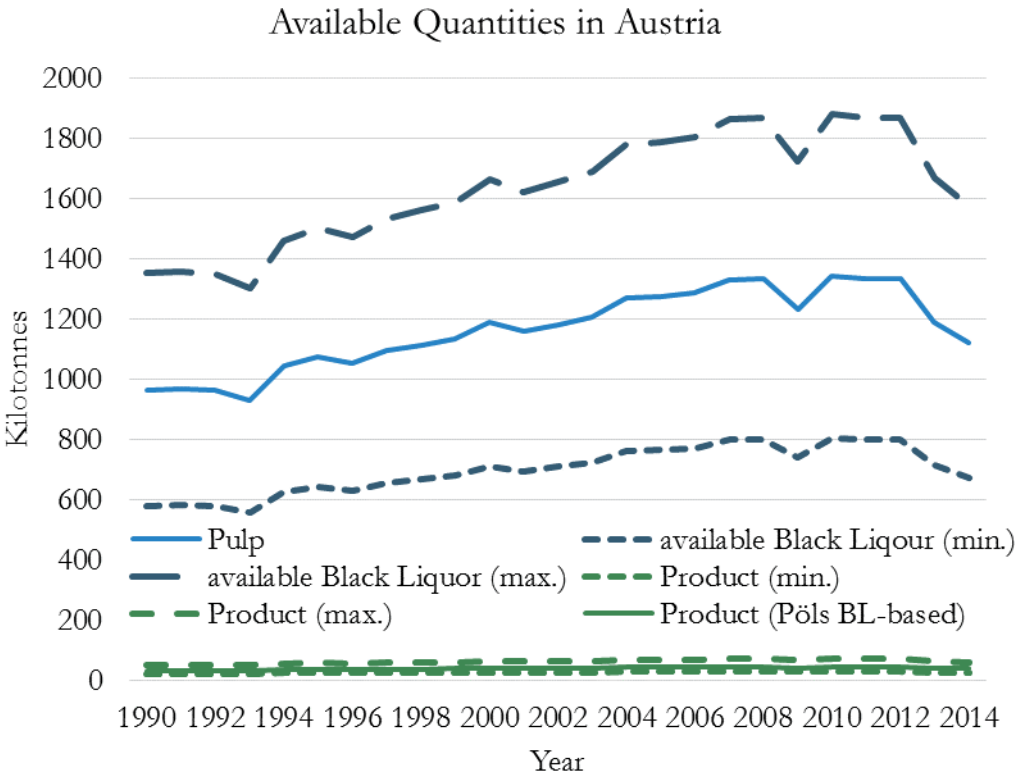


Figure 8-6: Annual Quantities of Pulp, Black Liquor and Liquid Product - Austria

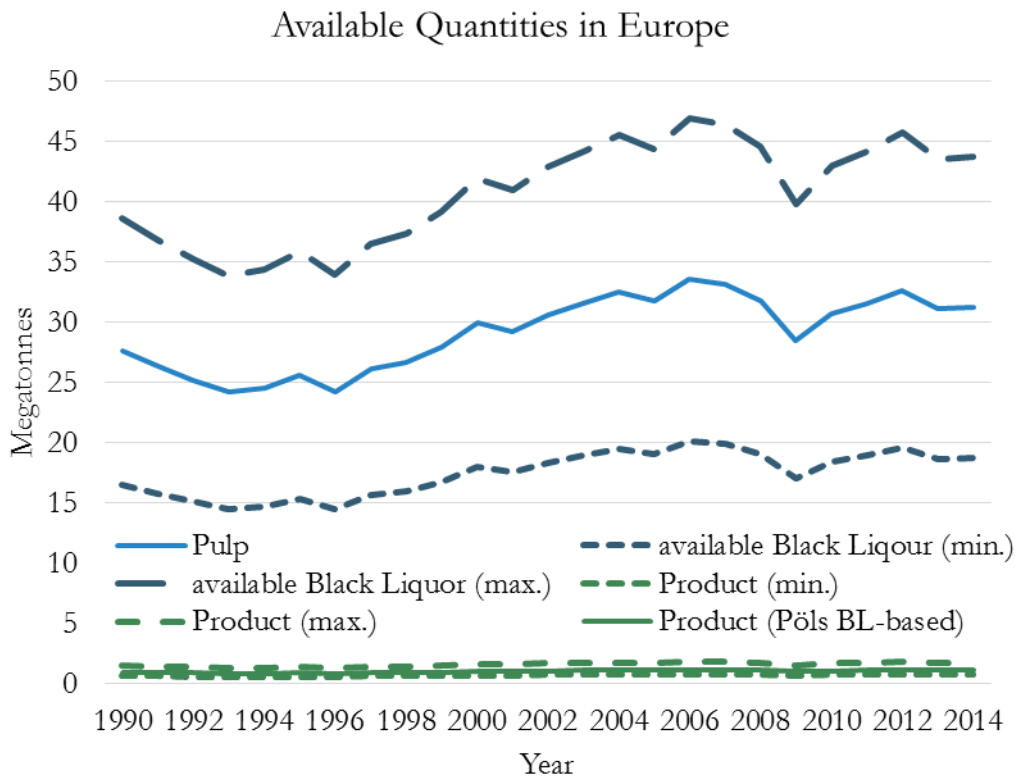


Figure 8-7: Annual Quantities of Pulp, Black Liquor and Liquid Product – Europe

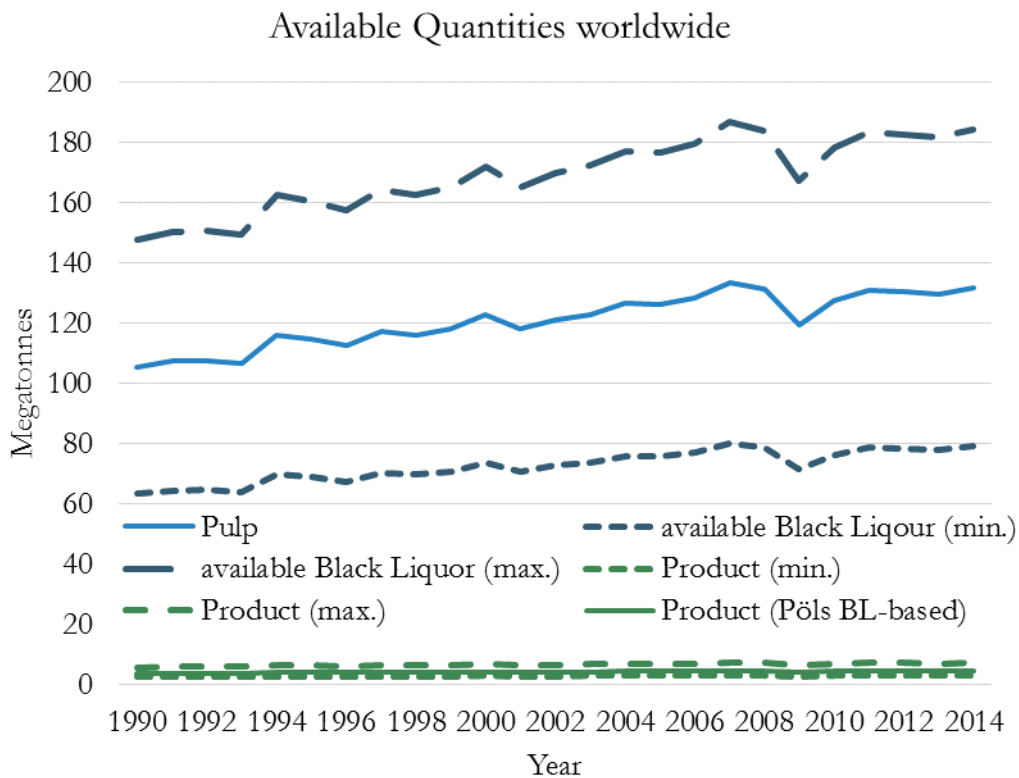


Figure 8-8: Annual Quantities of Pulp, Black Liquor and Liquid Product - worldwide

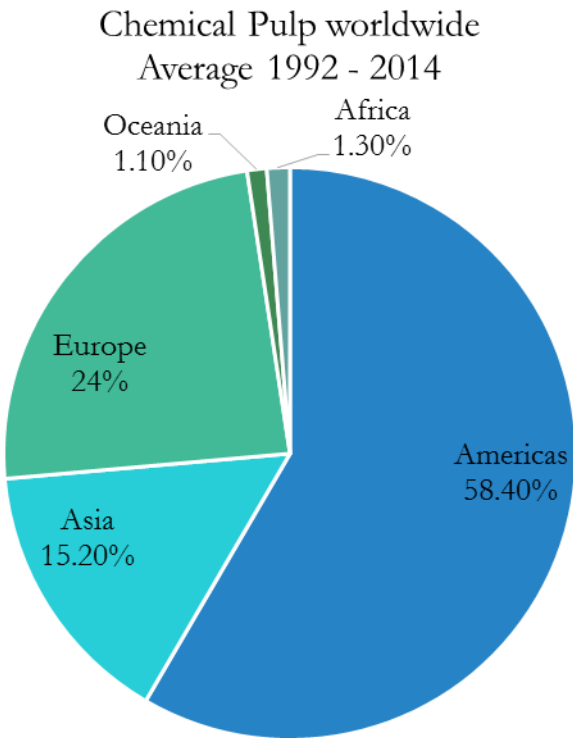


Figure 8-9: Chemical Pulp worldwide - average 1992 - 2014

9 Conclusion and forecast

In this chapter, the main findings and most important results are summarised. Table 9-1 shows the results of the calculation.

Table 9-1: Result summary

item	value	unit
liquefaction degree (black liquor organic content based)	35.8	[%]
carbon transfer degree (black liquor dry matter carbon in product)	45.2	[%]
carbon content of precipitation product	52.79	[%]
predicted yield of organic substance in the product	0.548	[-]
carbon content in liquid product	0.7345	[-]
hydrogen requirement (product-specific)	0.0306	[-]
upper heat value	39.17	[MJ/kg]

Concluding the initially postulated best case, process costs occur in a range between 0.42 and 0.76 billion €/a and a ton price between 1 700 and 3 050 €/t of product. These resulting operation cost estimations can be basis of calculations in future, e.g. capital cost estimations.

The idea of making fuels and chemicals from lignin is certainly a good one. A big disadvantage is that only parts of black liquor can be used for production of chemicals and fuels (10-20%) to avoid interference with paper mill energy management. However, some research and development still need to be done in order to increase the yield, the efficiency and thus the economy of the process. To improve further lignin valorization from black liquor, a validated pretreatment process is mandatory. Also, transport costs to refineries or chemical plants have to be decreased. In any case, there is potential in the development of the catalysts and in the optimization of the process management. Furthermore, there is the possibility to upgrade and market by-products. However, finally, the strongest dependence is connected with the oil or diesel price with which the idea lives and dies.

In the near future, legislation requires a significant reduction of CO₂ emissions. Conventional fuels and relating thereto engine and combustion techniques can most likely not fulfil these emission standards. At least in the commercial vehicle section, the combustion engine is indispensable in the next decades. In addition, the capacity of full electrification in the on-road vehicle sector is not given yet. Therefore, research in renewable fuels for combustion engines is necessary as well. Fuels from lignin may be a competitive alternative in the future.

10 Appendix

10.1 Credits

At the end of my master thesis it is time to say thank you to everyone who supported me during this intense time.

Thank you, Nikolaus, for supervising my work, for the expertise, for your vast resources of knowledge, for the hilarious stories and for the opportunity to enjoy such a great work environment. And, indeed, many thanks for your patience.

Thank you Univ.-Prof. Dipl.-Ing. Dr.techn. Matthäus Siebenhofer for the knowledge you imparted during my studies and the kind and harmonious handling of the people around you.

Thank you, Thomas, Klaus, Roland, Klara, Anna, Andrea, Michael, Joachim, Julia, Eli and Berndt, for the great and entertaining time in our office.

Thank you, Sarah, Tanja, Simon, Peter, Herta and the rest of the laboratory team for the practical assistance. The whole analytical work would not have been possible without your knowledge and experience.

Thank you, Mom and Dad, for encouraging me during all the years of my life.

(Dounkschei Mami und Vatl, dass' immer hinter mir g'stoundn seids.)

Thank you to my friends, especially Sebastian, Marco, Markus, Hannes, Christoph and Carmen for the necessary variety in my life as a student.

Thank you, Wilma and Neil, for your outstanding English language competence and the proof-reading.

Thank you to my colleagues from the AVL department where I worked during the last four years; above all Marko for supporting me with expertise and know-how.

10.2 Glossary

10.2.1 General acronyms

<i>BL</i>	Black Liquor
<i>WL</i>	White Liquor
<i>GL</i>	Green Liquor
<i>DWL</i>	Dissolved Wood Lignin
<i>ASL</i>	Acid-Soluble Lignin

10.2.2 Formula symbols

V_i	Volume [m ³]
ρ_i	Density [kg/m ³]
m_i	Mass [kg]
t	Time [s]

10.2.3 Formula indices

<i>I</i>	General index
<i>BL</i>	Black Liquor
H_2SO_4	Sulphuric acid
CO_2	Carbon dioxide
<i>F</i>	Filtrate
<i>C</i>	Filter Cake
<i>Ash</i>	Ash specific
<i>DS</i>	Dry matter specific

org Organic amount

in incoming

out outgoing

ξ Feed

meas measurement-based

pred predicted

exp experimental

sim simulated

10.3 Bibliography

- [1] D. C. Elliott, “Catalytic Hydrotreating of Black Liquor Oils,” pp. 102–109, 1991.
- [2] M. Helander, H. Theliander, M. Lawoko, G. Henriksson, L. Zhang, and M. E. Lindström, “Fractionation of technical lignin: Molecular mass and pH effects,” *BioResources*, vol. 8, no. 2, pp. 2270–2282, 2013.
- [3] S. Mesfun, J. Lundgren, C.-E. Grip, A. Toffolo, R. L. K. Nilsson, and U. Rova, “Black liquor fractionation for biofuels production – A techno-economic assessment,” *Bioresour. Technol.*, vol. 166, pp. 508–517, 2014.
- [4] P. Bajpai, *Biorefinery in the Pulp and Paper Industry*. 2013.
- [5] M. Hamaguchi, M. Cardoso, and E. Vakkilainen, “Alternative technologies for biofuels production in kraft pulp mills - potential and prospects,” *Energies*, vol. 5, pp. 2288–2309, 2012.
- [6] M. P. Pandey and C. S. Kim, “Lignin Depolymerization and Conversion: A Review of Thermochemical Methods,” *Chem. Eng. Technol.*, vol. 34, no. 1, pp. 29–41, 2011.
- [7] N. Schwaiger, R. Feiner, H. Pucher, L. Ellmaier, J. Ritzberger, K. Treusch, P. Pucher, and M. Siebenhofer, “BiomassPyrolysisRefinery - Herstellung von nachhaltigen Treibstoffen,” *Chemie-Ingenieur-Technik*, vol. 87, no. 6, pp. 803–809, 2015.
- [8] H. Pucher, N. Schwaiger, R. Feiner, L. Ellmaier, P. Pucher, B. Chernev, and M. Siebenhofer, “Biofuel production from liquid phase pyrolysis oil: A two-step HDO process,” *Green Chem.*, vol. 17, pp. 1291–1298, 2015.
- [9] H. Pucher, N. Schwaiger, R. Feiner, L. Ellmaier, P. Pucher, B. S. Chernev, M. Siebenhofer, H. Pucher, N. Schwaiger, R. Feiner, L. Ellmaier, P. Pucher, and B. S. Chernev, “Lignocellulosic Biofuels : Phase Separation during Catalytic Hydrodeoxygenation of Liquid Phase Pyrolysis Oil,” vol. 50, no. 18, pp. 2914–2919, 2015.
- [10] N. Schwaiger, D. C. Elliott, J. Ritzberger, H. Wang, P. Pucher, and M. Siebenhofer, “Hydrocarbon liquid production via the bioCRACK process and catalytic hydroprocessing of the product oil,” *Green Chem.*, vol. 17, no. 4, pp. 2487–2494, 2015.
- [11] R. Feiner, N. Schwaiger, H. Pucher, L. Ellmaier, M. Derntl, P. Pucher, and M. Siebenhofer, “Chemical loop systems for biochar liquefaction: hydrogenation of Naphthalene,” *RSC Adv.*, vol. 4, p. 34955, 2014.
- [12] E. Mateos-Espejel, M. Moshkelani, M. Keshtkar, and J. Paris, “Sustainability of the green integrated forest biorefinery: A question of energy,” *J. Sci. Technol. For. Prod. Process.*, vol. 1, no. 1, pp. 55–61, 2011.
- [13] “National Renewable Energy Laboratory.” [Online]. Available: <http://www.nrel.gov/>.
- [14] The Berkeley Center for Green Chemistry, “Green Chemistry Laboratory,” 2011. [Online]. Available: <https://bcgc.berkeley.edu>.
- [15] H. Sixta, “Advances in Biorefinery - Introduction to biorefineries including the historical background,” 2015.
- [16] T. Timmel, “Flipp^o,” 2013. [Online]. Available: <http://www.flippr.at>.
- [17] E. Sjöström, *Wood chemistry, Fundamentals and Applications*, 2nd editio., vol. 252. Academic

- Press, Inc., 1994.
- [18] F. Behrendt and N. Zobel, “Direktverflüssigung von Biomasse - Reaktionsmechanismen und Produktverteilungen,” 2006.
- [19] R. Shmulsky and P. D. Jones, *Forest products and wood science*, 6th ed. 2011.
- [20] K. Freudenberg and A. C. Neish, *Construction and Biosynthesis of Lignin*. Springer, 1968.
- [21] B. Saake and R. Lehnen, “Lignin,” in *Ullmann’s Encyclopedia of Industrial Chemistry*, Vol. 21., 2012, pp. 21–36.
- [22] M. Ek, G. Gellerstedt, and G. Henriksson, *Wood chemistry and biotechnology*, vol. 1. De Gruyter, 2009.
- [23] I. Brodin, *Chemical Properties and Thermal Behaviour of Kraft Lignins*. 2009.
- [24] H. Sixta, *Handbook of Pulp*. 2006.
- [25] H. Tran and E. K. Vakkilainen, “Advances in the Kraft Chemical Recovery Process,” in *International colloquium on Eucalyptus Pulp*, 2007.
- [26] V. Rajcoomar, “African Pulp and Paper Week 2004,” 2004. [Online]. Available: http://www.tappsa.co.za/archive2/APPW_2004/Title2004/Applying_best_sustainable_prac/applying_best_sustainable_prac.html.
- [27] Magnetrol®, “Level and Flow Solutions for Pulp and Paper Mill Production,” 2016. [Online]. Available: http://us.magnetrol.com/Industries_Individual.aspx?id=8.
- [28] M. S. Kannangara, “Development and Integration of Acid Precipitation based Lignin Biorefineries in Kraft Pulping Mills,” Université de Montréal, 2015.
- [29] P. Tomani, “The Lignoboost Process,” *Cellul. Chem. Technol.*, vol. 44, no. 1–3, pp. 53–58, 2010.
- [30] P. Tomani, P. Axegård, N. Berglin, A. Lovell, D. Nordgren, and I. Ab, “Integration of Lignin Removal Into a Kraft Pulp Mill and Use of Lignin As a Biofuel,” *Cellul. Chem. Technol.*, vol. 2, pp. 533–540, 2011.
- [31] W. Yang, H. Mu, and Y. Huang, “Treatment of black liquor from the papermaking industry by acidification and reuse,” *J. Environ. Sci.*, vol. 15, no. 5, pp. 697–700, 2003.
- [32] M. Alekhina, O. Ershova, A. Ebert, S. Heikkinen, and H. Sixta, “Softwood kraft lignin for value-added applications: Fractionation and structural characterization,” *Ind. Crops Prod.*, vol. 66, pp. 220–228, 2015.
- [33] O. Wallberg, “Design of ultrafiltration process for extraction of lignin from kraft black liquor,” 2005.
- [34] A. S. Jönsson and O. Wallberg, “Cost estimates of kraft lignin recovery by ultrafiltration,” *Desalination*, vol. 237, no. 1–3, pp. 254–267, 2009.
- [35] N. Schwaiger, “Reaktionstechnische Analyse für die Optimierung der Flüssigphasenpyrolyse,” TU Graz, 2011.
- [36] R. Feiner, “Hydrierende Verflüssigung biogener Einsatzstoffe,” TU Graz, 2014.

- [37] H. Pucher, “Entwicklung, Design und Modellierung eines Upgrading-Prozesses biobasierter flüssiger Energieträger,” TU Graz, 2014.
- [38] A. V. Bridgewater, *Research in Thermochemical Biomass Conversion*, 1st ed. Elsevier Ltd, 1988.
- [39] E. D. Nikitin, P. A. Pavlov, and A. P. Popov, “Vapour-liquid critical temperatures and pressures of normal alkanes with from 19 to 36 carbon atoms, naphthalene and m-terphenyl determined by the pulse-heating technique,” *Fluid Phase Equilib.*, vol. 141, pp. 155–164, 1997.
- [40] M. R. Riazi, *Characterization and Properties of Petroleum Fractions*, 1st ed., vol. 53, no. 9. Philadelphia, PA: American Society for Testing and Materials, 2005.
- [41] G. Holzer, *Einführung in die Simulationsprogramme*. 2012.
- [42] “SIS-CEN/TS 14775:2004: Solid biofuels – Method for the determination of ash content,” 2005.
- [43] W. Zhu and H. Theliander, “Equilibrium of lignin precipitation,” *Proc. 16th ISWFPC*, 2011.
- [44] W. Zhu, *Equilibrium of Lignin Precipitation - The Effects of pH, Temperature, Ion Strength and Wood Origins*. 2013.
- [45] W. Zhu, G. Westman, and H. Theliander, “The molecular properties and carbohydrate content of lignins precipitated from black liquor,” *Holzforschung*, vol. 69, no. 2, pp. 143–152, 2014.
- [46] W. Zhu and H. Theliander, “Precipitation of Lignin from Softwood Black Liquor: An Investigation of the Equilibrium and Molecular Properties of Lignin,” *BioResources*, vol. 10, no. 1, pp. 1696–1714, 2015.
- [47] S. Plappert and F. Liebner, “N-lignin,” BOKU, 2016.
- [48] M. Derntl, “Partielle Hydrierung polyzyklischer Kohlenwasserstoffe,” Graz University of Technology, 2013.
- [49] K. Annamalai and I. K. Puri, *Combustion Science and Engineering*. Texas A&M University: CRC Press - Taylor & Francis Group, 2007.
- [50] M. Tandl, “Ökonomische und ökologische Bewertung konventioneller Herstellung von Biodiesel aus Rapsöl,” Graz University of Technology, 2015.
- [51] J. Drack, “Ökonomische und ökologische Bewertung der Hydrierung von Pflanzenölen,” 2015.
- [52] T. Pichler, “Lignocellulose,” 2015.
- [53] T. Timmel and K. Eibinger, “Cost survey,” 2016.
- [54] A. Oasmaa, E. Kuoppala, A. Ardiyanti, R. H. Venderbosch, and H. J. Heeres, “Characterization of hydrotreated fast pyrolysis liquids,” *Energy and Fuels*, vol. 24, no. 9, pp. 5264–5272, 2010.
- [55] R. Manurung, D. A. Z. Wever, J. Wildschut, R. H. Venderbosch, H. Hidayat, J. E. G. van Dam, E. J. Leijenhurst, A. A. Broekhuis, and H. J. Heeres, “Valorisation of *Jatropha curcas* L. plant parts: Nut shell conversion to fast pyrolysis oil,” *Food Bioprod. Process.*, vol. 87, no. 3, pp. 187–196, 2009.

-
- [56] R. H. Venderbosch and W. Prins, “Fast Pyrolysis Technology Development,” *BIOFUELS Bioprod. BIOREFINING-BIOFPR*, vol. 4, no. 2, pp. 178–208, 2010.
- [57] M. Rudloff, “Herstellung von biogenem FT-Kraftstoff – „Sundiesel made by CHOREN“ – mit dem CHOREN-Verfahren,” in *Biokraftstoffe – ein neuer Wirtschaftszweig entsteht*, 2003.
- [58] M. Rudloff, “Bio-Syngas via CHOREN ’ s gasification technology - Operation of BTL Demo plant and future prospects -,” in *4th International Freiberg Conference on IGCC & XTL Technologies - IFC 2010*, 2010.
- [59] A. Althapp, “Kraftstoffe aus Biomasse Vergasungsverfahren,” pp. 218–227, 2003.
- [60] G. D. Ulrich and P. T. Vasudevan, “Chemical Engineering - Process Design and Economics - A Practical Guide.” 2004.
- [61] M. Kaltschmitt, H. Hartmann, and H. Hofbauer, *Energie aus Biomasse*. 2009.
- [62] K. Eibinger, “Black Liquor offset survey.” 2016.

10.4 Figures

Figure 1-1: Biomass Pyrolysis Refinery process.....	1
Figure 1-2: Biorefinery - value chain [15].....	2
Figure 1-3: Industrial (left) and scientific (right) project partners.....	4
Figure 2-1: Macro- and microstructure of wood [18]	7
Figure 2-2: Main lignin components [21].....	8
Figure 2-3: Chemical structure of Spruce Lignin [22], [23]	9
Figure 2-4: Principle behind the kraft pulping process [25].....	10
Figure 2-5: Kraft process - principle flow sheet [26]	10
Figure 2-6: Lignin decomposition pathways [6].....	11
Figure 3-1: The LignoBoost process	13
Figure 3-2: Ultrafiltration	14
Figure 3-3: Pöls black liquor behaviour of precipitation at different pH values	15
Figure 3-4: Mondi black liquor behaviour of precipitation at different pH values	15
Figure 3-5: “Alekhina” black liquor behaviour of precipitation at different pH values	16
Figure 3-6: Lignin removal behaviour of different black liquors	16
Figure 4-1: Equilibrium of tetralin-naphthalene-hydrogen system – difference between NRTL, Peng-Robinson and PSRK.....	19
Figure 6-1: Zellstoff Pöls AG precipitation pilot plant - process scheme	23
Figure 6-2: Precipitation pilot plant: reactor construction (left), chamber filter press (middle) and emptied filter chamber with cake residue (right)	24
Figure 6-3: Samples	26

Figure 6-4: Filter cake ash after the incineration	27
Figure 6-5: Filtrate ash after the incineration	28
Figure 6-6: Black Liquor ash after the incineration.....	28
Figure 6-7: Balance boundaries - precipitation with H ₂ SO ₄	29
Figure 6-8: pH drop induced by CO ₂	34
Figure 6-9: Lab scale precipitation experiment with CO ₂ as precipitant.....	34
Figure 6-10: Balance boundaries - depolymerisation	37
Figure 6-11: Depolymerisation balance.....	39
Figure 6-12: Depolymerisation lignin-based.....	40
Figure 6-13: Reaction pathway of naphthalene with hydrogen	46
Figure 6-14: Rehydrogenation reaction behaviour – mole fraction versus time.....	46
Figure 6-15: Rehydrogenation reaction behaviour - mass fraction versus time.....	47
Figure 6-16: Rehydrogenation balance boundaries	48
Figure 6-17: Rehydrogenation reaction behaviour - reduced dwell time	49
Figure 6-18: Rehydrogenation reaction behaviour - decalin prevention and low dwell time	50
Figure 6-19: Rehydrogenation reaction behaviour - maximum tetralin conversion.....	52
Figure 6-20: Simplified reaction equation.....	53
Figure 6-21: Van Krevelen plot.....	55
Figure 7-1: Principle process scheme	58
Figure 7-2: Precipitation simulation model – GUI	63
Figure 7-3: Precipitation simulation model	64

Figure 7-4: Precipitation simulation model - inner workings64

Figure 8-1: Liquefaction67

Figure 8-2: Carbon transfer.....68

Figure 8-3: Cumulative process costs – case #1.....70

Figure 8-4: Cumulative process costs - case #2.....72

Figure 8-5: Cumulative process costs - case #3.....73

Figure 8-6: Annual Quantities of Pulp, Black Liquor and Liquid Product - Austria74

Figure 8-7: Annual Quantities of Pulp, Black Liquor and Liquid Product – Europe.....75

Figure 8-8: Annual Quantities of Pulp, Black Liquor and Liquid Product - worldwide.....75

Figure 8-9: Chemical Pulp worldwide - average 1992 - 201476

Figure 10-1: Pump calibration97

10.5 Tables

Table 2-1: Organic constituents of wood [19]	8
Table 2-2: Elemental composition of wood [19]	8
Table 4-1: Carrier and products after depolymerisation and rehydrogenation	17
Table 4-2: Characterisation of tetralin, naphthalene and decalin	18
Table 4-3: Description of significant degradation products	18
Table 5-1: Dry matter and ash content analysis devices	21
Table 5-2: Elemental analysis device	22
Table 6-1: Black liquor input data	25
Table 6-2: H ₂ SO ₄ input data	25
Table 6-3: Outcome streams	25
Table 6-4: Sample overview	26
Table 6-5: Dry matter content	27
Table 6-6: Ash content	27
Table 6-7: Elemental analysis	28
Table 6-8: Mass balance result summary of precipitation with H ₂ SO ₄ as precipitant	31
Table 6-9: Carbon transfer result summary of precipitation with H ₂ SO ₄ as precipitant	33
Table 6-10: Depolymerisation process parameter	35
Table 6-11: Initial quantities of depolymerisation experiment	35
Table 6-12: Physical state distribution	36
Table 6-13: Output fractions	36

Table 6-14: Chemical composition of liquid carrier after reaction with lignin.....	36
Table 6-15: Elemental composition of depolymerisation educts and products.....	37
Table 6-16: Results of the depolymerisation mass balance.....	39
Table 6-17: Carbon conversion during the depolymerisation and liquid product elemental composition.....	44
Table 6-18: Rehydrogenation process conditions	45
Table 6-19: Mole fractions of components at dwell time for maximum tetralin concentration downstream rehydrogenation.....	46
Table 6-20: Mass fractions of components at dwell time for maximum tetralin concentration downstream rehydrogenation.....	47
Table 6-21: Mass fractions at low dwell time of maximum tetralin concentration without any decalin formation upstream and downstream rehydrogenation	51
Table 6-22: Mass fractions at high dwell time range for maximum tetralin creation without decalin	52
Table 6-23: Mass fractions at high dwell time range for maximum tetralin creation without decalin	54
Table 6-24: Elemental distribution in the liquid product - mole fraction.....	54
Table 6-25: Specific factors for the heat value estimation	56
Table 6-26: Upper and lower heat value of liquid product	56
Table 7-1: Stream table.....	59
Table 7-2: Block table	60
Table 7-3: Transport table.....	60
Table 7-4: Stream specification for distillation.....	66

Table 8-1: Annual operation time and product mass.....	69
Table 8-2: Material, transport and utility costs per reference unit [53]	69
Table 8-3: Cost impact factors	70
Table 8-4: Catalyst quantity for depolymerisation and rehydrogenation	72
Table 9-1: Result summary.....	77
Table 10-1: Elemental data	95
Table 10-2: Tetralin data	95
Table 10-3: Decalin data.....	96
Table 10-4: Hydrogen data.....	96
Table 10-5: Heating value calculation.....	96

10.6 Equations

(6-1)29

(6-2)29

(6-3)30

(6-4)30

(6-5)30

(6-6)30

(6-7)30

(6-8)30

(6-9)31

(6-10)31

(6-11)32

(6-12)32

(6-13)32

(6-14)32

(6-15)32

(6-16)32

(6-17)32

(6-18)32

(6-19)37

(6-20)38

(6-21)38

(6-22)38

(6-23)38

(6-24)38

(6-25)38

(6-26)38

(6-27)	38
(6-28)	39
(6-29)	41
(6-30)	41
(6-31)	41
(6-32)	41
(6-33)	41
(6-34)	41
(6-35)	41
(6-36)	42
(6-37)	42
(6-38)	42
(6-39)	42
(6-40)	42
(6-41)	42
(6-42)	43
(6-43)	43
(6-44)	43
(6-45)	43
(6-46)	43
(6-47)	43
(6-48)	43
(6-49)	43
(6-50)	43
(6-51)	43
(6-52)	43
(6-53)	44

(6-54) 44

(6-55) 44

(6-56) 53

(6-57) 53

(6-58) 53

(6-59) 53

(6-60) 55

(7-1) 65

(7-2) 65

(7-3) 65

10.7 Substance data

Table 10-1: Elemental data

Elemental data				
molar mass of elemental C	M_C	12.01	[kg/kmol]	
molar mass of elemental H	M_H	1.01	[kg/kmol]	
molar mass of elemental O	M_O	16	[kg/kmol]	
molar mass of elemental N	M_N	14.01	[kg/kmol]	

Table 10-2: Tetralin data

Tetralin data				
molar mass of tetralin	M_{tetralin}	132.2	[kg/kmol]	WP
density of tetralin	ρ_{tetralin}	970	[kg/m ³]	WP
tetralin C content	$\mu_{C,\text{tetralin}}$	0.9085	[-]	theoretical evaluated value
tetralin H content	$\mu_{H,\text{tetralin}}$	0.0917	[-]	theoretical evaluated value
melting point of tetralin	$T_{m,\text{tetralin}}$	-35.8	[°C]	WP
boiling point of tetralin	$T_{b,\text{tetralin}}$	208	[°C]	WP
critical temperature of tetralin	$T_{c,\text{tetralin}}$	446	[°C]	[1]
critical pressure of tetralin	$p_{c,\text{tetralin}}$	34	[bar]	[1]
critical volume of tetralin	$v_{c,\text{tetralin}}$	0.428	[m ³ /kg]	[1]
Naphthalene data				
molar mass of naphthalene	$M_{\text{naphthalene}}$	128.17	[kg/kmol]	WP
density of naphthalene	$\rho_{\text{naphthalene}}$	1140	[kg/m ³]	WP
naphthalene C content	$\mu_{C,\text{naphthalene}}$	0.9370	[-]	theoretical evaluated value
naphthalene H content	$\mu_{H,\text{naphthalene}}$	0.0630	[-]	theoretical evaluated value
melting point of naphthalene	$T_{m,\text{naphthalene}}$	80.3	[°C]	WP
boiling point of naphthalene	$T_{b,\text{naphthalene}}$	218	[°C]	WP
critical temperature of naphthalene	$T_{c,\text{naphthalene}}$	475	[°C]	[3]
critical pressure of naphthalene	$p_{c,\text{naphthalene}}$	41	[bar]	[3]

Table 10-3: Decalin data

Decalin data				
molar mass of decalin	M_{decalin}	138.25	[kg/kmol]	WP
density of decalin	Q_{decalin}	880	[kg/m ³]	WP
decalin C content	$\mu_{\text{C,decalin}}$	0.8687	[-]	theoretical evaluated value
decalin H content	$\mu_{\text{H,decalin}}$	0.1315	[-]	theoretical evaluated value
melting point of decalin	$T_{\text{m,decalin}}$	-43	[°C]	WP
boiling point of decalin	$T_{\text{b,decalin}}$	190	[°C]	WP

Table 10-4: Hydrogen data

Hydrogen data				
molar mass of hydrogen	M_{H_2}	2.02	[kg/kmol]	WP
density of hydrogen	Q_{H_2}	0.0899	[kg/m ³]	WP
melting point of hydrogen	$T_{\text{m,H}_2}$	14.01	[K]	WP
boiling point of hydrogen	$T_{\text{b,H}_2}$	21.15	[K]	WP
critical temperature of hydrogen	$T_{\text{c,H}_2}$	33.18	[K]	WP
critical pressure of hydrogen	$p_{\text{c,H}_2}$	13	[bar]	WP
critical volume of hydrogen	$v_{\text{c,H}_2}$	0.0332	[m ³ /kg]	WP

Table 10-5: Heating value calculation

Heating value calculation				
C multiplication factor for heat value evaluation	h_{C}	32.8	[MJ/kg]	
H multiplication factor for heat value evaluation	h_{H}	101.3	[MJ/kg]	
N multiplication factor for heat value evaluation	h_{N}	6.3	[MJ/kg]	
S multiplication factor for heat value evaluation	h_{S}	19.1	[MJ/kg]	
O multiplication factor for heat value evaluation	h_{O}	-9.8	[MJ/kg]	
H ₂ O multiplication factor for heat value evaluation	$h_{\text{H}_2\text{O}}$	-2.5	[MJ/kg]	

10.8 Experimental – amendment

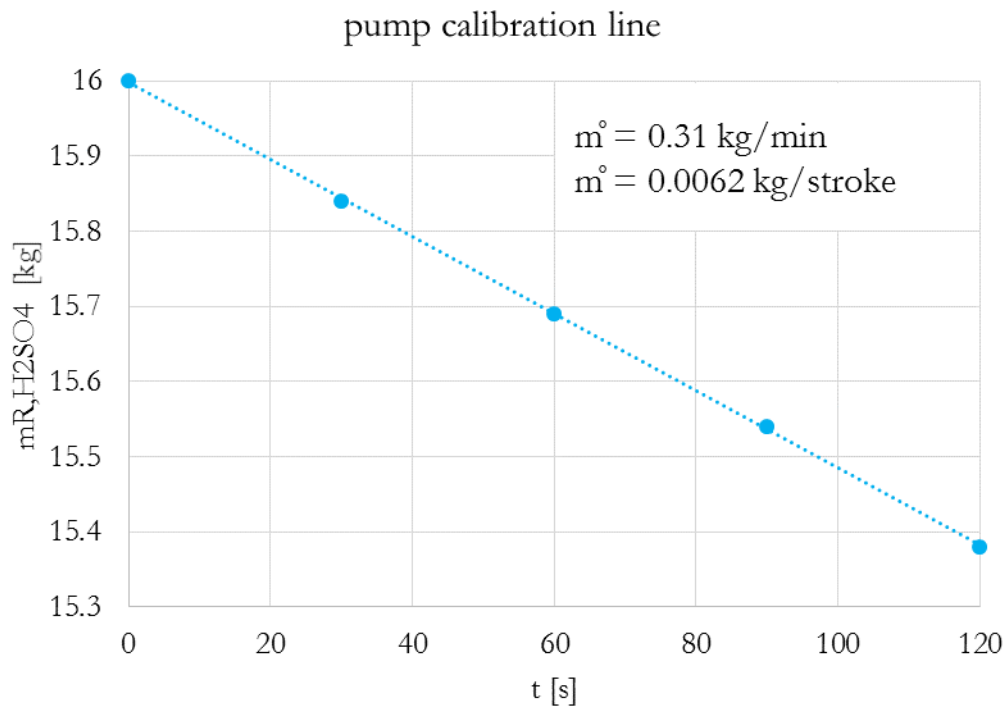


Figure 10-1: Pump calibration

10.9 Modelling

10.9.1 Matlab code

10.9.1.1 Main code

```
function varargout = LDGUI(varargin)
% LDGUI MATLAB code for LDGUI.fig
% LDGUI, by itself, creates a new LDGUI or raises the existing
% singleton*.
%
% H = LDGUI returns the handle to a new LDGUI or the handle to
% the existing singleton*.
%
% LDGUI('CALLBACK',hObject,eventData,handles,...) calls the local
% function named CALLBACK in LDGUI.M with the given input arguments.
%
% LDGUI('Property','Value',...) creates a new LDGUI or raises the
% existing singleton*. Starting from the left, property value pairs
are
% applied to the GUI before LDGUI_OpeningFcn gets called. An
% unrecognized property name or invalid value makes property applica-
tion
% stop. All inputs are passed to LDGUI_OpeningFcn via varargin.
%
% *See GUI Options on GUIDE's Tools menu. Choose "GUI allows only one
% instance to run (singleton)".
%
% See also: GUIDE, GUIDATA, GUIHANDLES

% Edit the above text to modify the response to help LDGUI

% Last Modified by GUIDE v2.5 23-Mar-2016 17:57:08

% Begin initialization code - DO NOT EDIT
gui_Singleton = 1;
gui_State = struct('gui_Name', mfilename, ...
                  'gui_Singleton', gui_Singleton, ...
                  'gui_OpeningFcn', @LDGUI_OpeningFcn, ...
                  'gui_OutputFcn', @LDGUI_OutputFcn, ...
                  'gui_LayoutFcn', [] , ...
                  'gui_Callback', []);
if nargin && ischar(varargin{1})
    gui_State.gui_Callback = str2func(varargin{1});
end

if nargout
    [varargout{1:nargout}] = gui_mainfcn(gui_State, varargin{:});
else
    gui_mainfcn(gui_State, varargin{:});
end
% End initialization code - DO NOT EDIT

% --- Executes just before LDGUI is made visible.
function LDGUI_OpeningFcn(hObject,~, handles, varargin)
% This function has no output args, see OutputFcn.
```

```

% hObject    handle to figure
% eventdata  reserved - to be defined in a future version of MATLAB
% handles     structure with handles and user data (see GUIDATA)
% varargin    command line arguments to LDGUI (see VARARGIN)

% Choose default command line output for LDGUI
handles.output = hObject;

% Update handles structure
guidata(hObject, handles);

% UIWAIT makes LDGUI wait for user response (see UIRESUME)
uiwait(handles.figure1);
% uiresume(handles.figure1);

% --- Outputs from this function are returned to the command line.
function varargout = LDGUI_OutputFcn(hObject, eventdata, handles)
% varargout  cell array for returning output args (see VARARGOUT);
% hObject    handle to figure
% eventdata  reserved - to be defined in a future version of MATLAB
% handles     structure with handles and user data (see GUIDATA)

% Get default command line output from handles structure
varargout{1} = handles.output;

function tracepath_Callback(hObject, eventdata, handles)
% hObject    handle to tracepath (see GCBO)
% eventdata  reserved - to be defined in a future version of MATLAB
% handles     structure with handles and user data (see GUIDATA)

% Hints: get(hObject,'String') returns contents of tracepath as text
%        str2double(get(hObject,'String')) returns contents of tracepath as
a double

% --- Executes during object creation, after setting all properties.
function tracepath_CreateFcn(hObject, eventdata, handles)
% hObject    handle to tracepath (see GCBO)
% eventdata  reserved - to be defined in a future version of MATLAB
% handles     empty - handles not created until after all CreateFcns called

% Hint: edit controls usually have a white background on Windows.
%        See ISPC and COMPUTER.
if ispc && isequal(get(hObject,'BackgroundColor'), get(0,'defaultUicontrolBackgroundColor'))
    set(hObject,'BackgroundColor','white');
end

function mf_BL_init_E_Callback(hObject, eventdata, handles)
% hObject    handle to mf_BL_init_E (see GCBO)
% eventdata  reserved - to be defined in a future version of MATLAB
% handles     structure with handles and user data (see GUIDATA)

```

```
% --- Executes during object creation, after setting all properties.
function mf_BL_init_E_CreateFcn(hObject, eventdata, handles)
% hObject    handle to mf_BL_init_E (see GCBO)
% eventdata  reserved - to be defined in a future version of MATLAB
% handles    empty - handles not created until after all CreateFcns called

% Hint: edit controls usually have a white background on Windows.
%         See ISPC and COMPUTER.
if ispc && isequal(get(hObject,'BackgroundColor'), get(0,'defaultUicontrolBackgroundColor'))
    set(hObject,'BackgroundColor','white');
end

% --- Executes on selection change in mf_BL_init_UPU.
function mf_BL_init_UPU_Callback(hObject, eventdata, handles)
% hObject    handle to mf_BL_init_UPU (see GCBO)
% eventdata  reserved - to be defined in a future version of MATLAB
% handles    structure with handles and user data (see GUIDATA)
val = get(hObject, 'Value');
str = get(hObject, 'String');
switch str{val}
    case 'kg/h' % Input in kg/h
        mf_BL_init_UF = 1;
    case 'kg/s' % Input in kg/s
        mf_BL_init_UF = 1/3600;
    case 't/h'  % Input in t/h
        mf_BL_init_UF = 1/1000;
    case 't/a'  % Input in t/a
        mf_BL_init_UF = 8.760;
end
assignin('base','mf_BL_init_UF',mf_BL_init_UF)
guidata(hObject, handles);

% --- Executes during object creation, after setting all properties.
function mf_BL_init_UPU_CreateFcn(hObject, eventdata, handles)
% hObject    handle to mf_BL_init_UPU (see GCBO)
% eventdata  reserved - to be defined in a future version of MATLAB
% handles    empty - handles not created until after all CreateFcns called

% Hint: popuptmenu controls usually have a white background on Windows.
%         See ISPC and COMPUTER.
if ispc && isequal(get(hObject,'BackgroundColor'), get(0,'defaultUicontrolBackgroundColor'))
    set(hObject,'BackgroundColor','white');
end

% --- Executes on button press in run_PB.
function run_PB_Callback(hObject, eventdata, handles)
% hObject    handle to run_PB (see GCBO)
% eventdata  reserved - to be defined in a future version of MATLAB
% handles    structure with handles and user data (see GUIDATA)

%% Setting up variables
display('Setting up variables in progress!')
```



```

missing=0;

% BL massflow
mf_BL_init = str2double(get(handles.mf_BL_init_E, 'String'));
assignin('base', 'mf_BL_init', mf_BL_init)
if (isnumeric(mf_BL_init) && (mf_BL_init > 0))
    set(handles.mf_BL_init_CB, 'String', 'ok');
else
    set(handles.mf_BL_init_CB, 'String', 'needed');
    missing = missing + 1;
end

% BL pH value
pH_BL_init = str2double(get(handles.pH_BL_init_E, 'String'));
assignin('base', 'pH_BL_init', pH_BL_init)
if (isnumeric(pH_BL_init) && (pH_BL_init > 0))
    set(handles.pH_BL_init_CB, 'String', 'ok');
else
    set(handles.pH_BL_init_CB, 'String', 'needed');
    missing = missing + 1;
end

% BL temperature
T_BL_init = str2double(get(handles.T_BL_init_E, 'String'));
assignin('base', 'T_BL_init', T_BL_init)
if (isnumeric(T_BL_init) && (T_BL_init > 0))
    set(handles.T_BL_init_CB, 'String', 'ok');
else
    set(handles.T_BL_init_CB, 'String', 'needed');
    missing = missing + 1;
end

% Acidification pH value set point
pH_BL_prec = str2double(get(handles.pH_BL_prec_E, 'String'));
assignin('base', 'pH_BL_prec', pH_BL_prec)
if (isnumeric(pH_BL_prec) && (pH_BL_prec > 0))
    set(handles.pH_BL_prec_CB, 'String', 'ok');
else
    set(handles.pH_BL_prec_CB, 'String', 'needed');
    missing = missing + 1;
end

%% Create an output cell array
% v{1,:} = {'mf_BL', num2str(mf_BL), 'UNIT', 'description'};
% v{2,:} = {'pH_init', num2str(pH_init), 'UNIT', 'description'};
% assignin('base', 'v', v)

%% Control function
ctrl = 0;

if missing == 0
    display('Setting up variables done!')
else
    msgbox(['ERROR: ' num2str(missing) ' Variable(s) missing!'], 'Error
message')
    ctrl = ctrl + 1;
end

parapathname = get(handles.parameter_test, 'String');

```

```
if exist(parapathname)
    display('Setting up parameters')
%     open(parapathname)
else
    msgbox('ERROR: No parameters defined!', 'Error message')
    ctrl = ctrl + 1;
end

modelpathname = get(handles.model_test, 'String');
if exist(modelpathname)
    display('Starting the model!')
    open(modelpathname)
else
    msgbox('ERROR: No model defined!', 'Error message')
    ctrl = ctrl + 1;
end

if ctrl == 0
    display('Running the simulation!')
    a = sim(modelpathname, 'SimulationMode', 'normal');
    b = a.get('testvalue');
    assignin('base', 'RESULTS', b);
else
    display('Something went wrong!')
end

uiresume(handles.figure1);
guidata(hObject, handles);

% --- Executes on button press in model_PB.
function model_PB_Callback(hObject, eventdata, handles)
% hObject     handle to model_PB (see GCBO)
% eventdata   reserved - to be defined in a future version of MATLAB
% handles     structure with handles and user data (see GUIDATA)
[filename pathname]=uigetfile({'*.slx'}, 'File Selector');
fullpathname=strcat(pathname, filename);
% open (fullpathname)
set(handles.model_test, 'String', fullpathname)

% --- Executes on button press in database_PB.
function database_PB_Callback(hObject, eventdata, handles)
% hObject     handle to database_PB (see GCBO)
% eventdata   reserved - to be defined in a future version of MATLAB
% handles     structure with handles and user data (see GUIDATA)
[filename pathname]=uigetfile({'*.xlsx'}, 'File Selector');
fullpathname=strcat(pathname, filename);
% open (fullpathname)
set(handles.parameter_test, 'String', fullpathname)

% --- Executes on button press in default_PB.
function default_PB_Callback(hObject, eventdata, handles)
% hObject     handle to default_PB (see GCBO)
% eventdata   reserved - to be defined in a future version of MATLAB
% handles     structure with handles and user data (see GUIDATA)
```

```

% --- Executes on button press in clear_PB.
function clear_PB_Callback(hObject, eventdata, handles)
% hObject    handle to clear_PB (see GCBO)
% eventdata  reserved - to be defined in a future version of MATLAB
% handles    structure with handles and user data (see GUIDATA)

% --- Executes on button press in pushbutton8.
function pushbutton8_Callback(hObject, eventdata, handles)
% hObject    handle to pushbutton8 (see GCBO)
% eventdata  reserved - to be defined in a future version of MATLAB
% handles    structure with handles and user data (see GUIDATA)

% --- Executes on button press in initial_PB.
function initial_PB_Callback(hObject, eventdata, handles)
% hObject    handle to initial_PB (see GCBO)
% eventdata  reserved - to be defined in a future version of MATLAB
% handles    structure with handles and user data (see GUIDATA)
defaultvalues
evalin('base', 'run(''defaultvalues.m'')')
set(handles.mf_BL_init_E,'String',mf_BL_init);
set(handles.pH_BL_init_E,'String',pH_BL_init);
set(handles.T_BL_init_E,'String',T_BL_init);
set(handles.pH_BL_prec_E,'String',pH_BL_prec);
guidata(hObject, handles);

function pH_BL_init_E_Callback(hObject, eventdata, handles)
% hObject    handle to pH_BL_init_E (see GCBO)
% eventdata  reserved - to be defined in a future version of MATLAB
% handles    structure with handles and user data (see GUIDATA)

% Hints: get(hObject,'String') returns contents of pH_BL_init_E as text
%        str2double(get(hObject,'String')) returns contents of pH_BL_init_E
as a double

% --- Executes during object creation, after setting all properties.
function pH_BL_init_E_CreateFcn(hObject, eventdata, handles)
% hObject    handle to pH_BL_init_E (see GCBO)
% eventdata  reserved - to be defined in a future version of MATLAB
% handles    empty - handles not created until after all CreateFcns called

% Hint: edit controls usually have a white background on Windows.
%        See ISPC and COMPUTER.
if ispc && isequal(get(hObject,'BackgroundColor'), get(0,'defaultUicontrolBackgroundColor'))
    set(hObject,'BackgroundColor','white');
end

% --- Executes on selection change in pH_BL_init_UPU.
function pH_init_UPU_Callback(hObject, eventdata, handles)
% hObject    handle to pH_BL_init_UPU (see GCBO)
% eventdata  reserved - to be defined in a future version of MATLAB
% handles    structure with handles and user data (see GUIDATA)

```

```
% Hints: contents = cellstr(get(hObject,'String')) returns pH_BL_init_UPU
contents as cell array
%         contents{get(hObject,'Value')} returns selected item from
pH_BL_init_UPU

% --- Executes during object creation, after setting all properties.
function pH_BL_init_UPU_CreateFcn(hObject, eventdata, handles)
% hObject    handle to pH_BL_init_UPU (see GCBO)
% eventdata  reserved - to be defined in a future version of MATLAB
% handles    empty - handles not created until after all CreateFcns called

% Hint: popupmenu controls usually have a white background on Windows.
%         See ISPC and COMPUTER.
if ispc && isequal(get(hObject,'BackgroundColor'), get(0,'defaultUicon-
trolBackgroundColor'))
    set(hObject,'BackgroundColor','white');
end

function T_BL_init_E_Callback(hObject, eventdata, handles)
% hObject    handle to T_BL_init_E (see GCBO)
% eventdata  reserved - to be defined in a future version of MATLAB
% handles    structure with handles and user data (see GUIDATA)

% Hints: get(hObject,'String') returns contents of T_BL_init_E as text
%         str2double(get(hObject,'String')) returns contents of T_BL_init_E
as a double

% --- Executes during object creation, after setting all properties.
function T_BL_init_E_CreateFcn(hObject, eventdata, handles)
% hObject    handle to T_BL_init_E (see GCBO)
% eventdata  reserved - to be defined in a future version of MATLAB
% handles    empty - handles not created until after all CreateFcns called

% Hint: edit controls usually have a white background on Windows.
%         See ISPC and COMPUTER.
if ispc && isequal(get(hObject,'BackgroundColor'), get(0,'defaultUicon-
trolBackgroundColor'))
    set(hObject,'BackgroundColor','white');
end

% --- Executes on selection change in T_BL_init_UPU.
function T_BL_init_UPU_Callback(hObject, eventdata, handles)
% hObject    handle to T_BL_init_UPU (see GCBO)
% eventdata  reserved - to be defined in a future version of MATLAB
% handles    structure with handles and user data (see GUIDATA)
val = get(hObject, 'Value');
str = get(hObject, 'String');
switch str{val}
    case '°C' % Input in °C
        T_BL_init_UA = 273.15;
    case 'K' % Input in K
        T_BL_init_UA = 0;
end
```

```

assignin('base','T_BL_init_UA',T_BL_init_UA)
guidata(hObject, handles);

% --- Executes during object creation, after setting all properties.
function T_BL_init_UPU_CreateFcn(hObject, eventdata, handles)
% hObject    handle to T_BL_init_UPU (see GCBO)
% eventdata  reserved - to be defined in a future version of MATLAB
% handles    empty - handles not created until after all CreateFcns called

% Hint: popupmenu controls usually have a white background on Windows.
%         See ISPC and COMPUTER.
if ispc && isequal(get(hObject,'BackgroundColor'), get(0,'defaultUicontrolBackgroundColor'))
    set(hObject,'BackgroundColor','white');
end

% --- Executes when entered data in editable cell(s) in uitable1.
function uitable1_CellEditCallback(hObject, eventdata, handles)
% hObject    handle to uitable1 (see GCBO)
% eventdata  structure with the following fields (see
MATLAB.UI.CONTROL.TABLE)
%   Indices: row and column indices of the cell(s) edited
%   PreviousData: previous data for the cell(s) edited
%   EditData: string(s) entered by the user
%   NewData: EditData or its converted form set on the Data property. Empty
if Data was not changed
%   Error: error string when failed to convert EditData to appropriate
value for Data
% handles    structure with handles and user data (see GUIDATA)

% --- Executes on selection change in LPS_PU.
function LPS_PU_Callback(hObject, eventdata, handles)
% hObject    handle to LPS_PU (see GCBO)
% eventdata  reserved - to be defined in a future version of MATLAB
% handles    structure with handles and user data (see GUIDATA)

% Hints: contents = cellstr(get(hObject,'String')) returns LPS_PU contents
as cell array
%         contents{get(hObject,'Value')} returns selected item from LPS_PU

% --- Executes during object creation, after setting all properties.
function LPS_PU_CreateFcn(hObject, eventdata, handles)
% hObject    handle to LPS_PU (see GCBO)
% eventdata  reserved - to be defined in a future version of MATLAB
% handles    empty - handles not created until after all CreateFcns called

% Hint: popupmenu controls usually have a white background on Windows.
%         See ISPC and COMPUTER.
if ispc && isequal(get(hObject,'BackgroundColor'), get(0,'defaultUicontrolBackgroundColor'))
    set(hObject,'BackgroundColor','white');
end

```

```
% --- Executes on selection change in popupmenu6.
function popupmenu6_Callback(hObject, eventdata, handles)
% hObject    handle to popupmenu6 (see GCBO)
% eventdata  reserved - to be defined in a future version of MATLAB
% handles    structure with handles and user data (see GUIDATA)

% Hints: contents = cellstr(get(hObject,'String')) returns popupmenu6 con-
tents as cell array
%         contents{get(hObject,'Value')} returns selected item from
popupmenu6

% --- Executes during object creation, after setting all properties.
function popupmenu6_CreateFcn(hObject, eventdata, handles)
% hObject    handle to popupmenu6 (see GCBO)
% eventdata  reserved - to be defined in a future version of MATLAB
% handles    empty - handles not created until after all CreateFcns called

% Hint: popupmenu controls usually have a white background on Windows.
%         See ISPC and COMPUTER.
if ispc && isequal(get(hObject,'BackgroundColor'), get(0,'defaultUicon-
trolBackgroundColor'))
    set(hObject,'BackgroundColor','white');
end

% --- Executes on button press in override_PB.
function override_PB_Callback(hObject, eventdata, handles)
% hObject    handle to override_PB (see GCBO)
% eventdata  reserved - to be defined in a future version of MATLAB
% handles    structure with handles and user data (see GUIDATA)

% --- Executes during object creation, after setting all properties.
function initial_PB_CreateFcn(hObject, eventdata, handles)
% hObject    handle to initial_PB (see GCBO)
% eventdata  reserved - to be defined in a future version of MATLAB
% handles    empty - handles not created until after all CreateFcns called

function pH_BL_prec_E_Callback(hObject, eventdata, handles)
% hObject    handle to pH_BL_prec_E (see GCBO)
% eventdata  reserved - to be defined in a future version of MATLAB
% handles    structure with handles and user data (see GUIDATA)

% Hints: get(hObject,'String') returns contents of pH_BL_prec_E as text
%         str2double(get(hObject,'String')) returns contents of pH_BL_prec_E
as a double

% --- Executes during object creation, after setting all properties.
function pH_BL_prec_E_CreateFcn(hObject, eventdata, handles)
% hObject    handle to pH_BL_prec_E (see GCBO)
% eventdata  reserved - to be defined in a future version of MATLAB
% handles    empty - handles not created until after all CreateFcns called
```

```

% Hint: edit controls usually have a white background on Windows.
%       See ISPC and COMPUTER.
if ispc && isequal(get(hObject,'BackgroundColor'), get(0,'defaultUicontrolBackgroundColor'))
    set(hObject,'BackgroundColor','white');
end

```

10.9.1.2 Default values

```

% Defining the default values
% Use default values for testing the simulation model
% M. J. Tendl, TUGraz, ICVT, Mar 3rd 2016

%% Definition of the process variables
mf_BL_init = 1000;      % [kg/h]
mf_BL_init_UF = 1;     % Factor, changes if unit is not [kg/h] via GUI
ds_BL_init = 0.21;    % [kg/kg]
pH_BL_init = 13;      % [-]
T_BL_init = 50;       % [°C]
T_BL_init_UA = 273.15; % Addend, changes if unit is not [°C] via GUI
pH_BL_prec = 9;      % [-]

%% Read in of the parameter sheets
[default, default_txt, default_description] = xlsread('parameter-
list.xlsx','default');
clear default_txt

pset = default;
pset_description = default_description;

for i = 2:length(pset_description(:,1)) % 2 as start because of the header
    k=i-1;
    name = pset_description{i,1};
    value = pset(k);
    eval([name '=value;'])
end
clear k i name value

%% Definition of the component parameter

%% Definition of the process parameter

%% Definition of the model parameter

```